ABSORPTION OF ULTRAVIOLET RADIATION BY MOLECULAR HYDROGEN AND OXYGEN

by

A.J.D. Farmer B.Sc.(Hons).
Department of Physics

A Thesis submitted for the degree of
Doctor of Philosophy
in the
University of Adelaide

April, 1969.

CONTENTS

SUMMARY

This thesis describes experiments carried out to measure absorption coefficients for molecular hydrogen and molecular oxygen in the vacuum-ultraviolet region of the spectrum.

The first four bands of the Lyman system in hydrogen (1060-1130Å) were investigated using a 1 metre, near-normal incidence monochromator having a best resolution of 0·1Å. This instrument was fitted with an argon discharge lamp and photoelectric detection methods were used. The digital data-handling system developed for the experiment is described in detail.

An equivalent width method of analysis was used and from the measured absorption coefficients, absolute values of cross-sections for the rotational lines in the bands were obtained.

Absorption cross-sections for the Schumann-Runge band system in molecular oxygen [(2-0) to (20-0) bands covering the wavelength region 1700-2000Å] were measured using a similar experimental arrangement to that described above. Modifications made to the data handling system to improve the accuracy of the raw data are described. The light source used was an A.C. discharge in hydrogen and

photoelectric detectors were again employed.

Oscillator strengths for the bands were calculated from the measured integrated absorption coefficients and are compared with those obtained by other authors. A comparison is also made between Franck-Condon factors obtained from the derived oscillator strengths in this thesis and various theoretical calculations.

PREFACE

This thesis contains no material which has been accepted for the award of any other degree of diploma in any University. To the best of the author's knowledge and belief it contains no material previously published or written by another person, except where due reference is made in the text.

A.J.D. FARMER

April, 1969.

ACKNOWLEDGEMENTS

The experiment on molecular hydrogen was performed in association with Dr. G. N. Haddad, and the experiment on molecular oxygen in association with W. Fabian and B. R. Lewis.

Thanks are due to Mr. E. J. Connock and the staff of the Physics Department workshop for their assistance in building some of the apparatus used in this work.

The author would like to thank most sincerely his two supervisors, Dr. K. H. Lokan, and Dr. L. W. Torop for their enthusiasm, help and encouragement during the course of this work.

Finally, the author would like to thank the Elder Professor of Physics, Professor J. W. Carver, for making it possible for the experiments to be performed.

CHAPTER 1

Introduction

Since the beginning of the twentieth century, there has been considerable interest in the subject of molecular spectroscopy in the vacuum ultraviolet region of the spectrum. At the start, the work was primarily stimulated by a desire to obtain information about the structures of the molecules concerned but more recently a large amount of interest has been shown in the application of molecular spectra to the fields of atmospheric physics and astrophysics.

This thesis presents a brief historical review of the field of vacuum ultraviolet spectroscopy and a summary of the theoretical development of the subject. A technique for the measurement of absorption spectra and the subsequent analysis of the raw data is given, and the absolute absorption coefficients for molecular hydrogen from 1060 Å - 1130 Å and molecular oxygen from 1750 Å - 2000 Å obtained using this technique are presented.

1.1 Experimental Vacuum Ultraviolet Spectroscopy

Spectroscopy, in the form generally recognised today, began in the early nineteenth century with Fraunhofer's observations of the absorption lines in the solar spectrum (Fraunhofer, 1817) and the discovery

in 1839 by Niepce and Daguerre (Weblette, 1930) of photographic detection methods allowed investigations to proceed into the ultraviolet region of the spectrum. About 1862, Stokes using quarts optics, a spark source and fluorescent detection methods, observed spectra to as low as 1830Å (Stokes, 1880) and this lower limit was not surpassed until the last few years of the nineteenth century. During this period, considerable advances were made in the field of wavelength measurements, probably the most notable contribution being made by Rowland in 1882 who invented the concave diffraction grating (Rowland, 1882).

The first experiments in the vacuum ultraviolet region of the spectrum were made by Schumann (Lyman, 1928) who in the years between 1890 and 1903 collected a vast amount of information regarding this region. He is to be particularly remembered for the development of the first vacuum ultraviolet spectrograph and the invention of the Schumann photographic plate. It has since been shown that using the vacuum spectrograph, which employed fluorite optics, Schumann was able to reach a limit of approximately 1267Å (Tousey, 1962). It seems a fitting tribute to the great work of this pioneer that

an excellent review of his work has been written by Lyman (1928) who, in 1906, by replacing the fluorite prism by a concave grating, was instrumental in extending the low wavelength limit to approximately 500Å. In the following years until about 1930, Lyman was extremely active in this field and excellent reviews of his and many other workers results up to this time have been published by Tousey (1962) and Boyce (1941).

Since 1930, considerable advances have been made in fields closely related to vacuum ultraviolet spectroscopy, in particular; grating efficiencies and spectrograph design, vacuum technology, ultraviolet light sources and photoelectric detectors. Reviews of work in these fields have been given by Watanabe (1958) and Samson (1967). Spectrographic measurements have progressed along with the developments mentioned above, and in particular a large number of high resolution measurements have been made for a variety of gases (e.g. Tilford et al. 1965, Herzberg and Howe, 1959 and Wonfils, 1965). These high resolution measurements have contributed greatly to the knowledge of energy levels and molecular constants for molecules. In contrast to this, there have been very few determinations of absolute

absorption coefficients for gases. Absolute absorption cross-sections of gases have wide applications to atmospheric and astrophysical problems and also may be used to provide additional information about molecular structure. For these reasons, it was decided to obtain measurements of absolute cross-sections for molecular hydrogen and molecular oxygen in regions where very little previous work of this kind has been attempted.

The results of the experiment on molecular hydrogen are presented as oscillator strengths (see Chapter 2) for the rotational lines of the first four bands in the Lyman series and a brief discussion on how these may be applied to interstellar absorption measurements is given. The oscillator strengths for the bands are also presented and compared with the theoretical predictions.

Oscillator strengths are also presented for the Schumann-Runge band system in molecular oxygen and these are used to determine the variation of the electronic transition moment with inter-nuclear separation.

CHAPTER 2.

Theory of Diatomic Molecules

To enable the data obtained from observed molecular spectra to be used as a tool for studying the structure of molecules, it is necessary to postulate theoretical models for the molecules and to investigate the types of spectra expected on the basis of these models. As the two gases of interest to this thesis are diatomic, this chapter will present a summary of the development of models for diatomic molecules. The notation used will be basically that of Herzberg (1950).

2.1 Emission and Absorption of Radiation

For emission or absorption of radiation by matter to occur, there must be an interaction between the electromagnetic field of the radiation and the matter involved. The frequencies of the emitted or absorbed radiation are determined by the eigenvalues for the Schrodinger equation for the system concerned and the probabilities of the transitions caused by the radiation are determined by the eigenfunctions of the states involved in the transitions. It is possible to think of the interaction of electromagnetic radiation (of wavelength greater than a few hundred angstroms) with a system as the interaction with the electric dipole moment for the system since this interaction is approxi-

mately five orders of magnitude greater than magnetic dipole interactions which are in turn approximately three orders of magnitude greater than electric quadruple interactions and magnetic quadruple interactions are weaker still. (Goody, 1964, Leighton, 1959). This approach has lead to the term "allowed transitions" being applied to electric dipole transitions, all other types of transitions being grouped together under the term "forbidden transitions" even though a finite probability exists for their occurrence.

The intensity of a dipole transition is between two states n and m is proportional to the square of the matrix element of the dipole moment M for the system; that is the probability is proportional to the absolute square of the quantity

$$r^{nm} = \int \psi_n^* M \psi_m \, d\tau \qquad (2.1.1)$$

where dr is a volume element of configuration space, and ψ_n and ψ_m are the wave-functions for the two states involved in the transition. The integration is taken over the whole of configuration space and the star denotes the complex conjugate.

The relations between the matrix element and the Einstein coefficients (A_{nm} - the Einstein transition probability of spontaneous emission, and B_{nm} - the Einstein probability for absorption) are given by wave mechanics for the case of dipole radiation as (Herzberg, 1950)

$$A_{nm} = \frac{64\pi^4 \nu_{nm}^3}{3h} |R^{nm}|^2 \qquad (2.1.2)$$

$$B_{nm} = \frac{8\pi^3}{3h^2 c} |R^{nm}|^2 \qquad (2.1.3)$$

These formulae only apply in the case of non-degenerate levels and the appropriate relations for degenerate levels will be introduced where necessary in the following chapters.

It can be seen, therefore, that if experimental quantities are measured which are related to the Einstein transition probabilities in equations (2.1.2) and (2.1.3) then these may be compared with theoretical quantities obtained on the basis of some molecular model and thus provide a test of the model.

2.2 Diatomic Molecules

When a diatomic molecule is considered in an ele-

mentary manner, it may be thought of as two stationary atomic nuclei separated from each other and bound by a cloud of electrons in various orbitals around the nuclei. As has been found for atoms (Herzberg, 1944) we would expect to find different electronic states for a molecule, depending on which orbitals are occupied by the electrons. However a diatomic molecule is not as simple as it may perform two types of motion. Firstly, it may rotate as a whole about an axis through the centre of gravity of the system and perpendicular to the line joining the nuclei; and secondly, the two nuclei may perform vibrations along the inter-nuclear axis. Thus a diatomic molecule is seen to be considerably more complicated than an atom, and a model of a diatomic molecule would need to take into consideration all of the above features if it is to account for the observed molecular spectra.

2.2.1 Separation of the Wave Equation

The total energy of a molecule is made up of the potential and kinetic energies of the electrons in the system and the potential and kinetic energies of the nuclei, and if the nuclei are considered as stationary, it can be seen that the electronic energy (the sum of

the potential and kinetic energies for the electrons) will be dependent on the internuclear distance. However, the nuclei are not stationary and the effect of their motion must be considered. Because of the large ratio of nuclear mass to electron mass, the electrons will move much more rapidly than the nuclei, and the electronic energy can be thought of as taking values corresponding to the momentary positions of the nuclei. Following this argument through, it can be seen that if the nuclei move, work must be supplied for the change in electronic energy as well as the work which is done against the Coulomb repulsion of the nuclei, and therefore, the potential energy under whose influence the nuclei perform their vibrations is the sum of the electronic energy and the Coulomb potential of the nuclei. The curves which show the variation of this potential energy with internuclear distance are called potential curves.

The above ideas indicating the potentials under which the nuclei vibrate may also be derived from a quantum-mechanical approach in which the Schrodinger equation for a diatomic molecule may be written (Herzberg, 1950):

$$\frac{1}{m}\sum_i\left(\frac{\partial^2\psi}{\partial x_i^2}+\frac{\partial^2\psi}{\partial y_i^2}+\frac{\partial^2\psi}{\partial z_i^2}\right)+\sum_k\frac{1}{M_k}\left(\frac{\partial^2\psi}{\partial x_k^2}+\frac{\partial^2\psi}{\partial y_k^2}+\frac{\partial^2\psi}{\partial z_k^2}\right)+$$

$$+\frac{8\pi^2}{h^2}(E-V)=0 \qquad (2.2.1.1)$$

where the electrons have coordinates x_i, y_i, z_i and mass m; and the nuclei have coordinates x_k, y_k, z_k and mass M_k. If, as an approximate solution to equation (2.2.1.1) the separated wave function

$$\psi=\psi_e(\ldots x_i,y_i,z_i,\ldots)\psi_{vr}(\ldots x_k,y_k,z_k,\ldots) \qquad (2.2.1.2)$$

is used; where ψ_e is the solution of the equation

$$\sum_i\left(\frac{\partial^2\psi_e}{\partial x_i^2}\ldots\right)+\frac{8\pi^2m}{h^2}(E^{el}-V_e)\psi_e=0 \qquad (2.2.1.3)$$

and ψ_{vr} is the solution of the equation

$$\sum_k\frac{1}{M_k}\left(\frac{\partial^2\psi_{vr}}{\partial x_k^2}\ldots\right)+\frac{8\pi^2}{h^2}(E-E^{el}-V_n)\psi_{vr}=0 \qquad (2.2.1.4)$$

then the wave equation (2.2.1.1) is satisfied provided that ψ_e only varies slowly with internuclear distance. That this is true in a majority of cases has been shown

by Born and Oppenheimer (1927). Equation (2.2.1.3) is seen to be the equation of the electrons moving in the field of the fixed nuclei with a potential energy V_e, and equation (2.2.1.4) is the equation of the nuclei moving under the influence of a potential E^{el} and V_n is the Coulomb potential of the nuclei, and so there is sufficient justification for using $E^{el} + V_n$ as the potential energy for the nuclear motion.

For a given electronic state, the minimum of the potential curve (the function $E^{el} + V_n$) is considered as the electronic energy of the state E_e and the excess of energy of the molecule over E_e may be considered as the sum of the vibrational and rotational energies, E_v and E_r respectively. Thus the total energy of the molecule may be written as

$$E = E_e + E_v + E_r \qquad (2.2.1.5)$$

It is common practice to express this equation in wave-number units (the wave-numbers are expressed as cm^{-1} and are 10^8 times the reciprocal of the wave length in angstroms) and the quantities are called Term Values. Thus equation (2.2.1.5) becomes

$$T = T_e + G + F \qquad (2.2.1.6)$$

2.2.2 Vibrational Energy

The simplest way of representing the vibrations of a diatomic molecule is the model of two atoms moving toward or away from each other with simple harmonic motion; that is the system is represented by a harmonic oscillator. The potential energy for such a system is given by (Herzberg, 1950)

$$U = 2\pi^2 \mu \nu_{osc}^2 x^2 \qquad (2.2.2.1)$$

where μ is the reduced mass of the molecule, x is the change in inter-nuclear distance from the equilibrium position and ν_{osc} is the frequency of oscillation. The potential curve given by equation (2.2.2.1) is seen to be a parabola. When this potential function is substituted in the wave-equation, satisfactory solutions are only found for values of energy given by (Herzberg, 1950)

$$E(v) = h\nu_{osc}(v+\tfrac{1}{2}) \qquad (2.2.2.2)$$

where v can only take values $0,1,2,3 \ldots$. A harmonic oscillator, therefore, gives equidistant energy levels which do not fit the observations, except near the equilibrium position of the potential curve.

However, the harmonic oscillator would not be

expected to give a good representation of the energy levels since the parabolic potential curve is not realistic for the potential in which the vibrations of the molecule occur. A typical potential curve would have a shape similar to that shown in figure 2.1. When the atoms are far apart, the energy of the system is just the sum of the energies of the two atoms, and so at large inter-nuclear distances, r, the potential function is expected to reach a constant value. For stable states, as the atoms approach each other there is a small attraction, increasing with decreasing r, and the potential function reaches a minimum value at the equilibrium separation $r = r_e$. For $r < r_e$, the value of the potential function should rise rapidly because of the repulsion of the two nuclei.

As a first approximation to the curve shown in figure 2.1, a cubic term may be added to the harmonic oscillator potential and we obtain

$$U = f(r - r_e)^2 - g(r - r_e)^3 \qquad (2.2.2.3)$$

where g is much smaller than f. This function is shown in figure 2.2, and is one type of potential curve which can be obtained if an anharmonic oscillator is used to represent the molecule. If the Schrodinger equation is

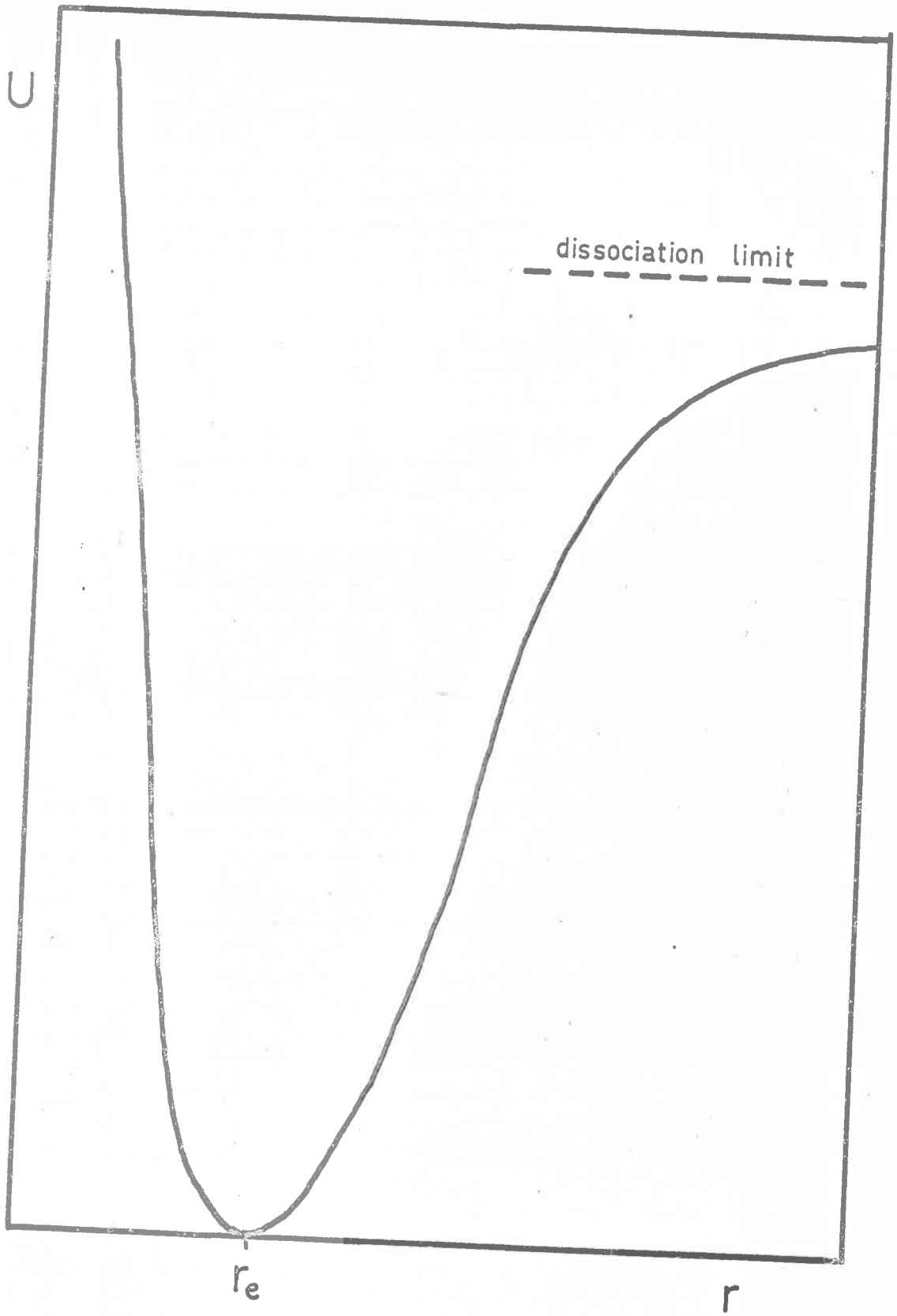

Fig. 2.1 Typical potential curve for diatomic molecules

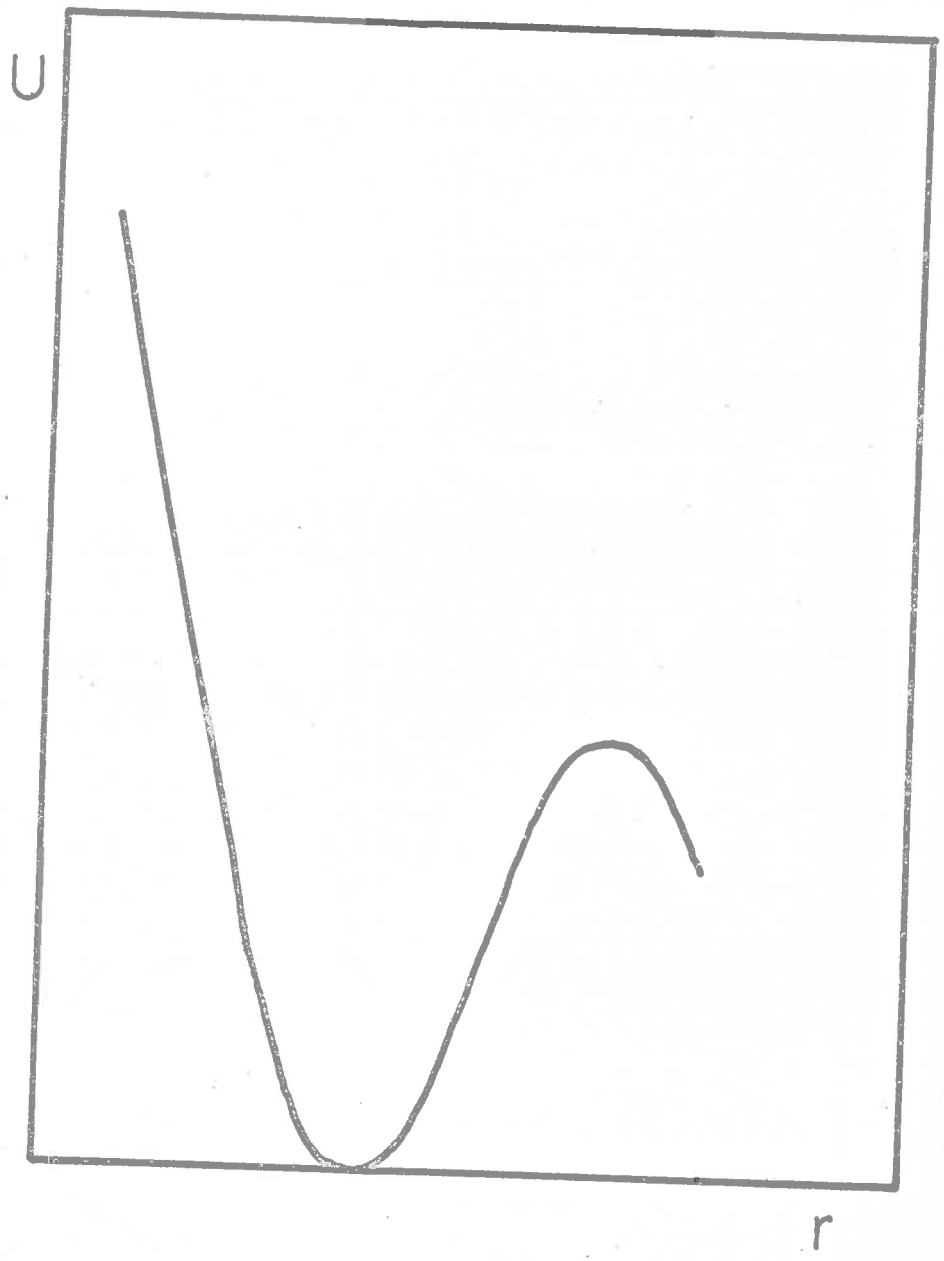

Fig. 2.2 Potential curve for a cubic harmonic oscillator (after Herzberg 1950)

now solved with equation (2.2.2.3) as the potential function (possibly with higher terms in $(r - r_e)$ present), the energy levels obtained are

$$E(v) = hc\omega_e(v+\tfrac{1}{2}) - hc\omega_e x_e(v+\tfrac{1}{2})^2 + hc\omega_e y_e(v+\tfrac{1}{2})^3 \ldots \qquad (2.2.2.4)$$

where $\omega_e, \omega_e x_e$ and $\omega_e y_e$ are constants of the molecule concerned ($\omega_e y_e \ll \omega_e x_e \ll \omega_e$ and ω_e and $\omega_e x_e$ are usually positive). The separation of these energy levels is slowly decreasing with increasing v, and if the function $E(v)$ may be adequately represented by a quadratic in $(r - r_e)$, then the dissociation energy for the molecule is given by (Herzberg, 1950)

$$D_e = \frac{\omega_e^2}{4\omega_e x_e} \qquad (2.2.2.5)$$

Because the simple potential functions described so far do not describe the energy levels very accurately, many more complicated mathematical expressions have been proposed as approximations to the true potential curve (Hylleraas, 1935, 1936, Coolidge et al. 1938, Hulbert and Hirschfelder, 1941, Morse, 1929 etc). One of the simplest of these potentials is that proposed by Morse (1929) and this has been the most commonly used. Morse put forward the potential

$$U(r-r_e) = D_e(1-e^{-\beta(r-r_e)})^2 \qquad (2.2.2.6)$$

This potential is shown in figure 2.3 and has a shape very similar to that shown in figure 2.1, the expected potential. As the internuclear distance becomes large, the value of $U(r-r_e)$ approaches D_e, the dissociation energy referred to the minimum of the potential curve; and the function equals zero at the equilibrium position r_e. One slight disadvantage of this potential is that for very small r, $U(r-r_e)$ although becoming large does not approach infinity as it must for a correct potential, but this is not of prime importance. The great advantage of equation (2.2.2.6) is that the Schrodinger equation with this as the potential energy function may be solved analytically yielding term values

$$G(v) = \beta\sqrt{\frac{D_e h}{2\pi^2 c\mu}}\,(v+\tfrac{1}{2}) - \frac{h\beta^2}{c8\pi^2\mu}\,(v+\tfrac{1}{2})^2 \qquad (2.2.2.7)$$

with no higher terms in $(v + \frac{1}{2})$ occurring. If this expression is compared with the term values obtained for the anharmonic oscillator, the constant β may be written in terms of the spectroscopic constants as

$$\beta = \sqrt{\frac{2\pi^2 c\mu}{D_e h}}\,\omega_e \qquad (2.2.2.8)$$

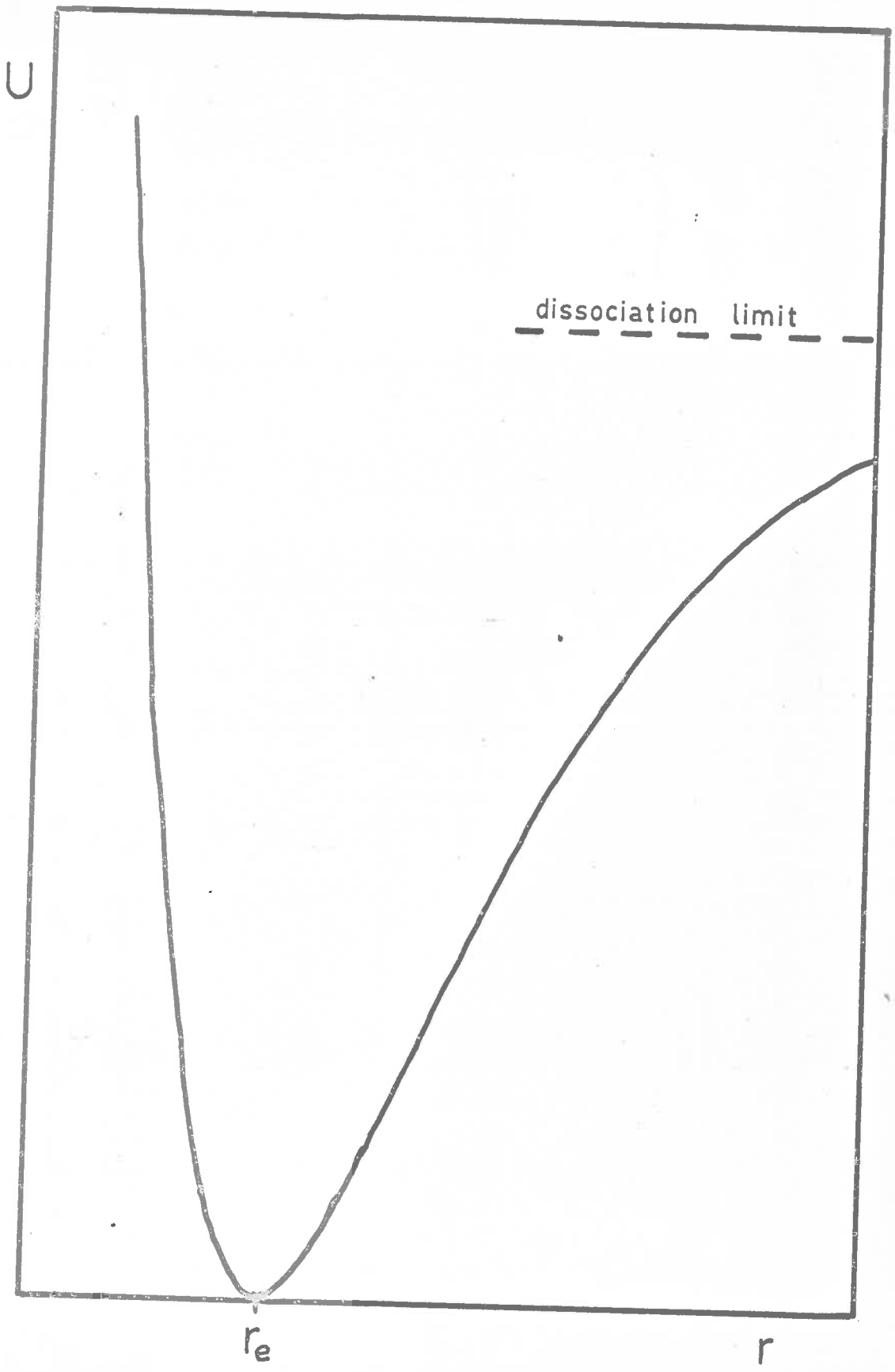

Fig. 2.3 Morse potential curve

This same relationship is found to hold when the coefficients of $(v + \frac{1}{2})$ and $(v + \frac{1}{2})^2$ are considered, and so it is possible to define the Morse constants in terms of the spectroscopic constants.

For most molecules, the Morse potential is a good representation of the bottom half of the true potential (e.g. for the B state of molecular oxygen, the Morse potential is good for approximately the first four vibrational levels) and for some states it may be even better than this.

As well as the abovementioned analytic representations, techniques have also been developed for deriving numerical potential curves. Considerable work has been done on the hydrogen molecule by Kolos and Wolniewicz (1965, 1966, 1968) who have used a variational approach to produce potentials, and a technique for developing potential curves from the observed energy levels was given by Klein (1932) and Rydberg (1931). The Klein and Rydberg method has been re-investigated by Rees (1947) and many other workers (Jarmain, 1960, Vanderslice et al. 1960, Gilmore, 1965, etc.), and a discussion of the potentials developed for the molecules of interest to this thesis will be given in the appropriate chapters.

2.2.3 Rotational Energy

The simplest way of considering the rotational energy of a diatomic molecule is to neglect the molecule's vibrations and think of the molecule as two point like atoms at each end of a rigid, massless rod; that is, as a rigid rotator. Using this model, Herzberg (1950) has shown that the resulting rotational term values are given by

$$F(J) = BJ(J+1) \qquad (2.2.3.1)$$

where $B = \frac{h}{8\pi^2 cI}$ is called the rotational constant, and I is the moment of inertia of the system.

A more realistic model is one which considers the rotation when the nuclei are allowed to move along the internuclear axis, that is a non-rigid rotator, and for such a model, Dunham (1930) and Pekeris (1934) have shown that the rotational term values for a given vibrational level may be written

$$F_v(J) = BJ(J+1) - DJ^2(J+1) \qquad (2.2.3.2)$$

where D is a constant and is usually less than $10^{-4}B$. This model, however, still considers the rotation of the system and the nuclear motions as two separate functions, and a more realistic model would be one which allows the

two motions to occur simultaneously. Such a model would be the vibrating rotator. Using this approach, Hylleraas (1936) has shown that since the period of vibration is small compared with the period of rotation, it is possible to use a mean value of B in equation (2.2.3.2) for the rotational constant in the vibrational state under consideration; this being

$$B_v = B_e - \alpha_e(v+\tfrac{1}{2}) + \ldots \qquad (2.2.3.3)$$

where $\alpha_e \ll B_e$, and B_e is the rotational constant corresponding to the equilibrium separation of the nuclei. Similarly, it is possible to write

$$D_v = D_e + \beta_e(v+\tfrac{1}{2}) \qquad (2.2.3.4)$$

where $\beta_e \ll D_e$. This D_e is not to be confused with the dissociation energy used in equation (2.2.2.5); it has been retained because of the conventional nomenclature.

Using this model of the vibrating rotator, and taking into consideration equation (2.2.2.4), the term values for the vibrating rotator are

$$\begin{aligned} T &= G(v) + F_v(J) \\ &= \omega_e(v+\tfrac{1}{2}) - \omega_e x_e(v+\tfrac{1}{2})^2 + \omega_e y_e(v+\tfrac{1}{2})^3 \ldots \\ &\quad + B_v J(J+1) - D_v J^2(J+1)^2 \end{aligned} \qquad (2.2.3.5)$$

Equation (2.2.1.6) may then be used to give the wave numbers of the spectral lines corresponding to the transitions between two different electronic states (if interactions between rotation and electronic motions are neglected) as

$$\nu = T'-T'' = (T_e'-T_e'') + (G'(v) - G''(v)) + (F_v'(J)-F_v''(J))$$

$$= \nu_e + \nu_v + \nu_r \qquad (2.2.3.6)$$

where the single prime letters refer to the upper state, and the double prime letters to the lower state.

A better model again for the molecule which only produces slight changes in the rotational term values, is the symmetric top model. This model, which has been described by Dennison (1926), Kronig and Rabi (1927) and others, takes into consideration the moment of inertia of the electrons about the line joining the nuclei, and thus introduces the quantum number A. This is the quantum number of the angular momentum of the electrons about the internuclear axis. Using the symmetric top model, it is possible to predict the transitions expected between two electronic levels.

For two given electronic levels, the term $\nu_e = T_e' - T_e''$, is a constant, and as there are no selection

rule restrictions on the vibrational quantum number v, the vibrational contribution to the transition energy is given by

$$\nu_v = \omega_e'(v'+\tfrac{1}{2}) - \omega_e x_e'(v'+\tfrac{1}{2})^2 + \omega_e y_e'(v'+\tfrac{1}{2})^3$$
$$- [\omega_e''(v''+\tfrac{1}{2}) - \omega_e x_e''(v''+\tfrac{1}{2})^2 + \omega_e y_e''(v''+\tfrac{1}{2})^3] \qquad (2.2.3.7)$$

The selection rules on J for the symmetric top are (Hersberg, 1950)

$\Delta J = J' - J'' = 0, \pm 1$ if $\Lambda \neq 0$ for at least one state

$\Delta J = J' = J'' = \pm 1$ if $\Lambda = 0$ for both states,

and the observed spectrum would therefore be expected to consist of two or three series of lines, whose wave numbers are given by

$$\text{for } \Delta J = +1 \; : \; \nu = \nu_0 + F_v'(J+1) - F_v''(J)$$
$$\text{for } \Delta J = 0 \; : \; \nu = \nu_0 + F_v'(J) - F_v''(J) \qquad (2.2.3.8)$$
$$\text{for } \Delta J = -1 \; : \; \nu = \nu_0 + F_v'(J-1) - F_v''(J)$$

where $\nu_0 = \nu_e + \nu_v$.

These series are called the R, Q, and P branches of the spectrum respectively. An example of these series is given in figure 2.4. The transitions shown are between the rotational levels of two vibrational states

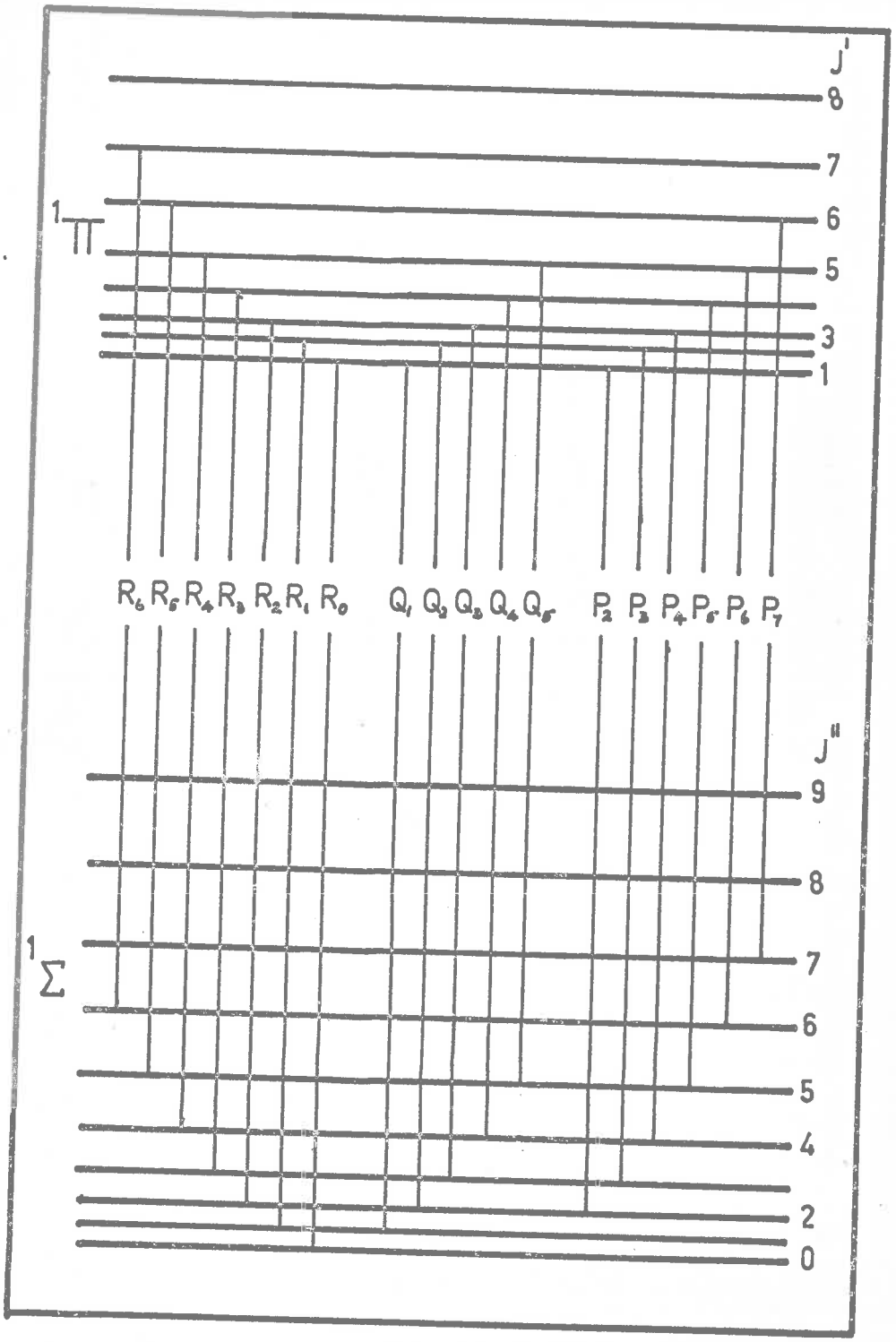

Fig. 2.4 P, Q, R, series for diatomic molecules (after Herzberg 1950)

in two different electronic states. For this particular case, $\Lambda = 1$ for the upper state and $\Lambda = 0$ for the lower state ($^1\Pi - {}^1\Sigma$ transition).

2.3 Band and Line Intensities

If transitions between the vibrational levels of two different electronic states are considered (neglecting the rotational structure for the present), then there are three main cases to be dealt with as far as transition intensities are concerned. These three cases are shown in figure 2.5. In figure 2.5a, the minimum of the two potential curves of the electronic states occur at approximately the same internuclear distance, and in figures 2.5b and 2.5c, the minimum of the upper curve lies at progressively larger values of the internuclear distance. These three cases give rise to the three distinct types of intensity distribution for absorption at room temperature (that is only the lowest vibrational level in the ground state is populated), and the distributions may be explained by the Franck-Condon Principle (Franck, 1925, Condon, 1928).

Franck's basic idea (developed mathematically by Condon) was that a transition from a level in the lower state to a level directly above it in the upper state

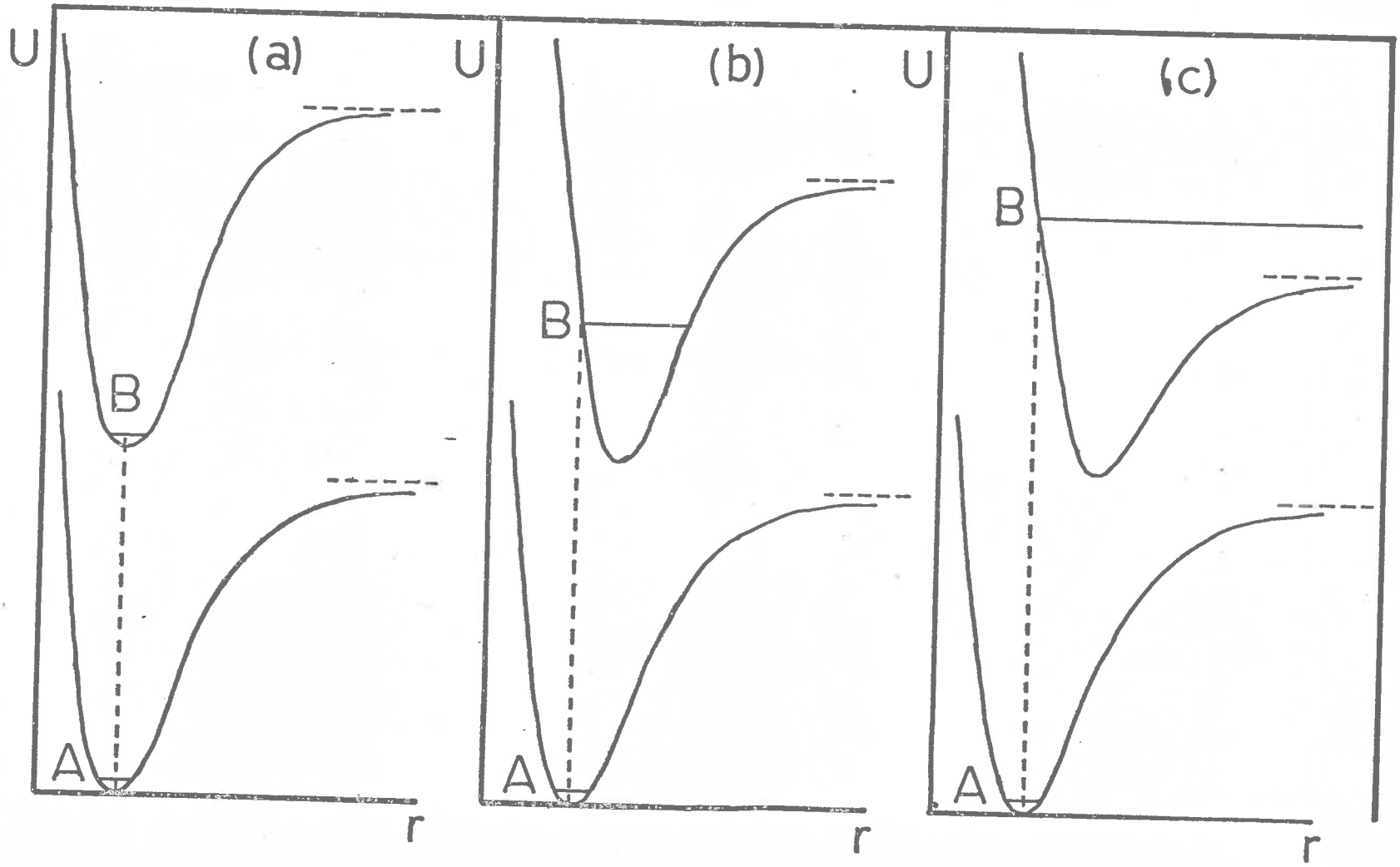

Fig. 2.5 Potential curves explaining absorption intensity by Franck-Condon principle (after Herzberg 1950)

(as represented by the line AB in figure 2.5) is the most probable transition and therefore gives rise to the most intense bands. The basis of this idea is that the nuclei are massive and move slowly compared with the electrons. The positions of the nuclei are therefore almost constant during a transition. This simple approach will explain approximately the three observed intensity distributions shown in figure 2.6 for the three cases in figure 2.5.

A more accurate approach is that given by Condon (1928) using wave mechanics. It was stated in section 2.1 that the probability of a transition between two states (having total wavefunctions ψ' and ψ'') is proportional to the absolute square of the matrix element of the electric moment. That is proportional to the quantity

$$R = \int \psi'^{*} M \psi'' d\tau \qquad (2.3.1)$$

where M is the electric moment for the system. It has been shown (Herzberg, 1950) that rotation of the molecule may be neglected. If the wavefunction is now separated into electronic and vibrational wavefunctions, the electric moment separated into electron dependent and nuclei dependent parts, and use is made of the ortho-

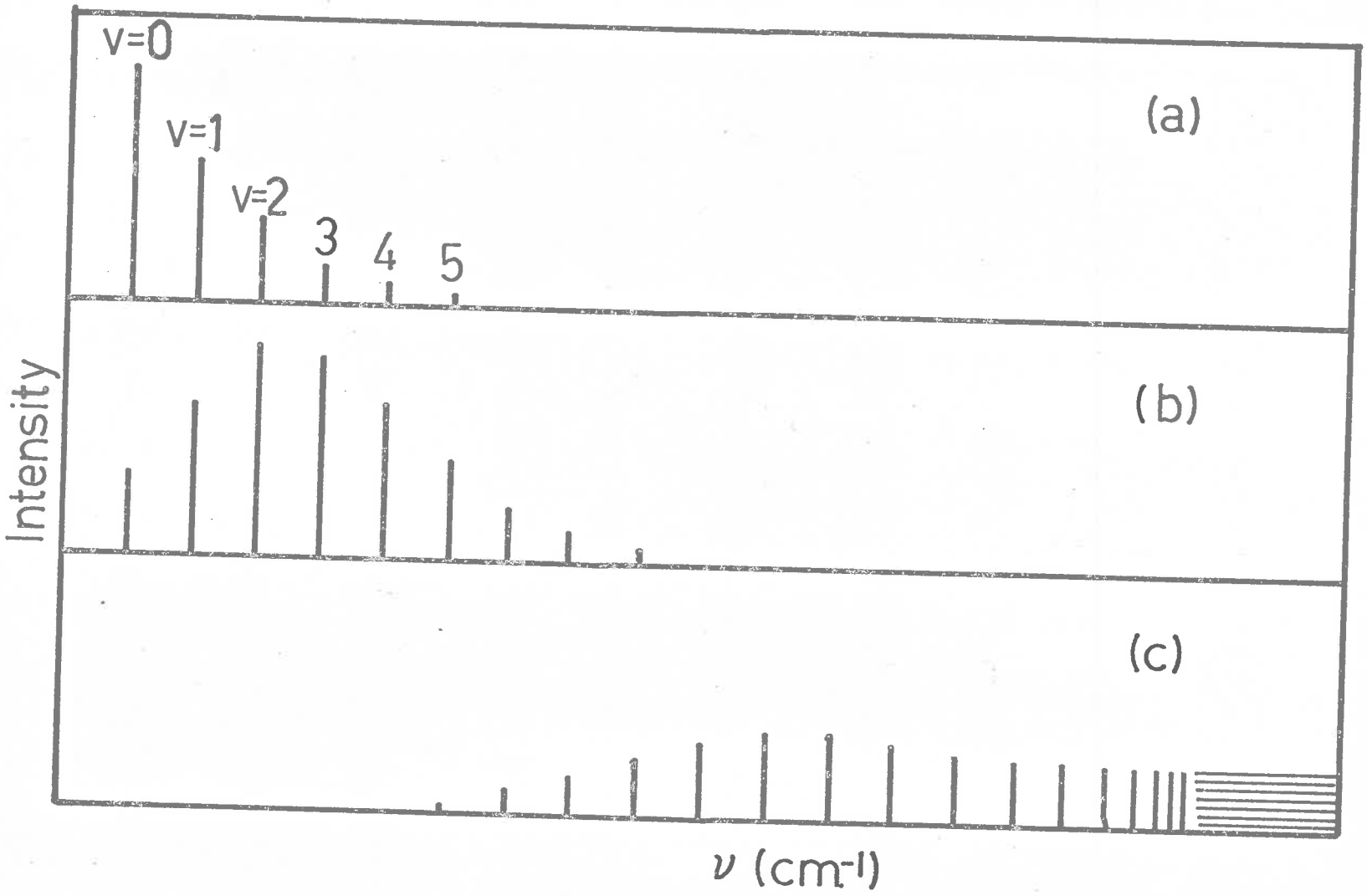

Fig. 2.6 Three types of absorption intensity distribution (after Herzberg 1950)

gonality relationship for the electronic wavefunctions, Herzberg (1950) has shown that equation (2.3.1) may be written

$$R = \int \psi'_v \psi''_v dr \int M_e \psi'_e \psi''_e dr_e \qquad (2.3.2)$$

where ψ'_v and ψ''_v are the vibrational wavefunctions and ψ'_e and ψ''_e are the electronic wavefunctions for the two states and M_e is the electron dependent part of the electric moment.

The second integral in equation (2.3.2) is the electronic transition moment

$$R_e = \int M_e \psi'_e \psi''_e dr_e \qquad (2.3.3)$$

and if the assumption is made that R_e is slowly varying with r, then it may be replaced by the average value $\bar{R}_e$, and we may write

$$R^{v'v''} = \bar{R}_e \int \psi'_v \psi''_v dr \qquad (2.3.4)$$

The transition probability and therefore the intensity is proportional to $R^{v'v''}$ (see section 2.1) and thus the square of the integral in equation (2.3.4) is representative of the intensity of a given transition. This integral is called the "overlap integral" and the absolute square of the overlap integral is called the

Franck-Condon factor, $q_{v'v''}$. That is

$$q_{v'v''} = \left|\int \psi'_{v'}\psi''_{v''}dr\right|^2 \qquad (2.3.5)$$

The transition for which the Franck-Condon factor is a maximum, is the most intense band in the series. Figure 2.7 shows an example of this where the maximum overlap for absorption at room temperature occurs for $v' = 2$. The v - value at which the maximum overlap occurs can thus be seen to depend upon the relative equilibrium internuclear distances for the states, and upon the shapes of the potential curves. The similarity between the wave-mechanical approach and Franck's "vertical transition" approach is easily seen since the wave-functions for all v - values (apart from $v = 0$) have a maximum on the left-hand limb of the potential curve (see figure 2.7). It is not surprising that the two approaches give similar results, as the large mass of the nuclei is precisely the fact which allows the wave-equation to be separated.

The intensity distribution of the rotational lines within a given band is essentially determined by the thermal distribution of the molecules in the rotational levels of the initial state of the transition. This is a Boltzman distribution and is modified by the statistical

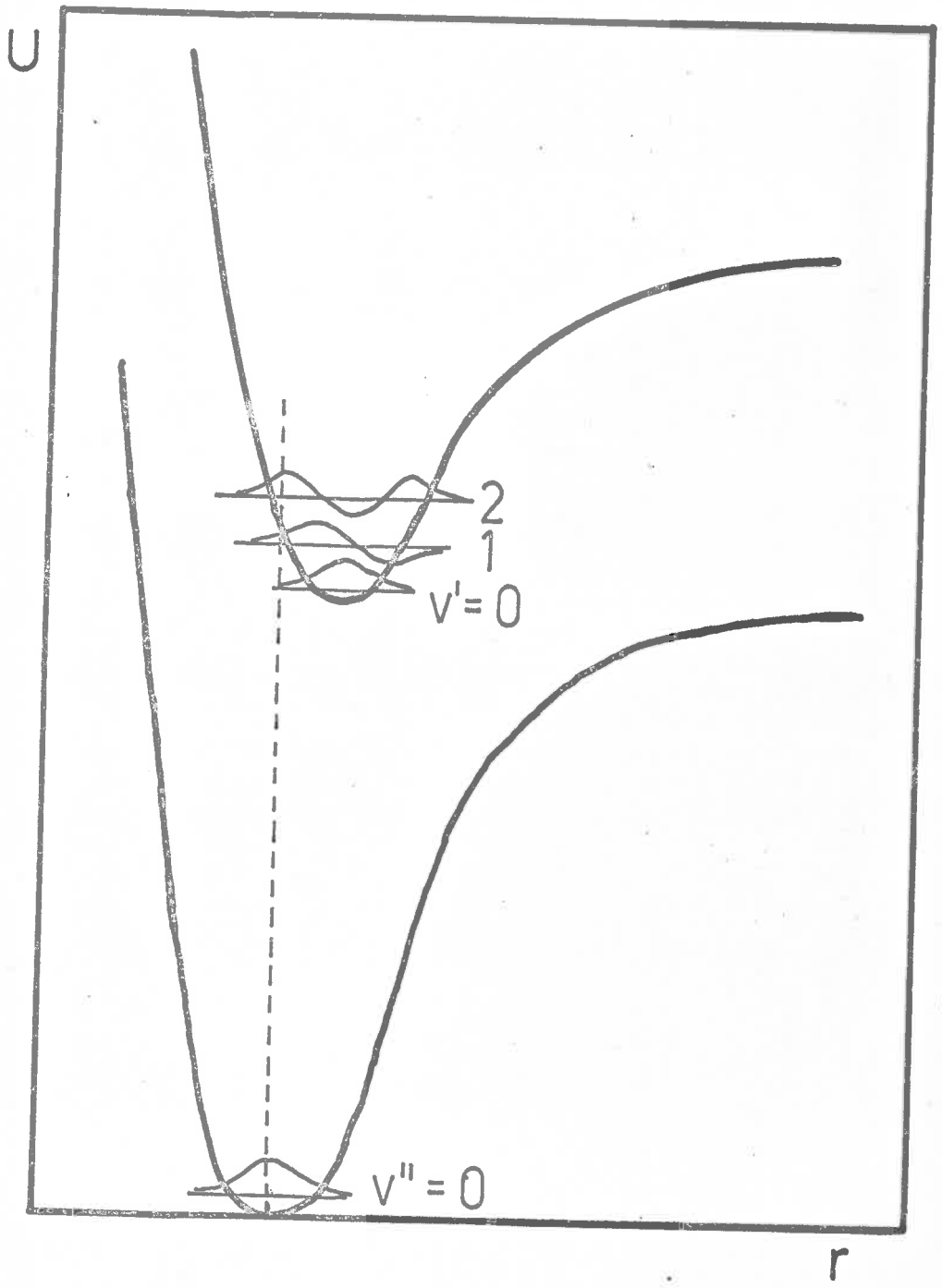

Fig. 2.7 Franck-Condon principle according to Wave Mechanics (after Herzberg 1950)

weights of the levels concerned. The statistical weights and degeneracies are discussed by Herzberg (1950) who gives the expression for the fraction of the molecules in a given level as

$$N = \frac{(2J''+1)\exp[-J''(J''+1)B''hc/kT]}{\sum_{J''}(2J''+1)\exp[-J''(J''+1)B''hc/kT]} \qquad (2.3.6)$$

Actually, the transition probability depends slightly on the rotational quantum number for the final state, and this may be accounted for when only P and R branches occur by using the following expression for N

$$N = \frac{(J'+J''+1)\exp[-J''(J''+1)B''hc/kT]}{\sum_{J''}(J'+J''+1)\exp[-J''(J''+1)B''hc/kT]} \qquad (2.3.7)$$

where J'' and J' refer to the initial and final stages respectively, and B'' is the rotational constant for the initial state. The transition strengths are also influenced by the selection rules for the states concerned, and the effect of these will be discussed where necessary for the molecules of interest to this thesis.

The foregoing sections have presented the development of models for a diatomic molecule and the validity of these models should be checked by comparing the

predicted spectral line positions, intensities etc. with the observed data. One way of obtaining absolute experimental intensities is to measure the absorption intensities over a given band system.

2.4 Oscillator Strengths

A knowledge of the absolute intensities of a given band system may be obtained from experimental absorption data, where the quantity usually measured is k_ν, the absorption coefficient at a given frequency ν, and defined by

$$I_\nu = I_\nu^0 e^{-k_\nu \Delta x} \qquad (2.4.1)$$

where I_ν and I_ν^0 are the light intensities before and after transmission through a length of gas Δx at 0 °C and 1 atmosphere pressure. If Δx is small, and I_ν^0 is assumed constant over the band, the light absorbed by the transitions between the two levels n and m is given by

$$I_{abs}^{nm} = \int_{band} (I_\nu^0 - I_\nu)\, d\nu = I_\nu^0 \Delta x \int_{band} k_\nu \, d\nu \qquad (2.4.2)$$

Using equation (2.4.2) it may be shown (Herzberg, 1950) that the integrated absorption coefficient (experimental) may be related to the theoretical quantity R^{nm},

the matrix element of the dipole moment, by

$$\int k_\nu \, d\nu = \frac{8\pi^3 \nu_{nm}}{3hc} N_m |R^{nm}|^2 \qquad (2.4.3)$$

where N_m is the number of atoms in the state m, and ν_{nm} is the frequency of the transition.

The oscillator strength for a given transition represents the ratio of the quantum theoretical to the classical value of the transition strength, and may be given in terms of R^{nm} as (Condon and Shortley, 1935)

$$f^{nm} = \frac{8\pi^2 me\nu_{nm}}{3he^2} |R^{nm}|^2 \qquad (2.4.4)$$

where m and e are the mass and charge of the electron.

The experimental results are frequently given as oscillator strengths

$$f^{nm} = \frac{mc^2}{\pi e^2 N_m} \int k_\nu \, d\nu \qquad (2.4.5)$$

If a is the fraction of molecules in the initial state, and N_0 is Loschmidt's number, we may write $N_m = aN_0$, and if we also use the substitution

$$\int k_\nu \, d\nu = \frac{10^8}{\lambda^2} \int k_\lambda \, d\lambda \qquad (2.4.6)$$

where λ is the wavelength in angstroms; equation (2.4.5) may be written

$$f^{nm} = \frac{4.203}{\alpha\lambda^2} \int k_\lambda \, d\lambda \qquad (2.4.7)$$

By making use of this result, we can therefore express the observed integrated absorption in terms of the dimensionless quantity f, the oscillator strength, which allows the experimental data to be easily compared with the theoretical predictions.

CHAPTER 3.

Curves of Growth

To make an ideal study of line spectra, the band-pass of the dispersing instrument being used should be very much smaller than the widths of the lines being observed. If this is the case, then the line shapes observed with the instrument will be true shapes. However, in the vacuum ultraviolet region of the spectrum, this is not usually true; that is true line widths are considerably smaller than the band-pass of the dispersing instrument. The conditions under which the experiments for this thesis were performed proved no exception. When this is the case, measurements of the transmission of radiation by a gas show significant departures from Beer's Law (absorption proportional to concentration). This can easily be seen if we consider a strong line which completely extinguishes at the line centre. If this is observed with an instrument whose band-pass is large compared with the line width, some transmission will still be recorded when the instrument is centred on the line centre. This does not give a true measure of the transmission at the particular wavelength, and the way in which the measured transmission departs from Beer's Law is dependent on the relationship between instrument band-pass and line width.

3.1 Equivalent Width

One way of overcoming this difficulty is to experimentally measure a quantity which is not dependent on instrument band-pass; such a quantity is the Equivalent Width of a line. If we consider a single absorption line of, as yet, unspecified shape, the absorption at a particular frequency ν can be written as

$$A_\nu = 1-T_\nu = 1-\exp(-k_\nu a) \qquad (3.1.1)$$

where T_ν is the transmission and k_ν is the absorption coefficient at a frequency ν, and a is the amount of absorbing material. Since the absorption comes from a single line, then the integral of equation (3.1.1.) over all frequencies is finite, and is called the Equivalent Width of the line W. That is

$$W(a) = \int_0^\infty A_\nu \, d\nu = \int_0^\infty [1-\exp(-k_\nu a)]d\nu \qquad (3.1.2)$$

If certain conditions are imposed on an experiment, it is possible to show that the equivalent width is a function which is independent of the instrument resolution function. These conditions, which are usually met in an experiment are:

1. That the instrument used to measure the absorption has a resolution shape function which is independent of the spectral setting of the instrument and represented by the function $\phi(\nu-\nu')$, where the instrument is set at a frequency ν'.

2. That the intensity of the radiation incident on the instrument is constant over the function $\phi(\nu-\nu')$ so that the radiation incident on the absorbing material is determined by the function $\phi(\nu-\nu')$.

Under these conditions, the measured transmission at a frequency ν' is given by

$$T'_{\nu'} = \frac{\int_0^\infty \phi(\nu-\nu')T_\nu \, d\nu}{\int_0^\infty \phi(\nu-\nu') \, d\nu} \qquad (3.1.3)$$

where T_ν is the true transmission at the frequency ν. If the function $\phi(\nu-\nu')$ is chosen such that

$$\int_0^\infty \phi(\nu-\nu')d\nu = \int_0^\infty \phi(\nu-\nu')d\nu' = 1 \qquad (3.1.4)$$

then the equation (3.1.3) may be written as

$$T'_{\nu'} = \int_0^\infty \phi(\nu-\nu')\,T_\nu\,d\nu \qquad (3.1.5)$$

The apparent equivalent width, $W'(a)$, is then given by

$$W'(a) = \int_0^\infty A'_{\nu'}\,d\nu' = \int_0^\infty (1-T'_{\nu'})\,d\nu' \qquad (3.1.6)$$

which, by using equation (3.1.5), may be written

$$W'(a) = \int_0^\infty d\nu'\left[1-\int_0^\infty \phi(\nu-\nu')\,T_\nu\,d\nu\right] \qquad (3.1.7)$$

If the normalisation of the instrument shape function in equation (3.1.4) is now used, we can write

$$W'(a) = \int_0^\infty d\nu'\left[\int_0^\infty \phi(\nu-\nu')\,d\nu - \int_0^\infty \phi(\nu-\nu')\,T_\nu\,d\nu\right]$$

$$= \int_0^\infty d\nu' \int_0^\infty (1-T_\nu)\,\phi(\nu-\nu')\,d\nu$$

$$= \int_0^\infty d\nu' \int_0^\infty A_\nu\,\phi(\nu-\nu')\,d\nu$$

$$= \int_0^\infty d\nu\,A_\nu \int_0^\infty \phi(\nu-\nu')\,d\nu'$$

and again making use of equation (3.1.4) we can write

$$W'(a) = \int_0^\infty A_\nu \, d\nu = W(a) \qquad (3.1.8)$$

Therefore, under the above conditions, which are usually met experimentally, the equivalent width is a quantity which is independent of the instrument resolution.

It can also be seen that $W(a)$ is the width of a completely absorbing rectangular line having the same absorption area as the line under consideration. The way in which the equivalent width $W(a)$ varies with the amount of absorbing material a, is called the Curve of Growth.

3.2 Small Absorption Region

In general, the shape of a curve of growth will depend on the shape function of the absorbing line, but it can be shown (Goody, 1964, Haddad, 1967) that for one particular region, the measured integrated absorption is independent of the line shape. This occurs if $k_\nu a \ll 1$.

If k_ν is written as $S.f(\nu-\nu_0)$, where S is the line strength and $f(\nu-\nu_0)$ defines the absorption line shape and is normalised such that

$$\int_0^\infty f(\nu-\nu_0)d(\nu-\nu_0) = 1 \qquad (3.2.1)$$

then provided that $k_0 a \ll 1$, we can say

$$W(a) = Sa \qquad (3.2.2)$$

(Goody, 1964, Haddad, 1967)

Unfortunately, when $k_0 a \ll 1$, it is difficult to measure $W(a)$ as it is small and it is therefore usually necessary to know the shape of the curve of growth apart from the region where $k_0 a \ll 1$.

3.3 Doppler Lines

The natural profile of a spectral line is Lorentzian (see section 3.4) whose half frequency width at half peak intensity is given by

$$a_N = 1/4\pi\tau \qquad (3.3.1)$$

where τ is the life-time of the excited state of the molecule. However, at the temperatures encountered in the laboratory, the shape of a spectral line is dominated (at low pressures) by its width due to Doppler broadening, and it is not necessary to discuss the curve of growth for natural line shapes.

The line shape resulting from Doppler broadening of a line centred at frequency ν_0 (caused by the thermal motion of the molecules) may be represented by the function (Goody, 1964)

$$f(\nu-\nu_0) = \left(\frac{mc^2}{2\pi kT\nu_0^2}\right)^{\frac{1}{2}} \exp(-mc^2(\nu-\nu_0)^2/2kT\nu_0^2) \quad (3.3.2)$$

where m is the mass of the molecule, T is the absolute temperature and k is Boltzmann's constant. Doppler lines have a width (half width at 1/e peak intensity) given by

$$\alpha_D = \frac{\nu_0}{c}\left(\frac{2kT}{m}\right)^{\frac{1}{2}} \quad (3.3.3)$$

It can be shown that if the shape of a line is completely determined by Doppler broadening, then the equivalent width of the line is given by (Goody, 1964)

$$W = \sqrt{\pi}\,\omega\alpha_D\left[1 + \sum_{n=1}^{\infty}(-1)^n \frac{\omega^n}{n!\sqrt{n}}\right] \quad (3.3.4)$$

$$\text{where} \quad \omega = S_a \Big/ \alpha_D\sqrt{\pi}$$

Goody has developed an asymptotic expansion for large ω given by

$$W = 2\alpha_D(\ell n\omega)^{\frac{1}{2}}\left[1 + \frac{0{\cdot}2886}{\ell n\omega} - \frac{0{\cdot}1335}{(\ell n\omega)^2} + \cdots\right] \quad (3.3.5)$$

Equations (3.3.4) and (3.3.5) then allow us to plot the curve of growth for a line of Doppler profile, and this is shown in figure 3.1. This treatment has been discussed by many authors (e.g. Struve and Elvey, 1934, Van der Held, 1931).

3.4 Pressure Broadening

Under conditions usually met in the laboratory, it is necessary to take pressure broadening effects on the line shape into consideration. The line profile determined solely by pressure broadening (collision effects) is found (Greene, 1957) to be given by the Lorents profile

$$f(\nu-\nu_0) = \frac{1}{\pi} \frac{\alpha_L}{(\nu-\nu_0)^2+\alpha_L^2} \qquad (3.4.1)$$

where α_L is the half width at half peak intensity of the line. The line profile for which a curve of growth is needed is therefore a combined Doppler-Lorents profile. This line is too complex for analytical solution, and numerical methods must be employed (Van der Held, 1931, Yamada, 1968), the final behaviour of W being shown in figure 3.2 where d is equal to $2\frac{\alpha_L}{\alpha_D}$.

In figures 3.1 and 3.2, the linear region occurring

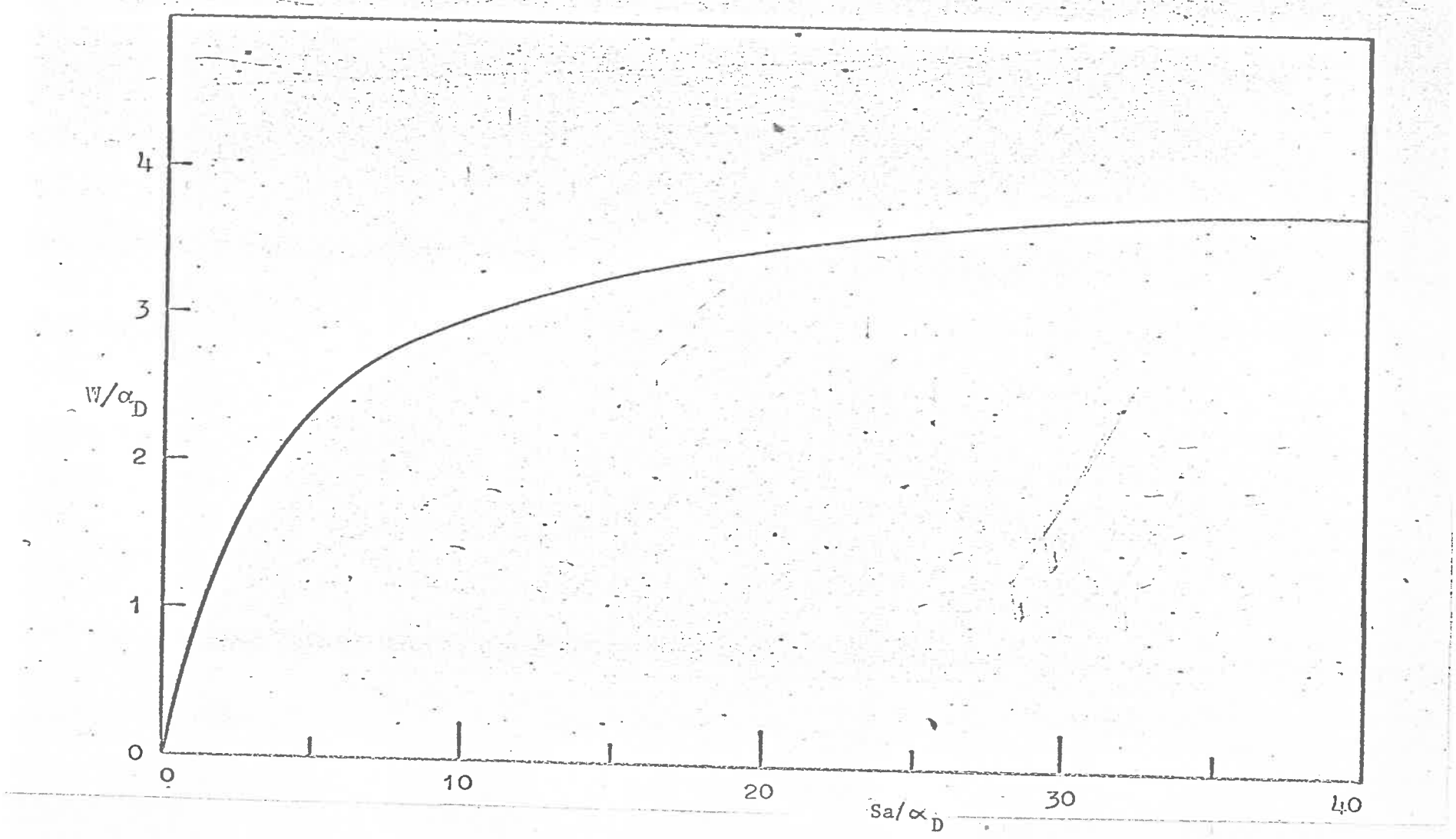

Fig. 3.1 Doppler curve of growth

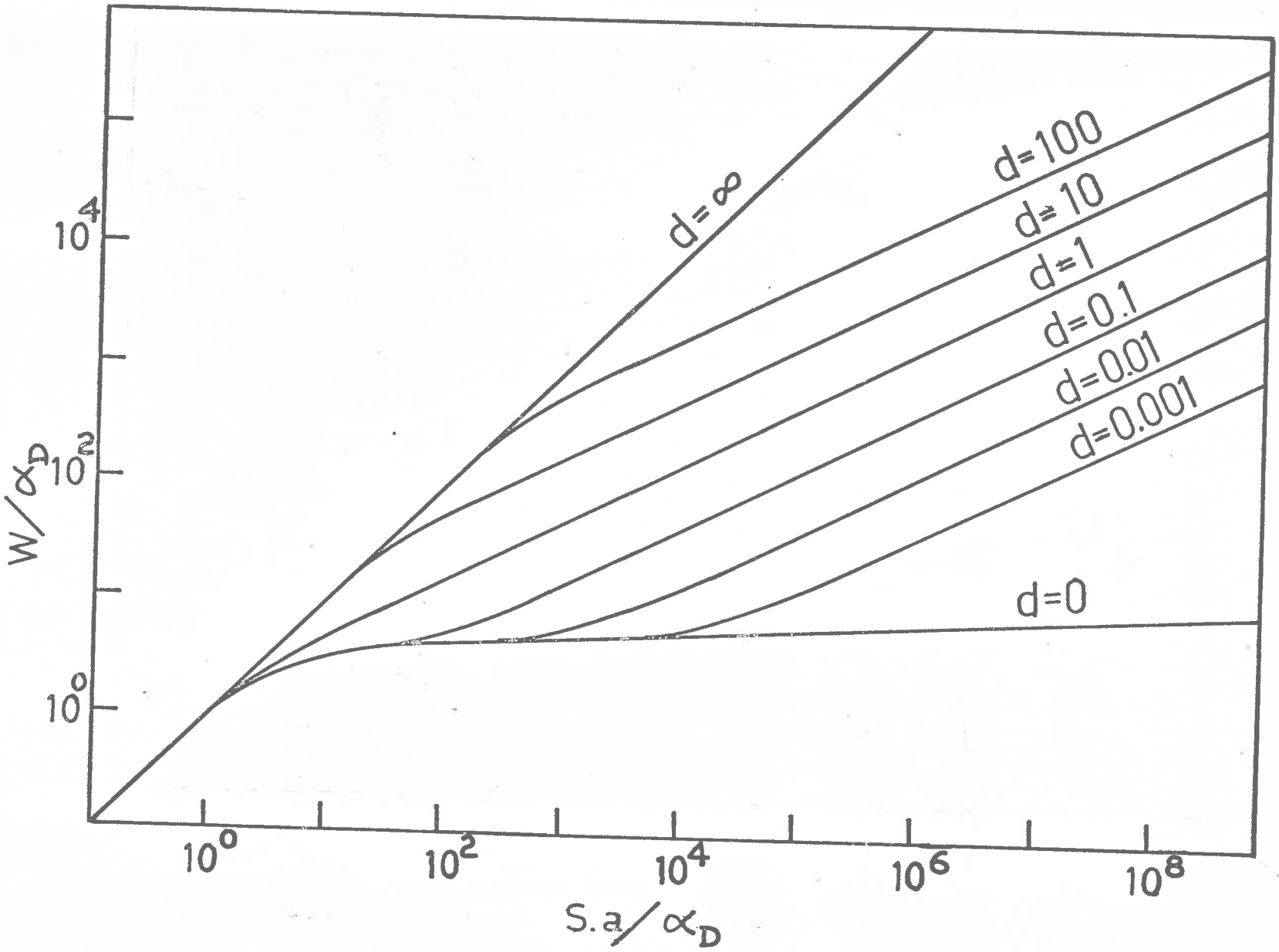

Fig. 3.2 Doppler-Lorentz curve of growth

at low values of absorbing material a, is the region where the small absorption approximation is valid. This approximation is seen to be valid (that is $W(a) \propto a$) until $W(a)$ is approximately equal to the Doppler width of the line.

3.5 Experimental Curves of Growth

Using the experimental system described in chapter 4, the equivalent width of the P_4 line of the (3-0) band in the Lyman system of molecular hydrogen was measured as a function of pressure in the absorption cell, and the resulting curve of growth is presented in figure 3.3. It can be seen that up to pressures $\sim$0·2 torr, the curve is basically that of a Doppler line. This line has been found to have a strength $S = 14$ (atmos.cm.)$^{-1}$ Å (Haddad, 1967) and using the asymptotic expansion (equation 3.3.5), retaining first order terms in $\xi n a$ only, a Doppler width of $a_D = 0{\cdot}0055$Å is obtained. If equation (3.3.3) is converted into wavelength units, one obtains

$$a_D = \frac{\lambda_0}{c}\left(\frac{2kT}{m}\right)^{\frac{1}{2}} \text{ Å} \qquad (3.5.1)$$

and this equation yields a value of 0·00556Å for the Doppler width of a line in the Lyman series of molecular

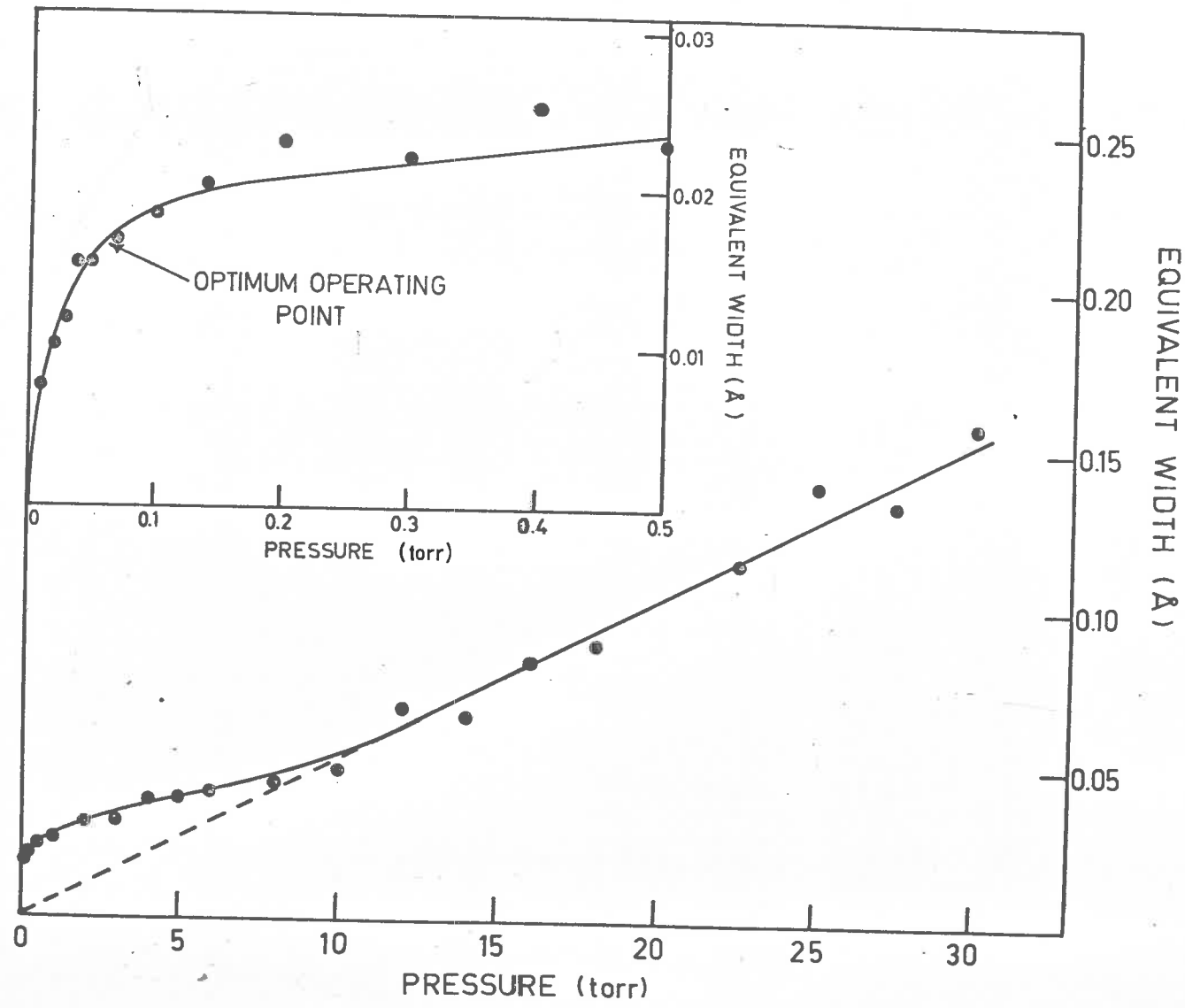

Fig. 3.3 Curve of growth for the P_4 line of the (3-0) band in H_2

hydrogen at 298 °K. Thus the experimental and the theoretical widths are in good agreement. Equivalent widths measured at higher pressures (in the pressure broadened region) were used to calculate a pressure broadening coefficient γ for this line, defined on the assumption that in the pressure broadened region, the width of a line is directly proportional to the pressure. The pressure broadening coefficient is defined as the constant of proportionality, and for this line is given as (Haddad, 1967)

$$\gamma = 6{\cdot}7 \times 10^{-6} \text{ Å/torr} \qquad (3.5.2)$$

In the experiment on molecular oxygen (see chapter 5), the resolution of the instrument was not sufficient to allow the triplet structure of the rotational lines to be resolved. The observed spectra appeared as though there was only a single P and a single R branch present. Because of this resolution effect, the nomenclature "line" will be taken to mean a group of three true lines.

As a preliminary exercise to the molecular oxygen experiment, an attempt was made to measure a curve of growth for an oxygen "line". However, the results of this experiment were not very encouraging; considerable

inconsistency arising in similar measurements made over the same "line", and quite different behaviours of W with pressure were obtained if different "lines" were considered. The reasons for this are probably two-fold. Firstly and more importantly, the "lines" of the Schumann-Runge system were not resolved with the instrument resolution being used (0·2Å - 0·3Å). At the lower pressure end of the curve of growth in particular, this overlapping of "lines", as well as the very bad statistics in this region, made it very difficult to assign a definite area to a given "line". Secondly, the separation of the lines comprising the triplets varies from triplet to triplet; and even within a given triplet, the separation of the lower wavelength pair of lines is not the same as that of the higher wavelength pair (Brix and Herzberg, 1954). As the gas pressure is raised and the lines begin to overlap, significant effects will be noticed in the curve of growth (e.g. as the region between two overlapping lines becomes strong enough to cause extinction of the incident radiation, the slope of the curve of growth will change as there are now only two line "wings" absorbing radiation instead of the original four). However, because of the different line separations involved, these effects will occur at

different pressures for different "lines", and the effects for a single "line" may be masked because there are two different separations involved in one "line". These difficulties caused by line separations will only be significant at high pressures where the pressure broadened width of the lines is of the same order as their separations.

Because of the difficulty experienced in obtaining curves of growth for a single "line" in molecular oxygen, a curve of growth was measured for the majority of the (12 - 0) band, thus allowing more accurate areas to be obtained as the statistical errors were averaged out over the band. The curve of growth obtained in this way is shown in figure 3.4.

The two experimental curves of growth described above for molecular oxygen and hydrogen have been used to determine the range of values of the equivalent width W which best suited the experimental conditions described in chapters 4 and 5. Details of the determining factors in each experiment are given in the appropriate chapters.

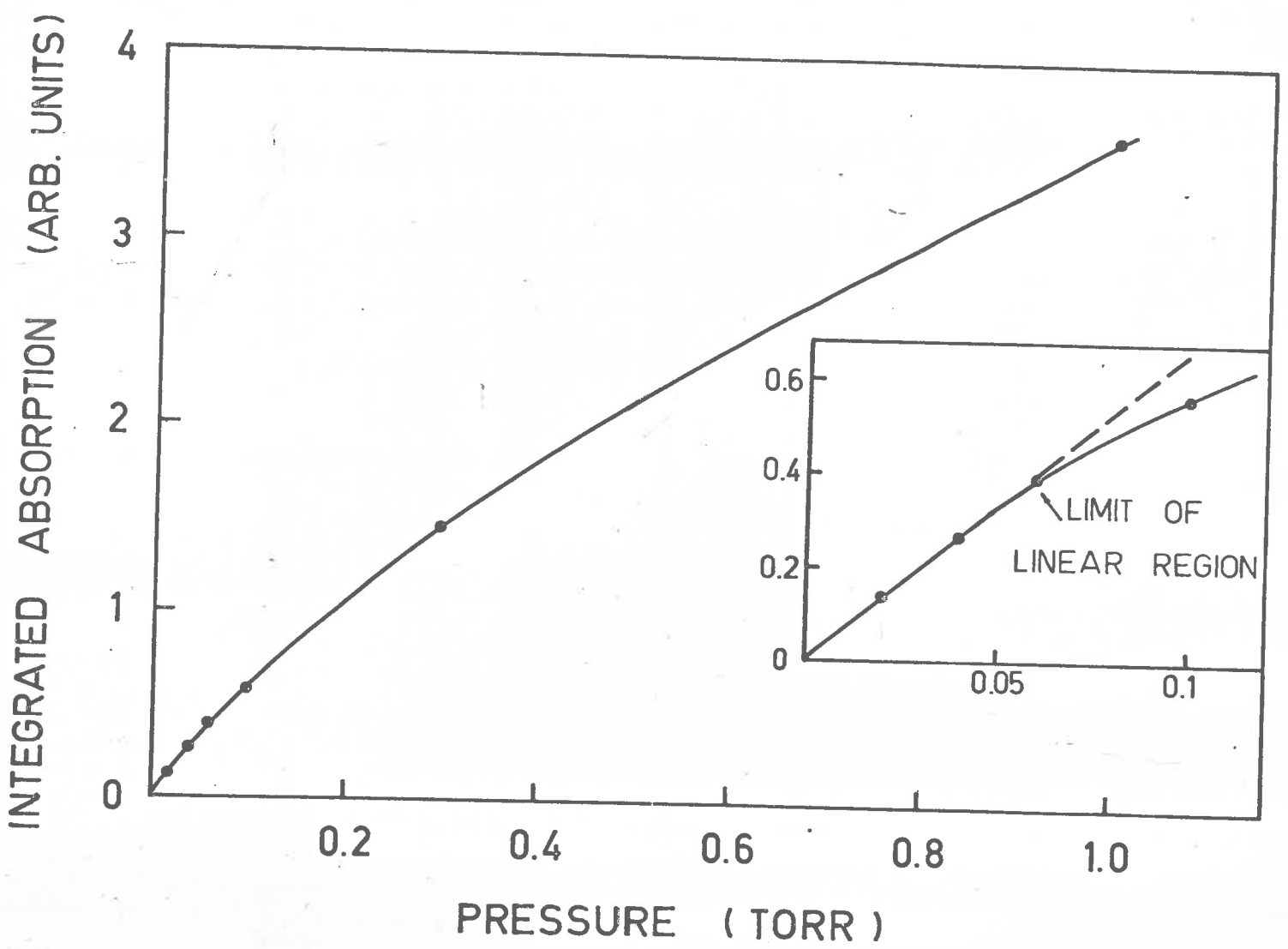

Fig. 3.4 Curve of growth for the majority of the (12-0) band of O_2

CHAPTER 4.

Molecular Hydrogen Absorption

In this chapter are presented the results of an experiment designed to measure the absorption in the Lyman bands of molecular Hydrogen between 1060Å and 1130Å ($B\ ^1\Sigma_u^+ \leftarrow X\ ^1\Sigma_g^+$). This work was carried out using a 1 metre near-normal incidence vacuum ultraviolet monochromator with a resolution of 0·3Å. The equivalent width-curve of growth approach was used in this work, and the basic principles of the method have been presented in the previous chapter. A description of the experimental apparatus is given, and since the low percentage absorptions required by the curve of growth method necessitated the building of a digital data-handling system, this is also described in some detail. The results of the experiment are presented as oscillator strengths for the individual rotational lines, and also as band oscillator strengths. These results and their relation to theoretical quantities are then discussed.

4.1 Previous Measurements

The first experiments performed on molecular hydrogen in the ultraviolet region were by Schumann (1901, 1903), who by using a vacuum spectrograph with fluorite optics was able to observe the spectrum as

far as 1267Å. Later, Lyman was able to extend the range of the spectrum to approximately 500Å (Lyman, 1928) as was discussed in chapter 1. During the development period of vacuum ultraviolet spectroscopy, the band systems of hydrogen in this region were studied by a large number of workers (Werner, 1926, Mori, 1927, Dieke and Hopfield, 1927, Hopfield, 1930, Beutler, 1934, 1935, Beutler et al. 1936, and others) and attempts were made to analyse the observed spectrum.

The first detailed study of the ultraviolet spectrum was carried out by Tanaka (1944) who performed a vibrational and rotational analysis for the Lyman and Werner band systems. Other rotational analyses have since been made on these band systems by Herzberg and Howe (1959), Herzberg and Monfils (1960), Monfils (1961a, 1961b, 1965) and Namioka (1964a, 1964b, 1965) with the result that the line positions and associated spectroscopic constants are now known quite accurately.

Measurements of absolute absorption coefficients were not made until 1952 (Lee and Weissler, 1952) who measured the absorption at about 50 wavelengths in the continuum region. Later absorption measurements have also been made by Bunch et al. (1958), Cook and Metzger

(1964) and Wilkinson and Byram (1965). The latter workers give no details on the observed line strengths.

The obvious lack of absorption coefficients for the band systems of hydrogen occurring at lower wavelengths than 1130Å has therefore been the main reason for performing the present experiment. In this chapter, reference is also made to an experiment performed by Hesser, Brooks and Lawrence (1968), which was completed after the one described in this thesis. Their experiment was designed to measure the absolute oscillator strengths for the part of the Lyman band system occurring below the lithium fluoride cut-off at 1050Å.

4.2 Theoretical Calculations

The hydrogen molecule, because of its extreme simplicity, has been studied by a large number of theorists over the years. As can be imagined, the quantum mechanical calculations for this system have reached a high degree of accuracy, and may be used for comparison with experimental results. Accurate potential energy curves for the two states involved in the Lyman bands ($B\ ^1\Sigma_u^+$ and $X\ ^1\Sigma_g^+$) have been calculated by Kolos and Wolniewicz (1965, 1966, 1968) and various other authors have calculated vibrational and rotational

levels and spectroscopic constants for these states which agree well with the experimental values (Wolniewicz, 1966, Poll and Karl, 1966, Cashion, 1966).

As well as these potential curve calculations, Nicholls (1965b) has calculated the Franck-Condon factors for the Lyman system based on a Morse potential (see section 2.2.2). Nicholls used the vibrational and rotational constants derived by Herzberg and Howe (1959). Franck-Condon factors based on an R.K.R. potential have recently been calculated by Spindler (1966) and Zare (Miller and Krauss, 1967), and these values as tabulated by Nesser, Brooks and Lawrence (1968) were used for theoretical comparisons.

4.3 Experimental Apparatus

The main dispersing instrument used in this experiment was a 1 metre near-normal incidence vacuum ultraviolet scanning monochromator*. This instrument was equipped with a 1200 lines per mm. grating which was blazed at 1200Å and had a dispersion in first order of 8·3Å per mm. The best attainable resolution with this instrument was approximately 0·1Å, although in this

---

* McPherson Model 225

particular experiment this resolution was never used because the narrow entrance and exit slits necessary to achieve it (approximately 10 microns) proved too severe a restriction on the flux available from the instrument. The "wavelength" emerging from the monochromator exit slit was able to be scanned continuously either by hand or by a synchronous motor, the scanning speeds available being variable between 0·25Å per min. and 2000Å per min.

For this experiment, a Hinterreger type discharge lamp was used as a light source. In order to produce continuum radiation in the region of interest, this lamp was operated with Argon at a high pressure (approximately 200 torr) in a condensed discharge mode. Because of the high lamp pressure, it was necessary to use a differential pumping arrangement between the lamp and the monochromator, and this enabled the pressure in the machine to be kept below 10^{-5} torr. However, severe clogging of the entrance slits was experienced (caused by aluminium oxide from the electrodes of the lamp), and the lamp was eventually modified so that it could be operated with a lithium fluoride window between it and the monochromator. With this mode of operation it was necessary to pump the gas away from the lamp with a small mechanical pump.

A schematic of the lamp is shown in figure 4.1.

Figure 4.2 shows a schematic diagram of the experimental system used. The radiation emerging from the exit slit of the monochromator was monitored by a sodium salycilate coated wire grid. When exposed to ultraviolet radiation, sodium salycilate fluoresces in the visible region of the spectrum, and this fluorescent radiation in this case was viewed by an E.M.I. type 9514S photomultiplier tube via a perspex light pipe. All photomultipliers used in this experiment were operated with their cathodes at negative high voltage (approximately -1500V), and electrostatic shields were placed around the tubes and connected to cathode potential. The electrostatic shields helped to decrease the noise levels of the tubes. The photomultipliers were housed in metal light-tight containers which were water cooled to help lower and stabilise their dark currents.

The absorption cell, which was situated immediately after the "beam-splitting" system, consisted of a 60 cm. long, 6" diameter copper tube, sealed at the entrance end by a 3/4" diameter lithium fluoride window. The far end of the cell was sealed by a 4" glass plate coated on the

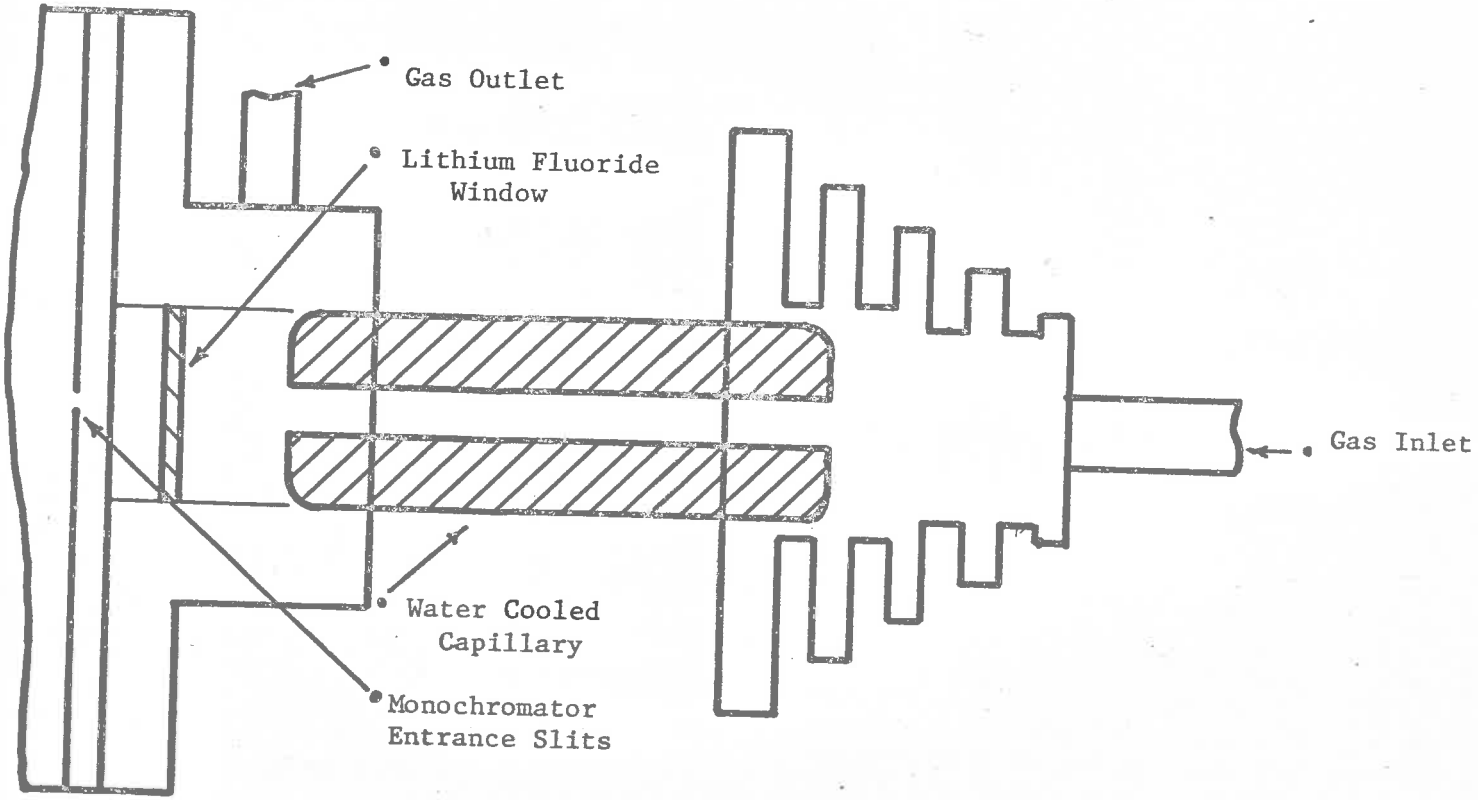

Fig. 4.1 Discharge lamp

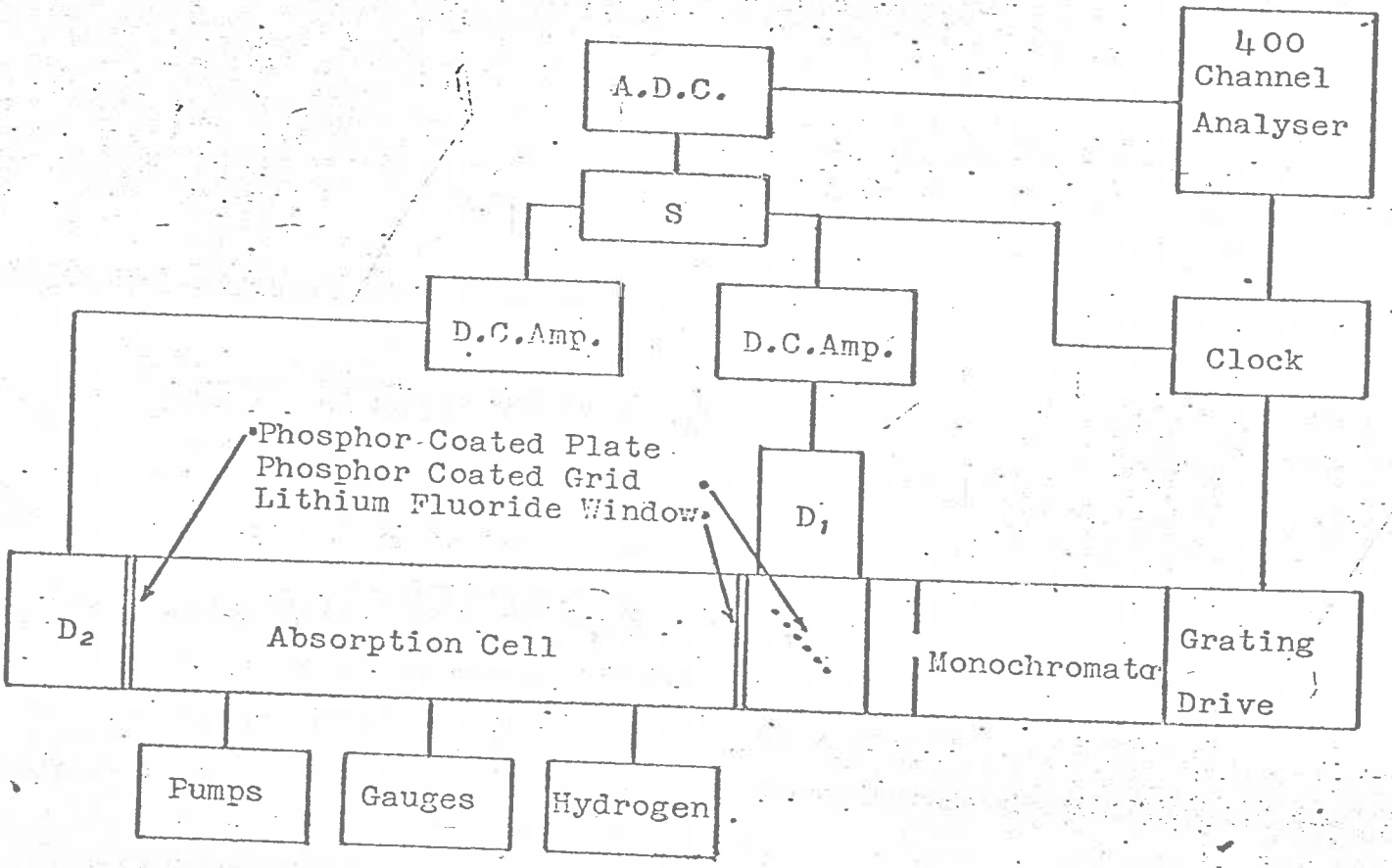

Fig. 4.2 Schematic of molecular hydrogen system

inside with sodium salycilate, and the fluorescent radiation coming from this plate was viewed by another E.M.I. type 95143 photomultiplier. Connected to the cell by means of a gate valve, was a 2" oil diffusion pump and liquid air trap backed by a mechanical pump, and this system enabled the absorption cell to be evacuated to approximately 10^{-5} torr when required. The pressure of the absorbing gas was measured with a differential capacitance manometer*, and the temperature of the gas in the cell was also monitored throughout the experiment.

When absorption measurements were to be made, the cell was isolated from the pumping system and hydrogen was admitted until the required pressure was attained. The hydrogen used was standard commercial grade gas and this was purified by passing it through an array of palladium diffusion tubes which could be heated with a tantalum strip heater. This particular filling technique was very reliable and allowed filling rates of up to 100 litre torr per minute.

4.4 Data-Handling System

As the results of this experiment were to be analysed by the curve of growth method, it was necessary

---

* MKS Barytron type 77H-XR.

to measure quite small amounts of absorption (see chapter 3 and section 4.5), and this required the design and construction of a data-handling system which would allow the statistical fluctuations present in the detector signals to be averaged out. Two main sources of random noise were present in the experiment; the random thermal emission from the photo-cathods of the photomultiplier tubes, and the random fluctuations in the light output from the lamp.

To achieve the averaging process, the photomultipliers signals were fed into an analogue to digital converter (A.D.C.). This A.D.C. was a continuously operating device, and details of the operation and circuits have been given by Haddad (1967). The memory unit used for accumulation of the outputs of the A.D.C. was a 400 channel multichannel analyser* used in time mode which provides the equivalent of 400 scalers which may be addressed sequentially. The signals from the two detectors are fed into two d.c. amplifiers and the analogue output signals from the amplifiers are then switched alternately into the A.D.C., the output of which is then fed into the multi-channel analyser. A

---

* RIDL model 34-12B

synchronous "clock" was built to control the switching of the inputs to the A.D.C. and also to control the channel of the analyser into which the digital signals are being fed. During a normal absorption scan, the sequence of events is as follows; at the same time as the wavelength drive of the monochromator is started, the analogue output of the amplifier on detector 1 is switched to the input of the A.D.C. and the output of the A.D.C. is fed into channel 0 of the analyser. After a given time interval (variable between 1/2000 min. and 2 min.) a pulse from the "clock" switches the output of the amplifier on detector 2 to the input of the A.D.C. and simultaneously switches the A.D.C. output into channel 1 of the analyser. When the same time interval has again elapsed, a "clock" pulse switches detector 1 back to the A.D.C. input and the A.D.C. output into channel 2 of the analyser, and so on until the 400 channels of the analyser have all been addressed. The data stored in the analyser consists, therefore, of two interlaced spectra, one from each detector.

The integration of the photomultiplier signals over the time spent in each channel of the analyser provides a means by which any short period fluctuations may be averaged out (e.g. the thermal fluctuations of the

photomultipliers) and if the above cycle is repeated several times, adding the new data on to the old, for the same wavelength region and same pressure, then the longer period fluctuations may also be averaged out (e.g. the lamp fluctuations). Any long term gain drifts are also averaged out by this process as long as the time taken for a single scan is smaller than the period of the drift. This data-handling system will therefore allow the determination of even very small amounts of absorption, the only requirement being that the spectral region is scanned enough times to make the statistical fluctuations small compared with the absorption being measured. The circuit details of the data-handling system are given in Appendix I.

A system was also designed and built (see Haddad, 1967) which enabled the memory of the analyser to be transferred on to punched cards in a form suitable for analysis by computer.

4.5 Measurements of Absorption

Before the absolute absorption measurements were taken, it was necessary to determine the positions and approximate strengths of all the lines whose absolute strengths were to be measured. The transmission spectra

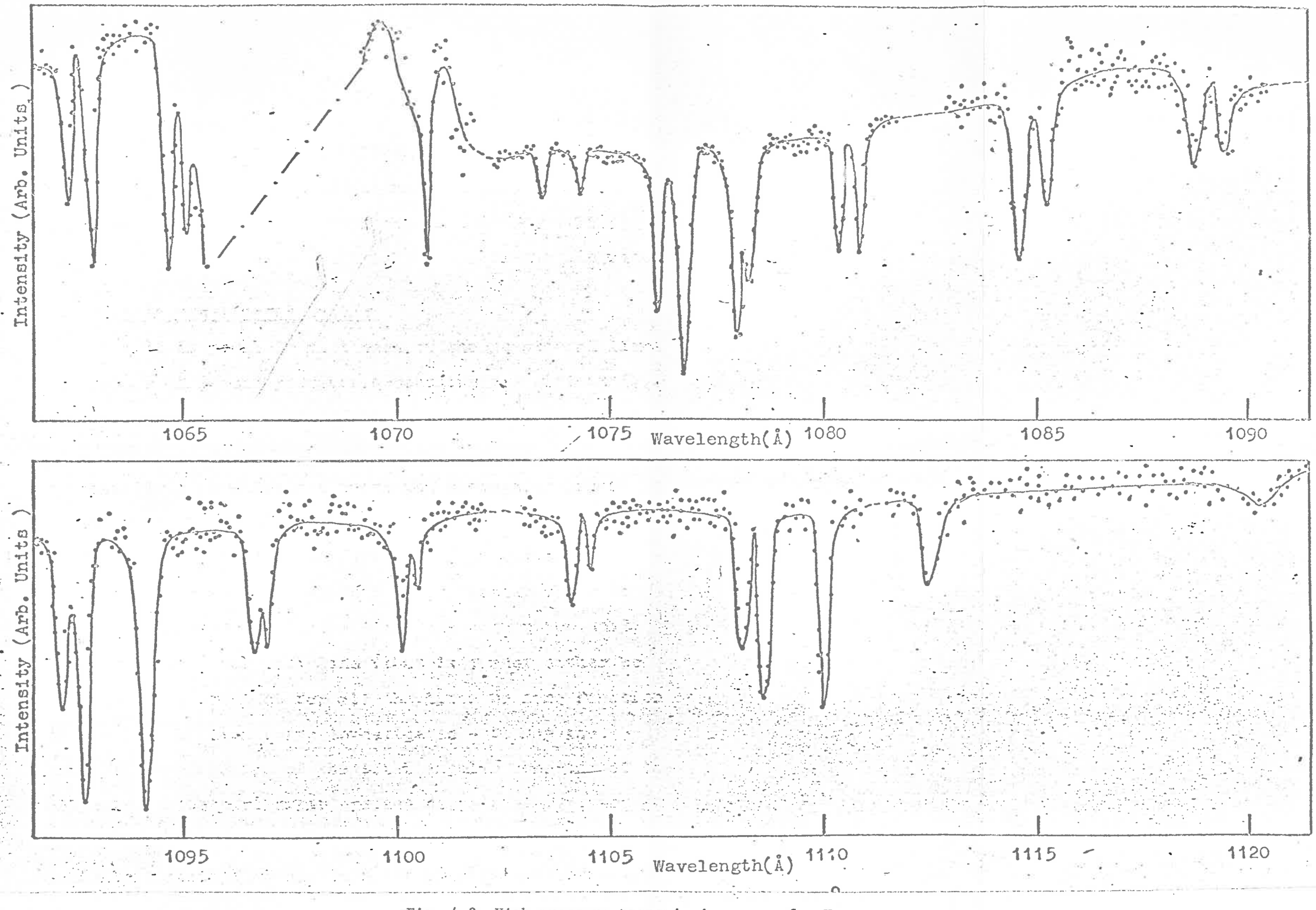

Fig. 4.3 High pressure transmission curve for H_2

used for identification purposes were taken at high gas pressures (up to 30 per cent absorption) with an instrument resolution of approximately 0·2Å, and a typical transmission curve is shown in figure 4.3. To obtain these spectra, a 10Å region of the spectrum was scanned by the monochromator, the detector outputs being stored in all 400 channels of the analyser, with the absorption cell evacuated. This procedure was then repeated with the cell filled to a given pressure of hydrogen, and then repeated again with the cell evacuated to allow for any drifts in gain of the system over the 40 minutes required to record each spectra. The data from each scan was recorded on punched cards and a simple computer program was used to obtain values of absorbance for all the accessible lines in the Lyman series. The wavelength data of Herzberg and Howe (1959) was used to identify the lines observed in the above manner. It was also noticed during the analysis of these "high pressure" spectra that there was no light emmited from the argon discharge lamp in the region 1066Å to 1069Å because of a self-absorption line which occurs in this region.

The spectra from which the absolute line strengths were obtained were recorded in a slightly different way since it was necessary to obtain these spectra using a

very small percentage absorption (see chapter 3 and later in this section). A 5Å region of the spectrum was all that was recorded at the one time. This portion of the spectrum was recorded in the first 200 channels of the analyser with the absorption cell evacuated, and it was then recorded in the last 200 channels with hydrogen in the cell. The cell was then once more evacuated and another spectrum added on to the first 200 channels, filled with hydrogen and a further spectrum added on to the last 200 channels and so on, until the fluctuations in the spectra were reduced to approximately 1/10th. of the peak absorption being measured at the time. Background levels from each detector were recorded in the last 10 channels of each block of 200 channels, and were subtracted from the signal levels in the final analysis.

There are three regions of the curve of growth for a line (chapter 3) where meaningful measurements of the absolute line strength may be made. The first of these is the "pressure broadened region" where the line has essentially a Lorentz shape and the absorption grows linearly with pressure. However, the slope of the curve of growth in this region gives a measure of the quantity $(\gamma S)^{\frac{1}{2}}$ (see Haddad, 1967 and chapter 3) and it is

therefore necessary to make some assumption about the pressure broadening coefficient γ in order to determine a value for S. The second region is the first linear region of the curve of growth where the absorption is independent of the line shape, however, the percentage absorptions which have to be measured to allow the linear approximation to be used are prohibitively small to enable this technique to be of any use in this particular experiment. (This region of the curve of growth was used in the experiment on molecular oxygen). The third region, that used in this experiment, requires a knowledge of the curve of growth for a line. If the curve of growth for a line is known, it is theoretically possible to obtain the true strength of the line from this curve. In particular, if the pressure at which the absorption is measured is such that the line shape will be predominantly Doppler, then figure 3.1 may be used to find the strength of the line. The values of W, the equivalent width of the line, are all either measured experimentally or able to be calculated, and therefore, the only unknown is S, the strength of the line, which may then be obtained from the graph. The most obvious portion of the curve in figure 3.1 to use for actual measurements is where the curve is changing most rapidly,

and therefore, it was decided to take all the absorption measurements at pressures so that W/α_D was approximately equal to 3. This is seen to be a compromise between a value of W/α_D which gives an average absorption too small to be measured accurately, and a value which lies in the region where a small error in the measured equivalent width can give a large error in the line strength.

Within a given band, the observed line strength for each individual rotational transition is proportional to the fraction (see section 2.3)

$$\frac{Y_{J''}\,(J'+J''+1)\,\exp\left[-J''(J''+1)B''hc/kT\right]}{\sum_{J'} Y_{J''}(J'+J''+1)\,\exp\left[-J''(J''+1)B''hc/kT\right]} \qquad (4.5.1)$$

where J'' and J' refer to the initial and final states respectively, B'' is the rotational constant for the initial state and $Y_{J''}$ is a factor dependent on the nuclear spin which gives rise in molecular hydrogen to the ortho and para varieties of the molecule. The value of $Y_{J''}$ was taken as 3 for odd J'' and 1 for even J'' (Herzberg 1950). This fraction, as was mentioned in section 2.3, takes into consideration the statistical weight of the initial state, and also the dependence on the final state of the transition.

In those cases where two non-overlapping lines

were not resolved because of the instrument resolution (e.g. most of the (0 - 0) band), the measured equivalent width for the combination was distributed between the two lines according to the fraction (4.5.1) for the appropriate transitions. It was also found that the R_1 lines in the (2 - 0) and (3 - 0) bands were so strong that it was not possible to obtain W/α_D equal to 3 even with the smallest layer thicknesses available for this experiment. The strengths of these lines were obtained by using the high pressure data which was used for line identification, and by comparing the lines with those produced by other similar transitions. These high pressure estimates of line strengths are not as accurate as the other measurements and are also rather higher than expected from the theoretical distribution. The values obtained for these two lines were therefore omitted in the final analysis of band oscillator strengths.

Figure 4.4 shows the measured line strengths for the lines of the (0 - 0), (1 - 0), (2 - 0) and (3 - 0) bands in the Lyman system of molecular hydrogen. The distribution of line intensities within a given band was calculated from equation (4.5.1) using $B'' = 59.303\ cm^{-1}$ (Hersberg 1950). This is shown in figure 4.5 where the R_1 line has been omitted and the

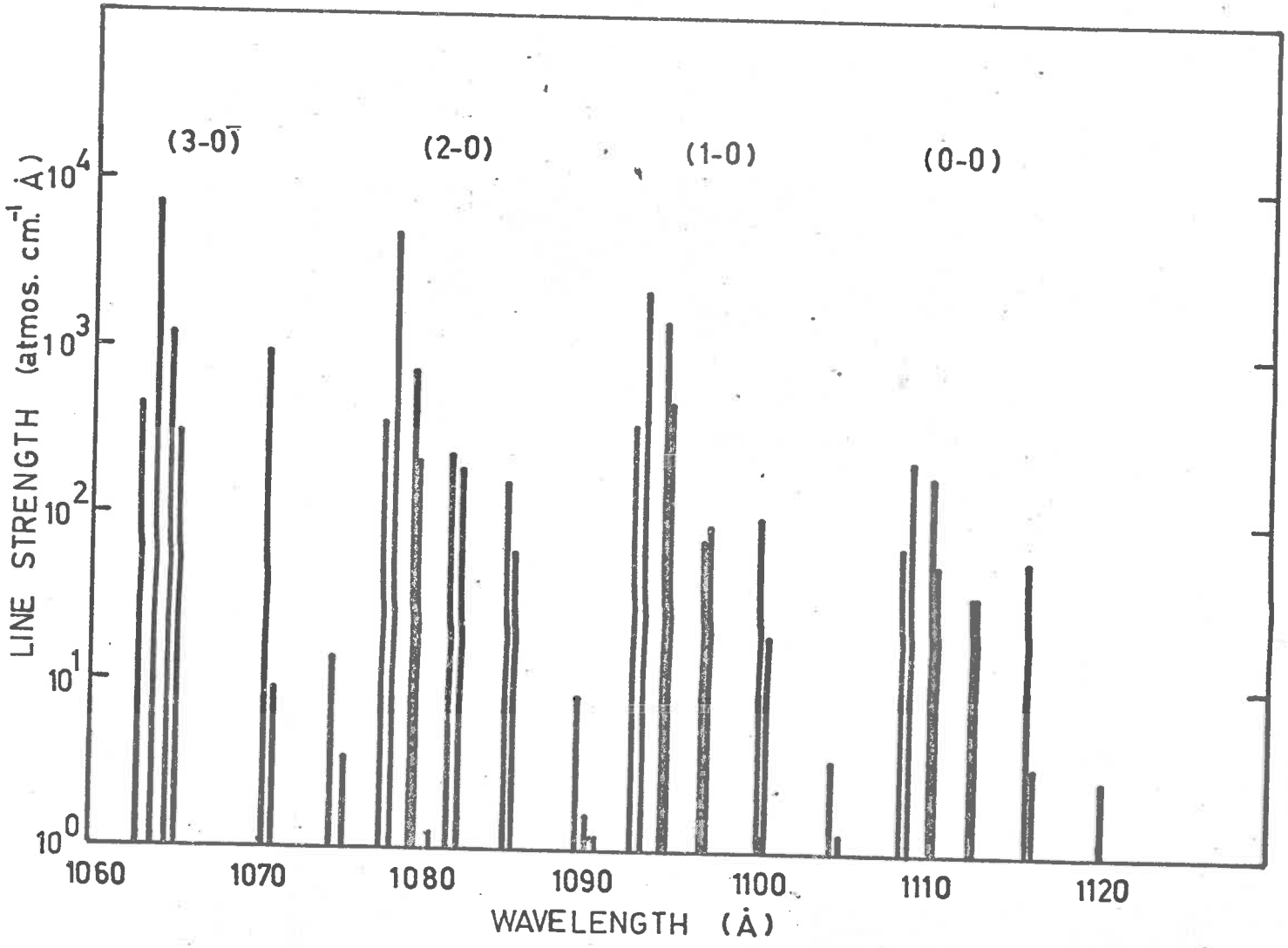

Fig. 4.4 Line strengths for the four bands of H_2

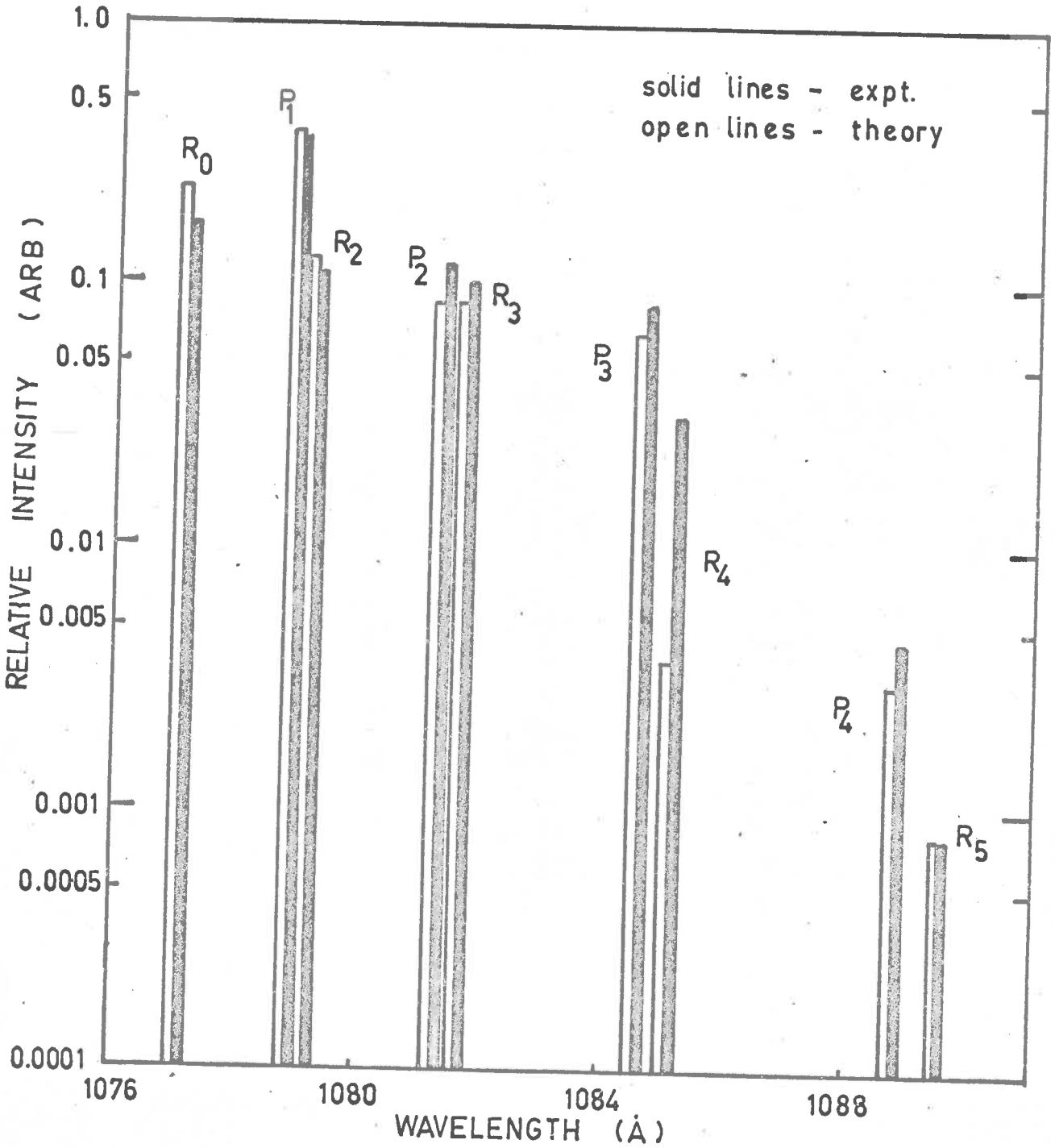

Fig. 4.5 Rotational distribution for the (2-0) band

remaining band strength has been normalised to have the value unity.

Figure 4.5 also contains the observed intensity distribution of the lines in the (2 - 0) band, where once again, the R_4 line has been omitted and the total band strength has been normalised as before. The agreement between the observed and expected values is seen to be good except for the R_4 line. A statistical analysis on the errors involved for each line was carried out (see section 4.8) and the probability that the observed value for the R_4 line is a good measurement was seen to be very small (see section 4.8). A similar comparison for lines in the (0 - 0) and (1 - 0) bands showed that all the lines agree, within the errors, with their expected values, and if the high pressure estimate of the R_4 line in the (3 - 0) band is omitted, the distribution for this band also agrees with the expected values.

4.6 Line Oscillator Strengths

Using equation (2.4.7), it is possible to express the measured line strengths $S = \int k_\lambda d\lambda$ in terms of the oscillator strengths for the transitions. Thus we may write

$$f = 4{\cdot}203\ S/a\lambda^2 \qquad (4.6.1)$$

where

f is the oscillator strength for the line,

S is the measured line strength,

λ is the wavelength of the transition, and

a is the fraction of molecules in a particular initial state. The population of the rotational levels in the ground vibrational-electronic level was assumed to be that given by the Boltzman distribution with a modification caused by the spin of the nuclei. It was assumed that the gas was at 25 °C and that the nuclear spin factors were given by (Herzberg, 1950)

$$g_J = \begin{cases} 3(2J+1) \text{ for odd } J \\ (2J+1) \text{ for even } J \end{cases} \qquad (4.6.2)$$

The values of a calculated in this manner are given in Table 4.1 for the first 6 rotational levels of the ground state.

TABLE 4.1

J	g_J	a
0	1	0·132
1	9	0·662
2	5	0·115
3	21	0·086
4	9	0·004
5	33	0·001

Using these values of α, the measured line strengths were used to calculate oscillator strengths for all the measured lines, and these values are given in Table 4.2. It is estimated that the statistical errors on the oscillator strengths are ± 50 per cent.

TABLE 4.2

Oscillator Strengths for some Rotational Lines in the Absorption Spectrum of Molecular Hydrogen

Band	Line	Wavelength (Å)	Strength	$fx10^3$
(0-0)	R_0	1108.130	67.7	1.75
	R_1	1108.636	228.8	1.18
	R_2	1110.126	53.0	1.57
	R_3	1112.598	35.8	1.41
	R_4	1116.048	3.25	2.75
	P_1	1110.066	169.5	0.88
	P_2	1112.502	33.9	1.00
	P_3	1115.911	58.0	2.27
	P_4	1120.238	2.8	2.34
(1-0)	R_0	1092.196	361	9.63
	R_1	1092.732	2167	11.51
	R_2	1094.294	464.4	14.17
	R_3	1096.729	91	3.69
	R_4	1100.182	20	17.36
	R_5	1104.596	0.58	2.00
	P_1	1094.054	1470.6	7.80
	P_2	1096.443	76	2.31
	P_3	1099.798	101	4.08
	P_4	1104.111	3.4	2.93

Table 4.2 (cont.)

Band	Line	Wavelength (Å)	Strength	fx10³
(2-0)	R_0	1077.136	348	9.55
	R_1	1077.687	4943*	27.02
	R_2	1079.200	220.6	6.92
	R_3	1081.672	197	8.22
	R_4	1085.094	61.4**	54.8
	R_5	1089.458	1.6	5.67
	P_1	1078.928	712.1	3.88
	P_2	1081.267	235	7.34
	P_3	1084.559	157	6.51
	P_4	1088.797	8.4	7.44
(3-0)	R_0	1062.871	437	12.3
	R_1	1063.422	7000*	39.3
	R_2	1064.917	310	9.98
	R_3	1067.350	-	-
	R_4	1070.712	9	8.24
	R_5	1074.989	3.48	12.65
	P_1	1064.607	1192	6.67
	P_2	1066.892	-	-
	P_3	1070.113	91	3.88
	P_4	1074.261	14	12.74

* high pressure estimates

** see section 4.8

4.7 Astrophysical Applications

It has been suggested (Haddad, 1967) that electronic transitions of the type studied in this thesis are useful for performing a quantitative study of the distribution, abundance and physical condition of molecular hydrogen in interstellar space. Any experiments to do this must obviously be performed from rockets or satellites, and two such programmes have been suggested (Varsarsky, 1966, Rogerson, 1963). An investigation of the spectrum of a typical B2 star (Morton, 1965) has shown that the best wavelength region for observing interstellar absorption is from 1090Å to 1105Å, which is the region occupied by the (1 - 0) band in the Lyman series of molecular hydrogen.

Haddad (1967) has calculated the equivalent widths expected for the lines of the (1 - 0) band on the basis of the oscillator strengths presented in Table 4.2. These calculations have been carried out for molecular hydrogen concentrations of 10^{19}, 10^{18}, 10^{17}, 10^{16} molecules per cm^2, and gas temperatures of 75 °K, 100 °K and 125 °K, and predict that an instrument having a resolution of up to 1·5Å would be able to detect the absorption. Haddad (1967) has also shown that if a high resolution instrument (~0·1Å) is used to measure the quantity

$$\frac{W_{P_3} + W_{R_4}}{W_{(1-0)}}$$

where W_{P_3}, W_{R_4} and $W_{(1-0)}$ are the equivalent widths of the P_3, R_4 lines and the (1 - 0) band, then this quantity changes by a factor of 5 over the temperature range 75 °K to 125 °K for a molecular hydrogen concentration of 10^{21} molecules per cm^2. A measure of this quantity would therefore provide an estimate of the temperature of the interstellar gas.

4.8 Band Oscillator Strengths

The oscillator strengths for the individual rotational lines presented in section 4.6 may be written as

$$f = f_e . f_v . f_r \qquad (4.8.1)$$

where f_e is a term involving the electronic transition moment and the transition energy. The factors f_v are the Franck-Condon factors for the transition (see section 2.3) and the rotational factors f_r are determined by the degeneracies of the rotational levels involved and may be written as (Hersberg 1950)

$$f_r = \frac{J'' + 1}{2J'' + 1} \quad \text{R Branch}$$

$$= \frac{J''}{2J'' + 1} \quad \text{P Branch} \qquad (4.8.2)$$

The product $f_e f_v$ is normally called the band oscillator strength.

If the line oscillator strengths from table 4.2 are used in conjunction with the f_r values (equation 4.8.2), then it will be seen that 9 or 10 independent estimates of the oscillator strength for each band may be obtained. As mentioned in section 4.5, the high pressure estimates of the R_4 lines in the (2 - 0) and (3 - 0) bands have been omitted from further calculations. When the independent measurements for each band are averaged and a root mean square deviation for the observed points is calculated, then it is seen that the agreement between the individual values and the mean is consistent within the limits of the statistical errors for the (0 - 0), (1 - 0) and (3 - 0) bands. For these three bands, the final value for the band oscillator strength is therefore given as the mean of the independent measurements with the appropriate statistical error. The one band where the agreement was not close, was the (2 - 0) band.

For the (2 - 0) band, if we include the R_4 line, the mean value for $f_e f_v$ is 24.7 with an R.M.S. deviation of 26. The value obtained from just the R_4 line is seen to be 98.6 which is nearly 3 standard

deviations from the mean and, as such, is a very doubtful measurement. If the R_4 line is omitted in the calculation of the mean, a value of 13.5 is obtained having an R.M.S. deviation of 3.0, and on the basis of these figures, the value from the R_4 line lies further than 25 standard deviations from the mean. Because of the reason given above, it was assumed that the measurement of the R_4 line was in error and it has been omitted from further calculations. No definite experimental reason for this large discrepancy has been found but it is quite possible that the lamp intensity changed on one of the scans across the R_4 line. This effect had been noticed several times during the experiment and was caused by material sputtered from the electrodes of the lamp adhering to the monochromator slits.

The values of the band oscillator strengths obtained by the above method are given in column 2 of Table 4.3. The errors quoted are the most probable errors for the mean obtained from the standard deviations. This error was found to agree well with the expected error calculated from the statistical fluctuations on the raw data, the errors involved in the pressure measurements being negligible.

TABLE 4.3

Band Oscillator Strengths

Band	Present Results (expt)	Geiger and Topschowsky ±25% (expt)	Dalgarno and Allison ±20% (theor)
0-0	0.0033 ± 0.0002	0.0018	0.0016
1-0	0.014 ± 0.002	0.0071	0.0057
2-0	0.014 ± 0.001	0.014	0.011
3-0	0.018 ± 0.002	0.017	0.017

The values presented in column 3 of table 4.3 are those obtained from the electron scattering experiment of Geiger and Topschowsky (Hesser et al 1968) and tabulated by Dalgarno and Allison (1968). The error estimate of ±25% placed on these results is that given by Hesser et al (1968). Column 4 of table 4.3 shows the theoretical values for band oscillator strengths presented by Dalgarno and Allison (1968). These values are expected to be more accurate than the previous "constant dipole moment" calculations (Nicholls 1965b, Spindler 1966). The present results are seen to be consistent with these other experimental and theoretical values for the (2 - 0) and (3 - 0) bands, but differ by a factor of 2 for the (0 - 0) and (1 - 0) bands.

It is interesting to note that if several lines in the (0 - 0) and (1 - 0) bands are omitted from the calculations (e.g. the P_3, R_3, P_4 lines in the (0 - 0) band), the average band oscillator strength is found to agree well with the other measurements. However, there seems to be no justification for omitting these measurements, as the line strengths are statistically in agreement with the theoretical distribution, and no experimental reason can be found for not using them. It is pleasing to find the agreement for the (2 - 0) and (3 - 0) bands but in view of the above discussion, it seems to be necessary to repeat the experiment in order to obtain better estimates of the band oscillator strengths. This experiment is planned for this laboratory together with a measurement of higher bands in the Lyman series.

It should be noted that the values obtained for band oscillator strengths in this thesis differ considerably from those obtained from the same basic data and presented by Haddad et al (1968). The values given by Haddad were obtained by numerically integrating line strengths over each band and not by calculating individual line oscillator strengths. The method used by Haddad did not make obvious the rather high values

obtained for some individual lines and also severely weighted the final answer in favour of the strong lines near the band heads. It is therefore felt that the analysis of the data in this thesis presents more accurate values for band oscillator strengths than those previously published.

CHAPTER 5.

Molecular Oxygen Absorption

Molecular oxygen becomes a strong absorber of ultraviolet radiation below 2000Å, the spectral region 1700Å to 2000Å being occupied by the Schumann-Runge band system which then develops into the strongly absorbing Schumann-Runge continuum which reaches a maximum at approximately 1425Å. This thesis presents oscillator strengths for the Schumann-Runge band system, (2 - 0) to (20 - 0) bands, obtained using low pressures of oxygen and an equivalent width method of analysis.

The $B\ ^3\Sigma_u^- \leftarrow X\ ^3\Sigma_g^-$ transition in molecular oxygen give rise to the Schumann-Runge system and for absorption at room temperature, only the transitions from the lowest vibrational level in the ground state need be considered. Both the initial and final states in this transition are triplet states, and the combination would normally give rise to three P branches and three R branches of similar intensities, and six weak satellite branches (Herzberg, 1950). However, molecular oxygen has zero nuclear spin, and every alternate triplet in each branch is missing.

5.1 Previous Measurements

The first observations of the Schumann-Runge band system were made by Schumann (Schumann, 1903) who

observed a strongly absorbing band structure from 2000Å to 1850Å with his vacuum spectrograph employing fluorspar optics. The rotational structure of the band system was resolved by Curry and Herzberg (1934) and Knauss and Ballard (1935) and subsequent rotational analyses were carried out by these workers. Watanabe, Inn and Zelikoff (1953) measured absorption coefficients between 1050Å and 1900Å using photoelectric detection methods, and Brix and Herzberg (1954) with much better resolution and lower pressures of oxygen than previous workers resolved the triplet splitting and extended the rotational analysis to the (21 - 0) band.

Using photographic techniques and moderate resolution, Ditchburn and Heddle (1953, 1954) calculated oscillator strengths from their measured absorption coefficients using an analysis which took account of line widths and instrument resolution. Band intensities have also been measured by Wilkinson and Mulliken (1957) who found pre-dissociation broadening occurring at the (12 - 0) band. Bethke (1959) made use of line broadening to overcome the problem of instrument resolution. He pressure broadened the rotational lines with argon, and measured integrated absorption intensities for each band. The pre-dissociation observed by Wilkinson and

Mulliken (1957) has been re-investigated by Carroll (1959) and Heddle (1960), both experimenters finding pre-dissociation occurring at much lower vibrational quantum numbers. Measurements of absorption coefficients in the Schumann-Runge continuum have also been made by several workers (e.g. Metzger and Cook, 1964, and Goldstein and Mastrup, 1966). Previous measurements have been carried out at Adelaide on the Schumann-Runge and other systems in molecular oxygen but these have been limited to oxygen layer thicknesses likely to be encountered in the upper atmosphere (Haddad, 1967, Blake et al. 1966).

The present measurements were made with an instrument resolution of 0·3Å which allowed a majority of the rotational structure to be resolved, and under conditions of small attenuation (2·4 per cent at the line centres). The measured integrated absorption under these conditions gave a direct measure of the absorption coefficients (see chapter 3).

5.2 Experimental Arrangement

The apparatus used for this experiment was basically the same as that used in the experiment on molecular hydrogen (see section 4.3). Once again, the 1 metre

vacuum ultraviolet scanning monochromator, the same absorption cell and the photomultipliers were used. A schematic of the experimental system is shown in figure 5.1.

The light source used for this experiment was again of the Hinterreger type, but was operated without a window between the lamp and the monochromator. This was possible because the gas pressure in the lamp was only 5-10 torr, and the pumping speed of the monochromator vacuum system was sufficient to enable the machine pressure to be kept below 10^{-5} torr under operating conditions. To produce a continuum radiation in the region of interest (1700Å - 2000Å) the lamp was operated at pressure of approximately 5 torr of hydrogen, and a 13KV, 50 cps. A.C. voltage was applied across the electrodes. As was the case in the molecular hydrogen experiment, it was not practicable to operate the monochromator at its best attainable resolution (0.1Å) because of the limited flux available from the lamp, and for this experiment, the resolution used was 0.3Å.

For the experiment, medical grade oxygen was purified by passing it through a thimble trap immersed in a freezing mixture of chloroform and carbon tetrachloride (frozen with liquid air) and then admitted to the cell

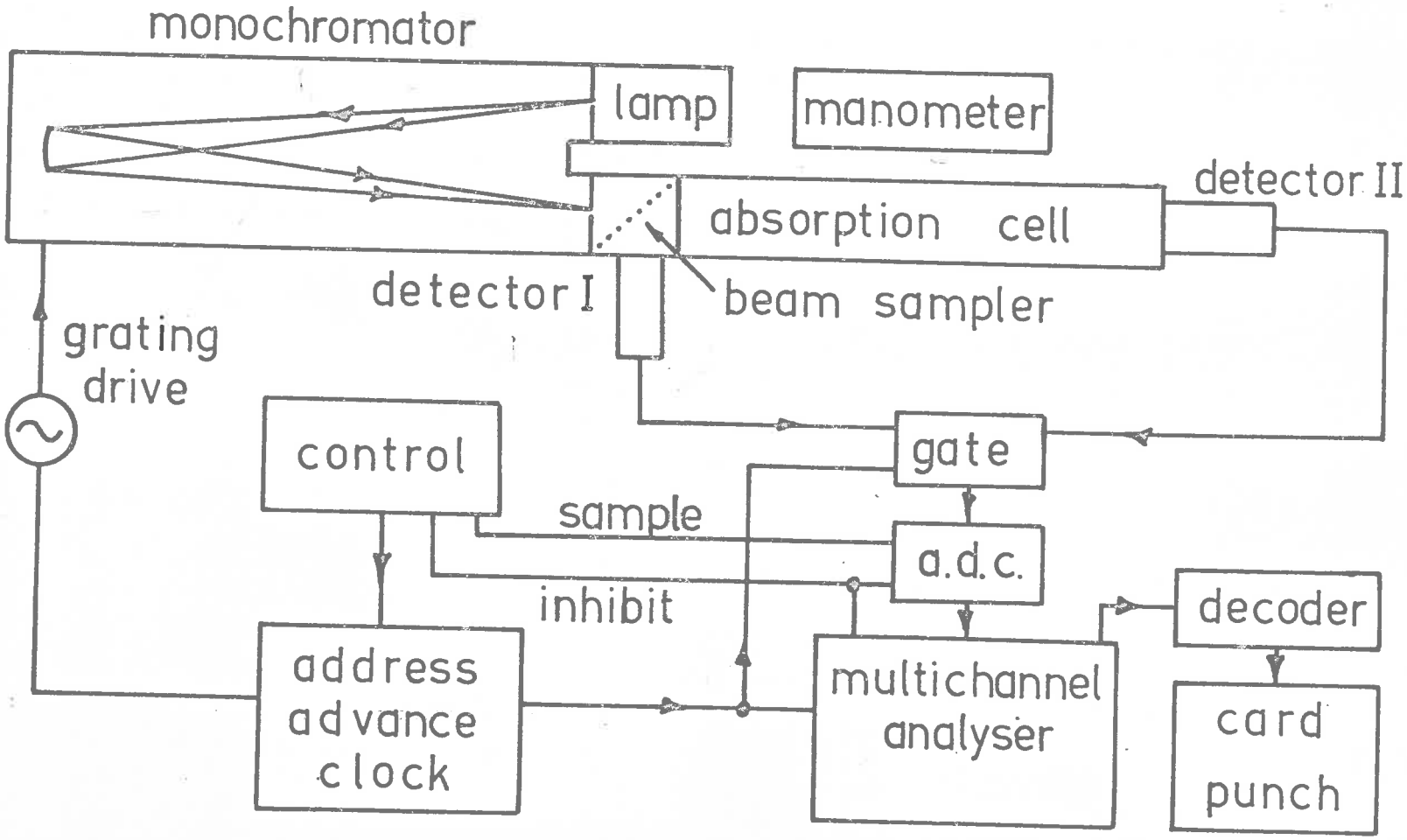

Fig. 5.1 Schematic of the experimental system

by means of a needle valve. The gas pressure in the cell was again measured with the differential capacitance manometer, and the accuracy of the pressure measurements is discussed in section 5.6.

The ease of repeatability of a given set of experimental conditions with the system described above was extremely useful for the multiple scanning technique used in the experiment (see section 5.4).

5.3 Data Recording

In view of the low attenuations to be measured, (see section 5.4) the logic of the data recording system used in this experiment was similar to that used in the molecular hydrogen experiment and described in section 4.4. That is, the analogue signals from the detectors are converted to digital form and fed into the appropriate channels of a 400 channel multi-channel analyser controlled by an "address-advance" clock synchronous with the 50 c.p.s. mains voltage. However, in the new system the two Hewlett-Packard D.C. amplifiers and the "home-made" analogue to digital converter were replaced by a commercial integrating digital voltmeter (Dynamco Model DM 2006) and all the associated electronics were designed around integrated circuits

instead of discrete components. This had the advantage of considerably improving the stability of the system (the digital voltmeter is stable to within 0·02 per cent per month), making the maintenance easier and saving space. The analogue signals from the detectors were switched alternately to the input of the digital voltmeter which sampled the input 50/3 times per second, taking a 50 m.secs. per sample, on command from the control unit. Provision was made for four analogue inputs to be switched to the digital voltmeter, and also for four digital inputs to be fed via the control unit into the multichannel analyser. Figure 5.1 gives a block diagram of the circuits and a detailed circuit is shown in Appendix II.

As mentioned in section 4.4, the main reason for using the digital system was to allow multiple scanning of wavelength regions in order to average the fluctuations in the output record. These fluctuations were again present for this experiment with magnitude comparable to the attenuation being measured, and therefore, in general, multiple scanning was used. The unit described in section 4.4 for transferring the contents of the memory of the analyser to punch cards was again used for this experiment.

5.4 Procedure

It was intended that the technique for this experiment would be similar to that described in section 4.5, that is to obtain a curve of growth for a single line and use this to interpret the results for the other lines. Several attempts were made to obtain a curve of growth for "lines" (actually triplets as discussed in section 3.5) in molecular oxygen, but these were unsuccessful. Reasons for this have been given in section 3.5.

It was shown in section 3.2 that the relationship between W(a), the experimental integrated absorption, and a, the amount of absorbing material, is linear until W(a) is approximately equal to the actual width of the absorbing line. For small values of the absorbing material a, the actual width of a line is dominated by the Doppler width of the line which is given by equation (3.5.1). Applying this equation to molecular oxygen at room temperature (293 ^{o}K), a Doppler width of $a_D \approx 0.0023$Å was obtained for the wavelength range of interest.

This means, therefore, that the linear relationship between W(a) and a will only be a true statement of fact

if a is kept small enough so that W(a) is less than 0·0023Å. As mentioned previously (section 5.1), the best attainable resolution of the monochromator was 0·3Å because of the limited flux available from the light source. If the instrument resolution shape is assumed to be triangular, with a full width at half maximum of 0·3Å, then the peak absorption of a single line must be kept less than 0·0023/0·3≈0·8 per cent, if the above linear relationship is to remain true. However, with an instrument resolution of 0·3Å, it is not possible to resolve the triplet structure of the rotational lines in the Schumann-Runge band system. These lines are sufficiently separated from each other so as not to overlap to any great extent at low pressures, and the measured absorption from a "line" may therefore be considered as the sum of the absorption from three individual lines. When this is taken into account, the requirement for a linear relationship between W(a) and a now becomes

$$W(a) \leq 0{\cdot}0023\text{Å} \times 3 = 0{\cdot}0069\text{Å} \qquad (5.4.1)$$

and this allows a maximum peak absorption for a "line" of 2·4 per cent.

As a check on the validity of this assumption, the integrated absorption of the majority of the (12 - 0) band was measured as a function of the pressure in the cell. The results have been plotted in figure 3.4, and the point labelled "limit of linear region" corresponds to the pressure at which the absorption from the strongest "line" first exceeded 2·4 per cent. The requirement that the peak absorption for a "line" must be less than 2·4 per cent for linearity between W(a) and a to be true thus seems to be a valid criterion.

The approximate positions and relative intensities of the "lines" in the (2 - 0) through to (20 - 0) bands of the Schumann-Runge system were obtained from absorption measurements made at relatively high pressures of oxygen (0·2 - 200 torr) producing peak absorptions of 10 - 15 per cent when an instrument resolution of 0·2Å was used. With this relatively large absorption, the fluctuations of the detector outputs, caused primarily by lamp fluctuations and noise levels in the detectors, were of no real significance and it was not necessary to use multiple scanning to obtain accurate results. The spectra for this part of the experiment were recorded in all 400 channels of the analyser (the last 10 channels

being used to record the background count of the detectors) representing a 10Å region of the spectrum. Also, as this was only a preliminary investigation of the bands, spectra with the absorption cell evacuated, to check the gains of the system, were not recorded. The data taken in the above manner was analysed very crudely and used to provide estimates of the pressures needed in the absorption cell to produce peak absorptions ≤ 2·4 per cent for the main absorption measurement. An example of the transmission data obtained in this way is shown in figure 5.2.

The main absorption measurements were taken with an instrument resolution of 0·3Å and the pressure in the absorption cell was varied between 0·06 and 60 torr depending on the strength of the line being measured. The multichannel analyser was used as two sets of 200 scalers, the data obtained for a given wavelength region with the cell evacuated being stored in one half of the memory, and that obtained for the same wavelength region with the cell containing oxygen in the other half. The last ten channels of each set of 200 were used to record the background count rates for the two detectors, and in the final analysis, these values were subtracted from the appropriate channels.

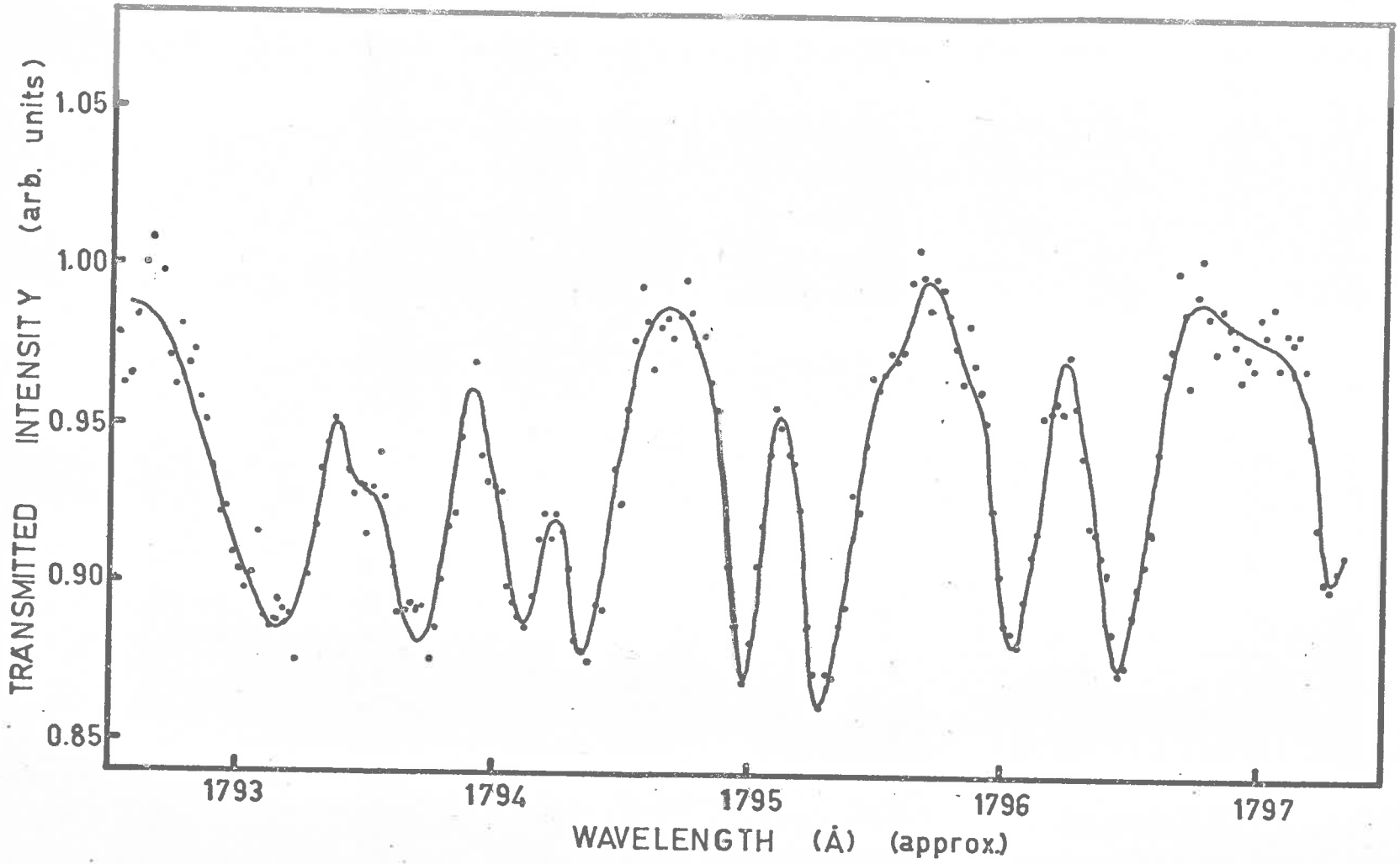

Fig. 5.2 High pressure transmission curve for O_2

Each set of 200 channels represented a 5Å wavelength region and successive scans over the region were added to each other in the sequence cell full, cell evacuated, cell full, etc. until the statistical fluctuations in the record were less than 0·2 per cent. Each individual scan took approximately ten minutes to complete and it was usually necessary to scan a given 5Å region for periods of 3 - 5 hours in order to reduce the fluctuations to the required level. The contents of the analyser memory were then transferred on to punch cards and the analysis was carried out by computer.

5.5 Discussion

Values for the transmission were obtained every 1/20Å by taking the ratio of the two detectors when the cell was full (allowing for background counts) and dividing it by the average value of this ratio when the cell was evacuated. Equations (3.1.2) and (3.2.2) were then used to calculate absorption coefficients (as seen by an instrument resolution of 0·3Å) from this transmission data and the absorption cell pressure. These results are plotted in figure 5.3.

The wavelength data obtained by Brix and Herzberg (1954) and Knauss and Ballard (1935) was used to

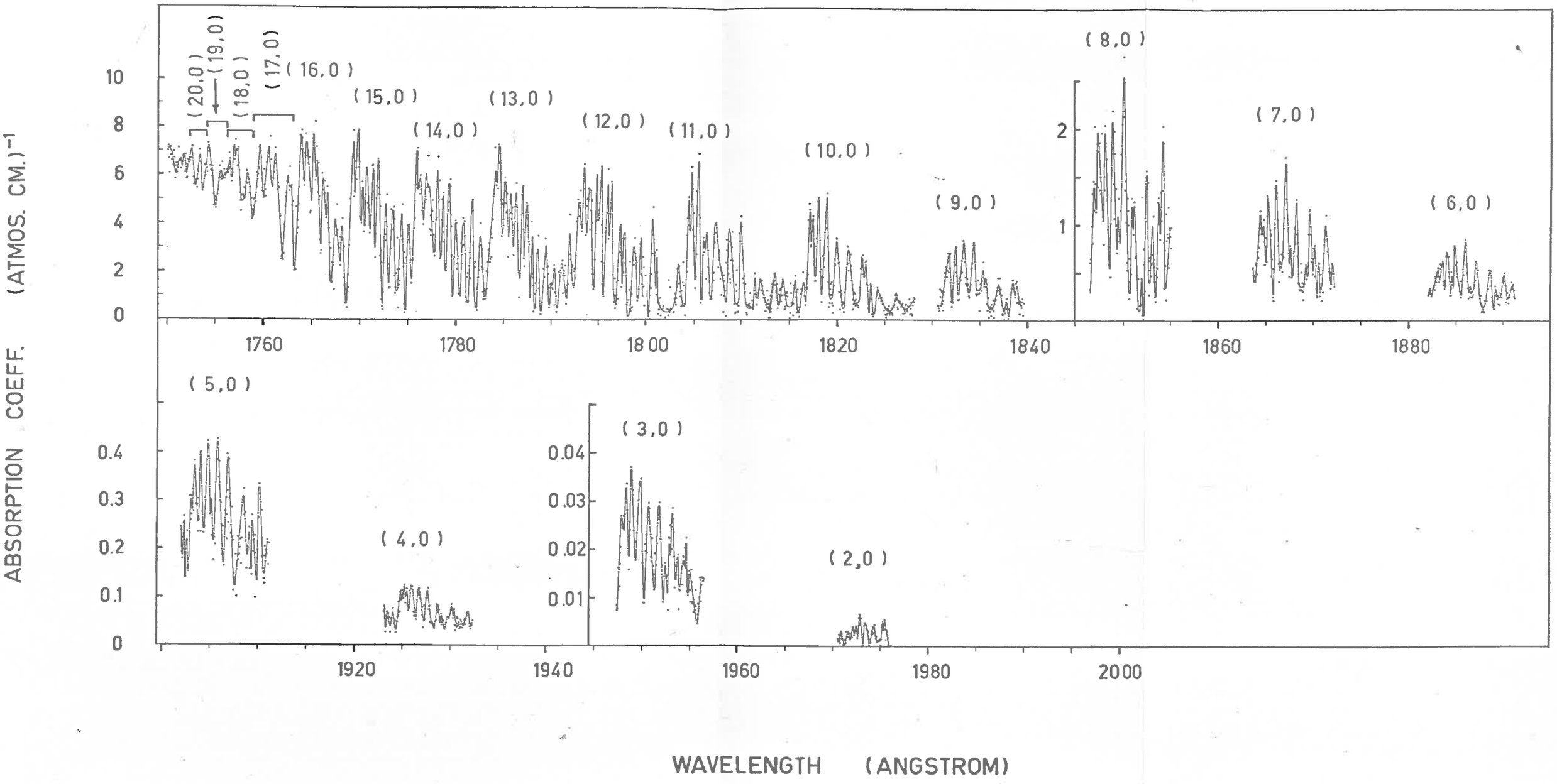

Fig. 5.3 Absorption coefficients for molecular oxygen

identify the observed rotational lines and to determine the wavelength range covered by each band. This was a necessary procedure as the wavelength scale on the monochromator was not absolute. The band strengths were obtained by integrating the absorption coefficients for each band from the band head to the last observed transition.

The total strength of a band is distributed between the rotational lines according to the statistical weights of the initial states of the transitions - that is the line strengths in this case are proportional to the fraction (Herzberg, 1950)

$$\frac{(K'+K''+1)\exp[-K''(K''+1)B''hc/kT]}{\sum_{K''}\left\{(K'+K''+1)\exp[-K''(K''+1)B''hc/kT]\right\}} \qquad (5.5.1)$$

where K' and K'' are the total angular momentums without spin of the initial and final states respectively, B'' is the rotational constant for the initial state and k is the Boltzman's constant.

Since equation (5.5.1) was used to correct the observed portions of some of the bands for the unobserved lines, the experimentally observed distribution of line strengths for the major part of the (12 - 0)

band was compared with that predicted by equation (5.5.1). This distribution of intensities was calculated for a temperature of 293 °K with a value for $B'' = 1{\cdot}43777\ cm^{-1}$ (Herzberg, 1950) and is shown in figure 5.4. The areas of the rectangles represent the theoretical line strengths for the lines shown and their total area is normalised to be equal to the measured integrated strength of the band up to and including the P_{15} line.

It can be seen from figure 5.3 that the observed sections of the bands (2 - 0) through to (8 - 0) do not overlap each other. The weakest band for which data was recorded was the (2 - 0) band, and in this band the weakest transition observed (for the remaining transitions the cross-section was too small to permit economical measurement) was the R_{11} "line". The range of integration for this band therefore covered 61 per cent of the total (2 - 0) band. For the bands (3 - 0) through to (8 - 0), the last observed transition was the P_{15} "line", and the range of integration therefore covered approximately 88 per cent of the bands. The integrated strengths for these bands were corrected for the unobserved portions using equation (5.5.1).

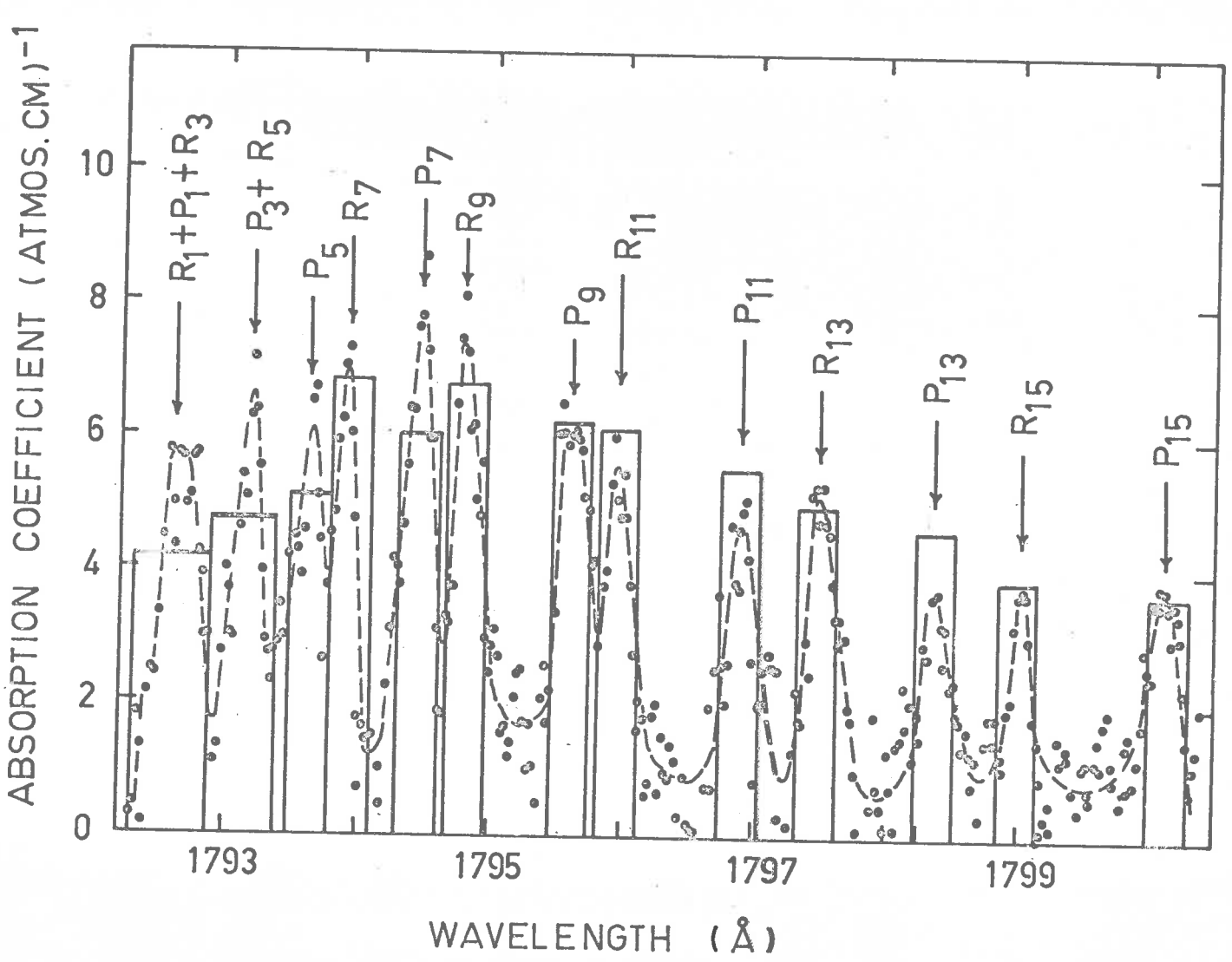

Fig. 5.4 Rotational distribution for the (12-0) band of O_2 .

The remaining bands, (9 - 0) through to (20 - 0) overlap each other, and a slightly different procedure was necessary for these bands. For the bands (9 - 0) to (16 - 0) the measured integrated strengths from band head to next band head provide a good measurement of the total band strength since the area lost by an incomplete integration (approximately 10 per cent of the total area) is gained from the overlap of the neighbouring band. This is an allowable approximation as the band strengths in this region do not change rapidly. The remaining bands, (17 - 0) through to (20 - 0) have a much greater degree of overlap, and although the same basic procedure outlined above is used for determining band strengths, a much larger uncertainty is placed on the assignment of individual band strengths. The integrated band strengths are given in Table 5.1 for the observed region of the band system. The standard deviation for each individual measurement is also given in Table 5.1.

Pre-dissociation occurring at the (12 - 0) band was observed by Wilkinson and Mulliken (1957) and also by Bethke (1959), which the former workers attribute to a $^3\Pi_u$ state intersecting the left limb of the potential curve for the B $^3\Sigma_u^-$ state. This pre-dissociation

TABLE 5.1

Band	Integrated Intensity $\int k(atm.cm^{-1})$	Band	Integrated Intensity $\int k(atm.cm^{-1})$
2-0	0·025 ± 0·001	12-0	27·6 ± 1·7
3-0	0·140 ± 0·006	13-0	27·8 ± 1·7
4-0	0·63 ± 0·03	14-0	27·8 ± 1·7
5-0	2·43 ± 0·10	15-0	28·2 ± 1·7
6-0	3·73 ± 0·15	16-0	24·6 ± 2·0
7-0	6·78 ± 0·27	17-0	23·4 ± 2·3
8-0	9·95 ± 0·40	17-0	15·0 ± 3·8
9-0	12·0 ± 0·5	19-0	12·9 ± 3·2
10-0	16·2 ± 0·7	20-0	9·9 ± 3·0
11-0	21·4 ± 1·3		

was also studied by Carroll (1959) who found strong pre-dissociation at the (4 - 0) band and possibly weak pre-dissociation at the (12 - 0) band, and Heddle (1960) who found evidence of pre-dissociation occurring at the (3 - 0) band. Carroll (1959) postulated several states which may account for his measurements, one of which was similar to that proposed by Wilkinson and Mulliken (1957). Most of the observations of pre-dissociation have relied on the apparent intensity increase, because of more diffuse lines (Herzberg, 1950), which occurs for the bands at which pre-dissociation takes place. This type of reasoning is not applicable to the present set of measurements since they have all been obtained with very small oxygen pressures (layer thicknesses) and thus fall into the "linear region of the curve of growth" where the measured absorption is independent of the line profile, as long as the line width is small compared to the instrument resolution. As would be expected, therefore, no apparent intensity increase was noticed for any bands in the present set of results, and it was therefore not possible to obtain any information regarding pre-dissociation.

5.6 Sources of Error

For the complete band system the estimated standard

deviations of the integrated band strengths were ± 4 per cent, and this is the only source of error for the bands (2 - 0) through to (10 - 0). For the remaining bands the pressure in the absorption cell was lower (0.06 torr) and the uncertainty in the pressure measurements was up to ± 4 per cent, thus increasing the total standard deviations. The bands (17 - 0) to (20 - 0) have a much larger deviation (±20 - 30 per cent) and this was a result of the severe overlap of the bands mentioned in section 5.5.

5.7 Oscillator Strengths

As was pointed out in section 2.4, it is common practice to present the measured absolute band absorption coefficients in terms of band oscillator strengths $f_{v'v''}$ by means of the equation

$$f_{v'v''} = \frac{4.203}{\alpha\lambda^2} \int_{band} k_\lambda d\lambda$$

where $\int_{band} k_\lambda d\lambda$ is the measured integrated absorption coefficient.

The absorption coefficients presented in section 5.5 were measured at room temperature and so α, the fraction of molecules in the initial state can be

taken as unity since almost all the molecules will be in the v = o vibrational level of the ground state. The oscillator strengths obtained for the (2 - 0) to (20 - 0) vibrational bands are presented in Table 5.2.

Prior to the present results, there have been only 3 publications giving oscillator strengths for the Schumann-Runge system. These were made by Ditchburn and Heddle (1954), Bethke (1959) and Halmann (1966).

Ditchburn and Heddle, using photographic techniques and a moderate resolution instrument, measured absorption coefficients for the (0 - 0) to (20 - 0) bands of the Schumann-Runge system and then used an analysis which took account of line widths and instrument resolution to obtain oscillator strengths for these transitions. The oscillator strengths they obtained are given in Table 5.2. Bethke (1959), used the results of Ditchburn and Heddle to calculate a value for $f_{e\ell}$, the electronic absorption oscillator strength for the transition, and obtained values which were about 30 times larger than expected from theoretical considerations.

Bethke subsequently made measurements on the band system using a vacuum ultraviolet grating spectrometer with a resolution of 0.4Å. The technique

TABLE 5.2

Band	Oscillator Strength (present results)	Oscillator Strength (Bethke)	Oscillator Strength (Fitchburn and Neddle)
2-0	$2 \cdot 69 \cdot 10^{-8}$	$2 \cdot 3 \cdot 10^{-8}$	$1 \cdot 18 \cdot 10^{-6}$
3-0	$1 \cdot 54 \cdot 10^{-7}$	$7 \cdot 4 \cdot 10^{-8}$	$8 \cdot 35 \cdot 10^{-6}$
4-0	$7 \cdot 11 \cdot 10^{-7}$	$2 \cdot 74 \cdot 10^{-7}$	$2 \cdot 76 \cdot 10^{-5}$
5-0	$2 \cdot 80 \cdot 10^{-6}$	$7 \cdot 28 \cdot 10^{-7}$	$6 \cdot 65 \cdot 10^{-5}$
6-0	$4 \cdot 40 \cdot 10^{-6}$	$1 \cdot 73 \cdot 10^{-6}$	$1 \cdot 37 \cdot 10^{-4}$
7-0	$8 \cdot 15 \cdot 10^{-6}$	$3 \cdot 56 \cdot 10^{-6}$	$3 \cdot 53 \cdot 10^{-4}$
8-0	$1 \cdot 22 \cdot 10^{-5}$	$6 \cdot 75 \cdot 10^{-6}$	$5 \cdot 94 \cdot 10^{-4}$
9-0	$1 \cdot 50 \cdot 10^{-5}$	$1 \cdot 07 \cdot 10^{-5}$	$6 \cdot 40 \cdot 10^{-4}$
10-0	$2 \cdot 05 \cdot 10^{-5}$	$1 \cdot 56 \cdot 10^{-5}$	$9 \cdot 45 \cdot 10^{-4}$
11-0	$2 \cdot 74 \cdot 10^{-5}$	$2 \cdot 16 \cdot 10^{-5}$	$1 \cdot 44 \cdot 10^{-3}$
12-0	$3 \cdot 58 \cdot 10^{-5}$	$2 \cdot 81 \cdot 10^{-5}$	$1 \cdot 31 \cdot 10^{-3}$
13-0	$3 \cdot 66 \cdot 10^{-5}$	$3 \cdot 17 \cdot 10^{-5}$	$4 \cdot 04 \cdot 10^{-4}$
14-0	$3 \cdot 69 \cdot 10^{-5}$	$3 \cdot 24 \cdot 10^{-5}$	$8 \cdot 42 \cdot 10^{-4}$
15-0	$3 \cdot 77 \cdot 10^{-5}$	$3 \cdot 26 \cdot 10^{-5}$	$2 \cdot 79 \cdot 10^{-3}$
16-0	$3 \cdot 31 \cdot 10^{-5}$	$3 \cdot 16 \cdot 10^{-5}$	$5 \cdot 55 \cdot 10^{-3}$
17-0	$3 \cdot 16 \cdot 10^{-5}$	$2 \cdot 94 \cdot 10^{-5}$	$6 \cdot 63 \cdot 10^{-3}$
18-0	$2 \cdot 03 \cdot 10^{-5}$		$6 \cdot 93 \cdot 10^{-3}$
19-0	$1 \cdot 74 \cdot 10^{-5}$		$7 \cdot 58 \cdot 10^{-3}$
20-0	$1 \cdot 35 \cdot 10^{-5}$		$8 \cdot 25 \cdot 10^{-3}$

he used was exactly the opposite of the equivalent width approach used in the present work. He pressure broadened the oxygen with argon to such an extent that the rotational structure of the bands was smoothed out, thus making his instrument resolution small compared with the width of the bands. This procedure allowed him to obtain band integrated absorption coefficients. The oxygen partial pressures used by Bethke were very large compared with the pressures used in the present work - for the weak bands, he found it necessary to raise the oxygen partial pressure above one atmosphere. The values obtained by Bethke are presented in Table 5.2 and these can be seen to be about 100 times less than those published by Ditchburn and Heddle (1954).

The present results are seen to agree with those of Bethke much better than with Ditchburn and Heddle although on closer investigation there is seen to be a factor of 2 or 3 discrepancy between the two sets of results, particularly for the (3 - 0) - (8 - 0) bands.

The (2 - 0) to (8 - 0) bands of the present results did not overlap each other and consequently their analysis was carried out slightly differently from the remaining bands (see section 5.5). This was first considered as a possible reason for the discrepancy.

However, the types of errors which may have appeared in the analysis would only produce, at most, a 15 per cent correction to the final answer and this is not large enough to bring the two sets of results into agreement. Other possible sources of errors in the present results have been discussed in section 5.6 but again, the possible corrections occurring from them do not resolve the discrepancy.

Since Bethke's (1959) results were obtained at very high pressures, distortion effects on the molecules because of this may have had an influence on the results. Bethke's analysis technique used extrapolation procedures to eliminate effects of charge distortion and formation of "O_4 molecules" and there appears to be no reason to doubt the validity of this approach. However, the present results obtained without the uncertainty of high pressure effects should provide a more certain estimate of the band oscillator strengths.

While experimenting with isotope effects for the oxygen molecule, Halmann (1966) measured oscillator strengths for the Schumann-Runge bands using an experimental arrangement and analysis technique identical to Bethke (1959). The results obtained agree well with those of Bethke within the experimental errors but

this measurement does not make the present results less valid as the same possible sources of error can be found in Halmann's (1966) high pressure measurements as in those of Bethke (1959).

Other measurements of absorption coefficients for the $v'' = o$ transitions of the Schumann-Runge bands have been made by Watanabe et al (1958) and Blake et al (1966) but in both these experiments, the resolution was not sufficient to allow the rotational structure to be resolved and oscillator strengths can not be calculated from them. The absorption coefficients so obtained are very dependent on the pressure at which they were measured, and the instrument resolution used. Because of this, no direct comparison can be made with the present results.

Trenoar and Wurster (1960) have used shock-tube techniques to measure absorption coefficients for the higher v'' bands and vibrational transition probability measurements for these higher bands have also been measured by Hébert and Nicholls (1961) in emission. These two sets of results are not directly comparable to the present oscillator strengths but their relationship to these will be discussed in Chapter 6.

CHAPTER 6.

The Electronic Transition Moment

In this chapter, the theory used in deriving values for the electronic transition moment from the experimental oscillator strengths is developed, and the way in which the r-centroid approach can be used to study the variation of the electronic transition moment with internuclear distance is shown. To be able to use this approach it is necessary to have accurate Franck-Condon factors for the transitions of the molecule in question, and this in turn requires accurate potential-energy curves. Therefore, the development of various potential curves and the Franck-Condon factors derived from them is discussed with particular reference to the oxygen molecule. The formulae derived in the early portion of this chapter are then used to obtain absolute values for the variation of the electronic transition moment with internuclear distance.

6.1 Theory of Electronic Transition Moments

To be able to use the oscillator strengths obtained in the previous chapter as a tool for studying the electronic transition moment, it is necessary to find a relationship between these two quantities. For a diatomic molecule with degenerate states, equation (2.4.4) may be written (Herzberg, 1950) for absorption as

$$f_{v'v''} = \frac{8\pi^2 m c \nu_{v'v''}}{3he^2} |R^{v'v''}|^2 \qquad (6.1.1)$$

where $f_{v'v''}$ is the oscillator strength for the transition $v'' \rightarrow v'$

$|R^{v'v''}|^2$ is the transition probability summed over the degenerate levels,

$\nu_{v'v''}$ is the wave-number of the transition,

d is the degeneracy of the state involved,

m is the electron mass,

e is the electronic charge, and

c is the velocity of light in a vacuum.

Equation (6.1.1) may then be written (Herzberg, 1950, section 2.4) as

$$f_{v'v''} = \frac{8\pi^2 m c \nu_{v'v''}}{3he^2 d} |\psi_{v'} Re(r) \psi_{v''} dr|^2 \qquad (6.1.2)$$

where $\psi_{v'}$ and $\psi_{v''}$ are the wave-functions of the upper and lower vibrational levels respectively, and the electronic transition moment

$$R_e(r) = \int \psi_{e'}^* M \psi_{e''} dr_e \qquad (6.1.3)$$

where $\psi_{e'}$ and $\psi_{e''}$ are the electronic wave-functions of the two states, dr_e is the element of configuration space of the electrons, M is the part of the electric moment

depending on the electrons and r is the internuclear separation.

Until recently, the approximation applied to equation (6.1.2) was to assume that $R_e(r)$ had almost no dependence on r, and to extract an average value of $R_e(r)$. This approach leads to the equation

$$f_{v'v''} = \frac{8\pi^2 m\sigma\nu v'v''}{3he^2 d} |\overline{R_e(r)}|^2 |\int \psi_{v'}\psi_{v''} dr|^2 \qquad (6.1.4)$$

This approximation now allows the use of the Franck-Condon factors

$$q_{v'v''} = |\int \psi_{v'}\psi_{v''} dr|^2 = (v',v'')^2 \qquad (6.1.5)$$

and establishes a relationship between the experimental oscillator strengths $f_{v'v''}$ and the theoretical Franck-Condon factors $q_{v'v''}$. This relationship (equation 6.1.4) has been used (section 6.4) to allow the present oscillator strengths to be compared with the Franck-Condon factors of Jarmain (1963a, 1963b).

However, one would expect a variation of the electronic transition with internuclear separation as the wave-functions are, in general, dependent on r (Nicholls, 1956), and some attempts have been made to take this into

account (e.g. Bates, 1949). A more recent development in this field has been made by Fraser, Jarmain and Nicholls (Fraser, 1954, Nicholls and Jarmain, 1956, Nicholls, 1956).

In performing their many calculations of Franck-Condon factors, Nicholls and Jarmain have calculated the integrals

$$(v',rv'') = \int \phi_{v'}\, r\phi_{v''}\, dr \qquad (6.1.6)$$

and

$$(v',r^2v'') = \int \phi_{v'}\, r^2\phi_{v''}\, dr \qquad (6.1.7)$$

and noticed the property

$$(v',rv'')/(v',v'') = (v',r^2v'')/(v',rv'') \qquad (6.1.8)$$

Fraser (1954) has studied the validity of the equation

$$(v',rv'')/(v',v'') = (v',r^nv'')/(v',r^{n-1}v'') \qquad (6.1.9)$$

and concludes that an upper limit of n approximately equal to 10 is to be expected for this relationship.

The quantity $\bar{r}_{v'v''}$, the r-centroid, which may be thought of as an average value of r for a given transition $v' \leftarrow v''$, was defined by Nicholls and Jarmain (1956)

as $$\bar{r}_{v'v''} = (v', rv'')/(v', v'') \qquad (6.1.10)$$

A further equality was put forward by Fraser (1954) which was based on the validity of equation (6.1.9) and the definition, equation (6.1.10), and this equality may be written

$$(v', f(r)v'') = f(\bar{r}_{v'v''}) \cdot (v', v'') \qquad (6.1.11)$$

This equation is valid provided that $f(r)$ is expressible as a polynomial in r whose powers do not exceed about 10.

Equation (6.1.11) is extremely useful in a study of the electronic transition moment, $R_e(r)$, as this quantity is not expected to have a dependence on r to higher powers than about 2 (Herzberg, 1950). This approach allows us to write equation (6.1.2) as

$$f_{v'v''} = \frac{8\pi^2 m c \nu_{v'v''}}{3he^2 d} R_e^2(\bar{r}_{v'v''}) q_{v'v''} \qquad (6.1.12)$$

where $R_e(\bar{r}_{v'v''})$ is the electronic transition moment at the r-centroid of the $v' \leftarrow v''$ transition. Nicholls and Jarmain (1966) have also shown that a linear relationship exists between $\bar{r}_{v'v''}$ and $\nu_{v'v''}$ and we may therefore write $R_e(\bar{r}_{v'v''})$ as $R_e(\nu_{v'v''})$.

In order to use the experimental oscillator strengths and the theoretical Franck-Condon factors (Jarmain 1963b) for the Schumann-Runge transitions in molecular oxygen, equation (6.1.12) may be written as below where δ, the degeneracy, is equal to 3 (Brix and Herzberg, 1954).

$$R_e^2(\nu_{v'v''}) = \frac{f_{v'v''}}{q_{v'v''}} \cdot \frac{9he^2}{8\pi^2 mc\nu_{v'v''}} \qquad (6.1.13)$$

The electronic transition moment is usually expressed in atomic units, and so it is desirable to write equation (6.1.13) in a form which allows easy calculation in these units. The atomic unit of electric moment is the product of the electron charge (e) and the Bohr radius (a_0), and so equation (6.1.13) is written in atomic units as

$$R_e^2(\nu_{v'v''}) = \frac{f_{v'v''}}{q_{v'v''}} \cdot \frac{9he^2}{8\pi^2 mc\nu_{v'v''}} \cdot \frac{1}{e^2 a_0^2} \qquad (6.1.14)$$

In this equation, $f_{v'v''}$ and $q_{v'v''}$ are dimensionless.

Now
$$a_0 = h^2/4\pi^2 me^2 \qquad (6.1.15)$$

therefore equation (6.1.14) becomes

$$R_e^2(\nu_{v'v''}) = \frac{f_{v'v''}}{q_{v'v''}} \cdot \frac{9}{hc\nu_{v'v''}} \cdot \frac{2\pi^2 me^4}{h^2} \quad \text{(atomic units)} \qquad (6.1.16)$$

If use is now made of the expressions

$$E_H = 2\pi^2 me^4/h^2 = 13{\cdot}6 \text{ eV} \qquad (6.1.17)$$

and

$$E_{v'v''} = h c \nu_{v'v''} \qquad (6.1.18)$$

for the total energy of the ground state of the hydrogen atom, and the energy of the $v'' \rightarrow v'$ transition respectively, we can write the electronic transition moment in atomic units as

$$R_e^2(\nu_{v'v''}) = (f_{v'v''}/q_{v'v''}) \cdot (9E_H/E_{v'v''}) \qquad (6.1.19)$$

6.2 Potential Curves

As was shown in the previous section, the experimental measurements may be used to determine the variation of the electronic transition moment provided that the Franck-Condon factors for the bands are known. To calculate these Franck- Condon factors it is necessary to propose potential energy curves for the states in question, and from these curves, the wave-function for the appropriate vibrational levels are computed. To obtain accurate Franck- Condon factors, it is therefore necessary to have a satisfactory potential curve to begin with.

As was seen in section 2.2.2, many analytic expressions for the potential curves of diatomic molecules have been put forward, one of the most satisfactory being that proposed by Morse (1929) who suggested the potential be represented by the expression

$$V(r-r_e) = D_e(1-e^{-\beta(r-r_e)})^2 \qquad (6.2.1)$$

where the notation is as given in section 2.2.2. This Morse function is a very good representation of the potential curve in the region of the equilibrium position for most molecules (Herzberg, 1950) and as such may be used to give reliable values for the energies and wavefunctions of the first few vibrational levels. Since at room temperature, all the molecules may be considered as being in the v = 0 vibrational level of the ground state, it is therefore possible to use the Morse function to represent the ground state for this analysis. However, for the B $^3\Sigma_u^-$ state of molecular oxygen, the Morse function is not a particularly good representation (Nicholls, 1960) and more sophisticated approximations to the "true" curve must be found.

Many other analytic expressions for the potential curve have been proposed (Hylleraas, 1935, Coolidge et al. 1938, Hulbert and Hirschfelder, 1941 etc.) but

more success, particularly with the recent accessibility of electronic computers, has been obtained with numerical techniques for obtaining potential curves. One of the most significant advances in this field was made by Rydberg (1931) and Klein (1932) who put forward a method enabling the classical turning points of a potential curve to be expressed in terms of the vibrational quantum number v. This was a semi-classical procedure which used as a starting point the observed energy levels for the states in question. Rees (1947) reinvestigated the approach of Rydberg and Klein, and developed an analytic method based on the same idea. The basic technique of these three workers, with various modifications, is one of the most used methods for obtaining numerical curves. It is generally referred to as the R.K.R. method.

Some of the more recent calculations applying this method to the B $^3\Sigma_u^-$ state of molecular oxygen have been performed by Vanderslice et al. (1960) Singh and Jain (1962), Jarmain (1960, 1963a, 1963b), Richards and Barrow (1964), Ginter and Battino (1965) and Gilmore (1965). All of these calculations employ various approximations to the original equations of Rees which have been designed to make the calculations simpler, and as such, these recent calculations were only thought

to apply rigorously to certain sections of the potential curves (e.g. near the equilibrium position, or near the dissociation limit). However, it is generally accepted now that most of these calculations are accurate over a major portion of the curves. Of these calculations, only that of Richards and Barrow (1964) does not require the known energy levels to be represented by an analytic function, although Richards and Barrow state that their procedure is only economical for the higher vibrational levels. The curves of Vanderslice et al., Singh and Jain and Jarmain show an anomalous increase in the position of the left hand turning point above v = 15 which is not apparent in the other curves, and this is explained by Richards and Barrow (1964) as being brought about by the type of function used to represent the energy levels. The method of Jarmain (1960) is usually referred to as the Klein-Dunham method as it was developed from Klein's original equations and Jarmain found it equivalent to an earlier procedure used by Dunham (1932).

6.3 Franck-Condon Factors

Until very recently, most of the Franck-Condon factors available were those which had been derived

using wave-functions obtained from a Morse or modified Morse potential. The major advantage in using a Morse-type potential is that the wave-functions obtained in solving the Schrodinger equation are analytic functions, and this greatly simplifies the process of computing overlap integrals. A complete summary up to 1965 of the published Franck-Condon factors for a large number of molecules is given in a review article by Spindler (1965). In particular for molecular oxygen, the large number of papers published by Fraser, Jarmain and Nicholls (Fraser and Jarmain, 1953, Jarmain and Fraser, 1953, Fraser, 1954, Nicholls, 1965a etc.) as well as providing results which allow comparison between theory and experiment, have contributed significantly to the development of the subject as a whole. One example of this is the approximation, by using a mean value for the constant in the Morse expression, which allows analytic integration of the overlap integrals (Fraser, 1954, Fraser and Jarmain, 1953, Jarmain and Fraser, 1953). Franck-Condon factors based on Morse potentials for a number of molecules and their isotopes have been calculated by Halmann and Laulicht (1966 etc.) for use in their study of isotope effects, and Wacks (1964) and Childs (1964) have also published Morse-type potential

Franck-Condon factors for several molecules.

The B $^3\Sigma_u^-$ state of molecular oxygen (the upper state involved in the Schumann-Runge transitions) is not particularly well represented by a Morse potential and the Franck-Condon factors derived from this potential are only "indicative of trends". For example, the Franck-Condon factors calculated from a Morse potential, with constants as given by the spectroscopic constants, form an increasing series with increasing vibrational quantum number v' (with v" = 0) (e.g. Nicholls, 1960); whereas the experimental results predict a maximum transition probability occurring at v' = 15 (Bethke, 1959 and the present results). A modification put forward by Ory and Kittlemann (1964) was to use the experimental value for the dissociation limit of the upper state in the Morse calculations, instead of the one predicted by the spectroscopic constants which is approximately twice the observed value. This modification had the desired result of producing a maximum in the Franck-Condon array at v' = 17, but the absolute values of the results were considerably smaller than those expected.

The oxygen molecule is rather abnormal since it

has a rather large internuclear separation between the equilibrium positions of the two states involved in the Schumann-Runge transitions, the equilibrium position of the ground state being considerably less than that of the upper state. Because of this, it might be expected that the increasing series of Franck-Condon factors obtained by Nicholls (1960) were correct in form. However, the "true" potential of the B $^3\Sigma_u^-$ state is very much broader than the Morse potential near the dissociation limit, which means that the wave-functions for the higher vibrational levels are "spread" over a much larger region. This implies that the magnitude of the wave-function in the region of the left-hand limb of the curve is smaller than that of the Morse wave-functions, and since this is where the maximum "overlap" with the ground state wave-function occurs, the corresponding Franck-Condon factors will be diminished. Thus a maximum in the Franck-Condon distribution might be expected. The maximum occurring in the results of Ory and Gittlemann (1964) bears out this argument as their procedure of lowering the value of the dissociation limit used in the Morse potential has the same effect basically as broadening the potential well near the top.

Recently, the availability of electronic computers has made practicable the calculation of Franck-Condon factors based on R.K.R. and other numerical potential curves. Jarmain (1960) suggested that if Morse potentials were fitted to various portions of a numerical potential, then the Morse curves could be used to calculate wave-functions for the vibrational levels, but this technique has not been used as yet to calculate Franck-Condon factors for molecular oxygen.

Other approaches using numerical potential curves have been applied to other molecules (Zare, 1965, Jain, 1964) but for the Schumann-Runge system, the only available Franck-Condon factors based on a numerical potential are those of Jarmain (1963a, 1963b). These values have been based on the Klein-Dunham potential developed by Jarmain (1960), and the wave-functions were computed using the method of Numerov (1933). The wave-functions for the ground state were derived from a Morse potential which is a good representation of the ground state potential (see section 6.2). These Franck-Condon factors are the best available to the present time for the v" = 0 progression of the Schumann-Runge band system.

6.4 Comparison of Theory and Experiment

A quick means of comparing theoretical Franck-Condon factors with experimental oscillator strengths is available if use is made of the approximation which lead to equation (6.1.4). This approximation neglects any effects due to the electronic transition moment, and attributes all the variation in the transition probability to the variation in the Franck-Condon factor distribution. That is, the Franck-Condon factors may be thought of as giving the manner in which the total oscillator strength for the $B\ ^3\Sigma_u^- \leftarrow X\ ^3\Sigma_g^-$ transition is divided amongst the bands. That is we may write

$$f_{v'0} = f_{e\ell} \cdot q_{v'0} \qquad (6.4.1)$$

where $f_{e\ell}$ is the total oscillator strength for the electronic transition. If a value of $f_{e\ell} = 0{\cdot}162$ (Haddad, 1967) is used in conjunction with the Franck-Condon factors of Jarmain (1963a, 1963b) a set of "theoretical" oscillator strengths for the band system is obtained. Figure 6.1 shows a comparison of these "theoretical" oscillator strengths and the experimental values obtained in the present work. The agreement between experiment and theory is seen to be remarkably good, particularly for the transitions to the higher values of v'. This

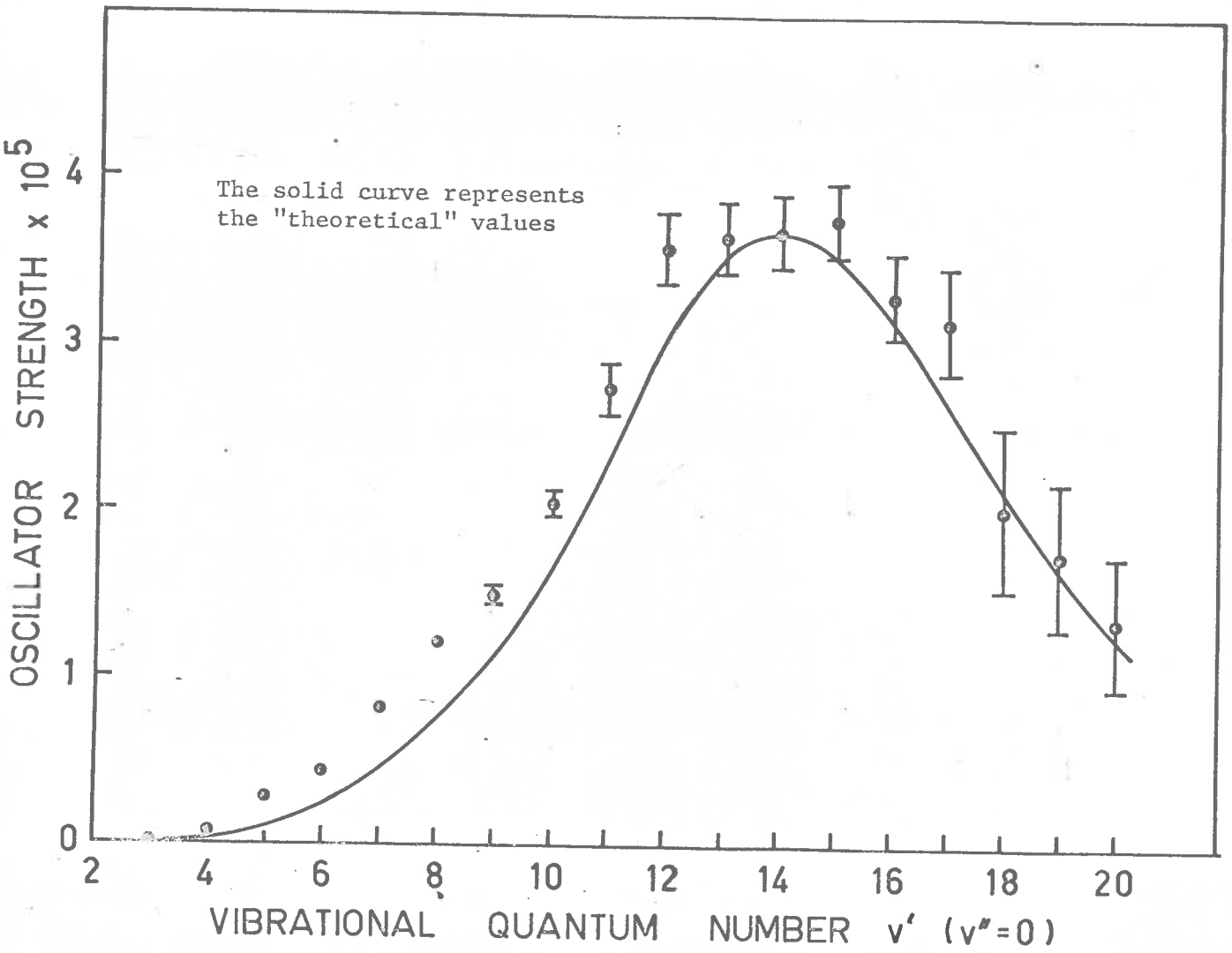

Fig. 6.1 Comparison of experimental and "theoretical" oscillator strengths

approach is also useful in that it can give an idea of the accuracy of the potential curve used in obtaining the Franck-Condon factors. The overlap integral is largely controlled by the magnitude of the ground state wave-function at the classical turning point of the potential curve for the upper state, and if a Morse wave-function is used for this wave-function, the Franck-Condon factors are seen to be extremely dependent on the position of the upper state potential curve. In fact, if the inside edge of the potential curve used by Jarmain were moved towards the ground state by as little as 0·01Å, then the magnitude of the ground state wave-function near the classical turning point of the $v' = 8$ level would be increased by about a factor of two. Thus the agreement between the two sets of results shown in figure 6.1 is seen to be quite good even for the lower lying transitions. It is interesting to note that if the Franck-Condon factors given by Nicholls (1960) are used in equation (6.4.1), the oscillator strengths obtained are very close to the experimental ones up to about $v' = 6$, and the potential used by Nicholls is displaced from that used by Jarmain (1960) at the $v' = 8$ level by roughly 0·01Å. This displacement is, in the light of the above argument, approximately

that required to bring the experimental and "theoretical" results into agreement.

As was shown in section 6.1, it is possible to use the experimental oscillator strengths to calculate values of the electronic transition moment R_e at the r-centroids of the transitions $(\bar{r}_{v',v''})$, provided the Franck-Condon factors for the band system are known. Since an accurate set of Franck-Condon factors for the Schumann-Runge band system have been calculated by Jarmain (1963a, 1963b, see the above discussion), these values and the experimental band oscillator strengths were used in equation (6.1.19) to obtain the electronic transition moment as a function of the wave-number of the transition. The values are presented in Table 6.1 and also in figure 6.2. For completeness, the oscillator strengths obtained by Bethke (1959) have been used to calculate values for the electronic transition moment by the same procedure, and these are also presented in Table 6.1 and figure 6.2. Figure 6.2 is seen to point out clearly the discrepancy between the present results and those of Bethke (1959) which was discussed in chapter 5.

Marr (1964) has used the results of Bethke (1959),

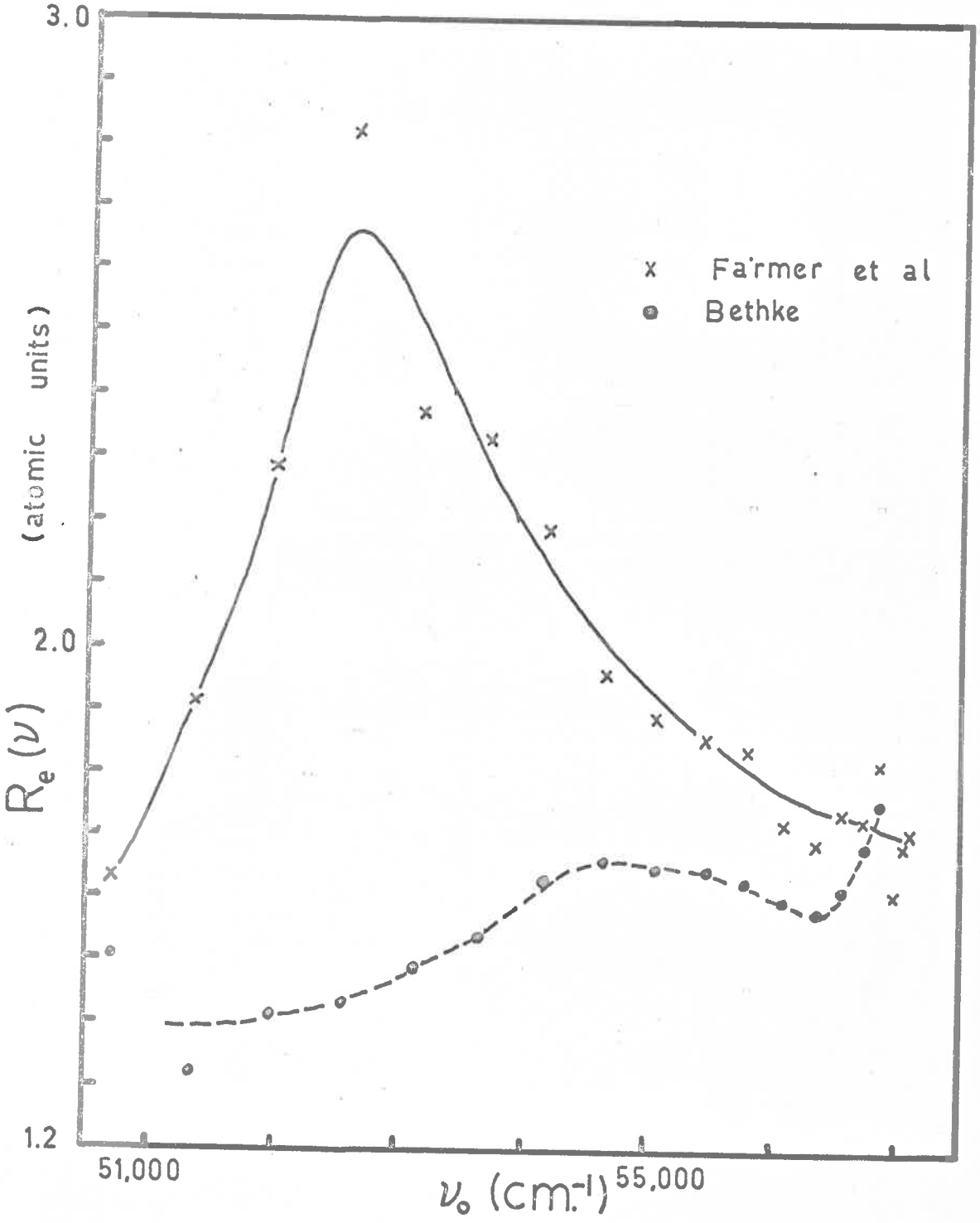

Fig. 6.2 Variation of the electronic transition moment (R_e)

TABLE 6.1

Band	Wave number (ν) (cm^{-1})	$R_e(\nu)$ Present results (a.u)	$R_e(\nu)$ Bethke (a.u)
2-0	50711	1·63	1·51
3-0	51352	1·91	1·32
4-0	51970	1·28	1·41
5-0	52563	2·82	1·43
6-0	53124	2·37	1·48
7-0	53659	2·33	1·54
8-0	54159	2·19	1·63
9-0	54624	1·96	1·66
10-0	55053	1·89	1·65
11-0	55442	1·86	1·65
12-0	55785	1·84	1·63
13-0	56086	1·72	1·60
14-0	56340	1·69	1·58
15-0	56551	1·74	1·62
16-0	56720	1·73	1·69
17-0	56852	1·83	1·76
18-0	56955	1·61	
19-0	57030	1·69	
20-0	57083	1·71	

Ditchburn and Heddle (1953, 1954) and Watanabe, Inn and Zelikoff (1953) to obtain the variation of the electronic transition moment with wave number for the $v'' = 0$ band progression and the associated continuum using Franck-Condon factors from a Morse potential. He suggests that the continuity of R_e over the dissociation limit found with Bethke's results indicates that they are more consistent with the photodissociation measurements than are the results of Ditchburn and Heddle. The discontinuity of the slope of R_e at the dissociation limit was attributed to the inadequacy of the Morse potential for the upper state above $v' = 3$.

Marr (1964) has also compared the variation of R_e derived from Bethke's results (using R.K.R. Franck-Condon factors) with that derived from the higher v'' absorption work of Treanor and Wurster (1960) and emission work of Hébert and Nicholls (1961) (using Morse Franck-Condon factors). To show this more clearly he shows a figure in which R_e is displayed as a function of internuclear separation r, covering the range $r = 1.2\text{Å}$ to 1.8Å. The data over most of this region is very sparse and the errors associated with the points are quite large (up to 30%) but Marr has tentatively suggested a linear variation of R_e with r, decreasing to higher r values. Since the publication

of this figure, R.K.R. Franck-Condon factors for at least some of the bands studied by Treanor and Wurster and Hébert and Nicholls have been published (Harris et al 1969) but these do not appear to differ by more than 10% from the Morse values. Consequently, the variation of R_e with r for these bands derived by Marr is still expected to be quite accurate.

As was mentioned earlier in this section, the variation of R_e derived from the present results differs from that derived from Bethke's results by up to a factor of two (see fig. 6.2) but, in view of the errors associated with these and the higher v'' values, one could still tentatively draw a linear variation of R_e with r as was done by Marr, the only possible difference being that the absolute value of R_e may be slightly higher. In view of the sparseness of data in this region and the errors involved in the measured values, all one can say is that the $v'' = 0$ band system and the higher v'' band systems give values for R_e which agree within a factor of two and as such are not inconsistent with each other. To obtain an accurate representation of the way in which R_e varies with r, it will probably be necessary to provide more data for other v'' band systems in the region r = 1.3Å to 1.8Å.

A similar procedure was follwed by Jarmain and Nicholls (1964), who used Franck-Condon factors obtained from a Klein-Dunham potential to predict the variation of the electronic transition moment with wave number. Their results, obtained from the absorption coefficients of Bethke (1959) for the band system, suggest continuity of R_e and its slope at the dissociation limit, but a definite statement can not be made as there is no information for R_e in the limiting cases as the dissociation limit is approached from higher or lower wave-numbers. Jarmain and Nicholls (1964) have also tentatively assigned the dip in R_e from $v' = 11$ to $v' = 16$ to the predissociation observed strongly at $v' = 11$ by Wilkinson and Mulliken (1957).

Figure 6.2 shows that the electronic transition moment variation derived from the present results approaches that derived from Bethke's results for $v' \geq 11$, and the present results will therefore give continuity of R_e with the continuum results of Jarmain and Nicholls (1964). However, continuity of slope is not quite as obvious, but this does not seem to be very serious as the Franck-Condon factors near the dissociation limit are possibly less accurate than those for lower transitions. It is also obvious from figure 6.2

that the dip obtained between $v' = 11$ and $v' = 16$ when Bethke's results are used is not apparent when the calculations are performed on the present results. As mentioned previously, Carroll (1959) found strong predissociation occurring at $v' = 4$, the effect becoming weaker towards higher v' values. Because of this, one is tempted to explain the structure around $v' = 4$ which is observed in the R_e values inferred from the present results, by this phenomena. However, there appears to be no justification for this as the curve derived from the present results is quite smooth.

The discussion presented above indicates that before a definite statement can be made about the structure of the variation of the electronic transition moment with wave number, detailed investigations are necessary in several fields. In particular, more accurate oscillator strengths are required for the band system and the continuum, more details are required about the predissociation phenomena and related topics, and more accurate Franck-Condon factors are required in the neighbourhood of the dissociation limit.

Using the experimental techniques described in this thesis, it would be possible to obtain more accurate oscillator strengths, but it is feared that the time

required to perform the experiment under the existing conditions would become prohibitively large. This can be overcome by using a more intense light source or a dispersing instrument having better resolution, or both; and it is thought that an experiment incorporating these features will eventually produce oscillator strengths of the desired accuracy.

APPENDIX I

Circuits for Molecular Hydrogen Data-Handling System

The block diagram of the circuits used in this data-handling system is shown in figure I(a), and the detailed individual circuits are shown in the figures I(b), (c), (d) and (e).

The synchronous "clock" described in section 4.4, consists of a full or half wave rectifier circuit (providing a 100c/s or 50c/s waveform) whose output is used to fire a Schmidt trigger and a monostable multivibrator. The monostable output is then fed into a dividing network of binary dividing stages. The dividing stages are controlled by series gates so that the initial 600 c/min. or 3000 c/min. from the monostable may be divided as shown in figure I(a) by 3,6,30,60...6000. The output of the dividing network ("clock pulses") are fed directly to the address advance input of the multi-channel analyser and via a bi-stable to two reed relays with gold plated contacts (the switch S). The circuit for the switch is shown in figure I(f).

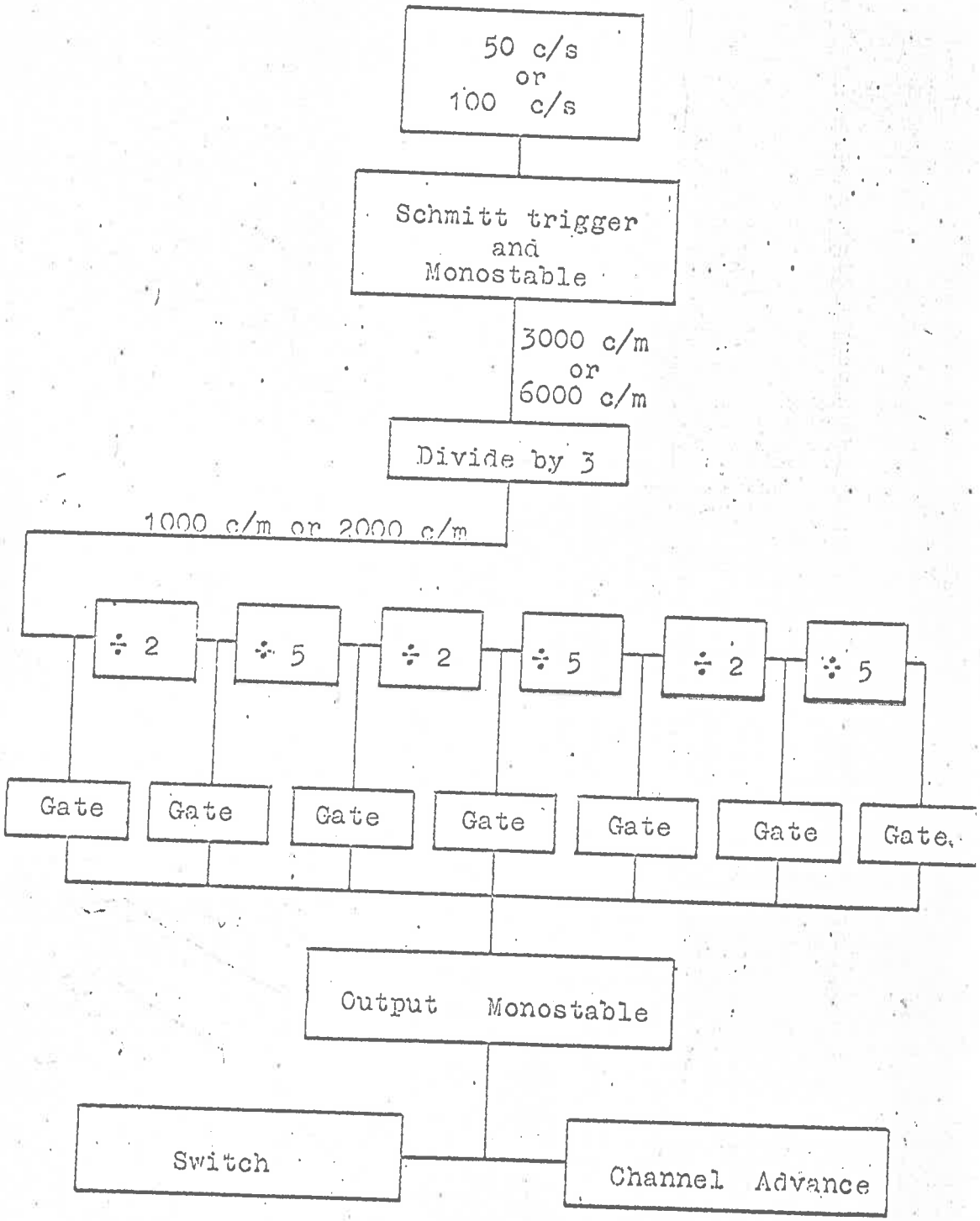

Fig. I(a) Schematic of the subsidiary circuits

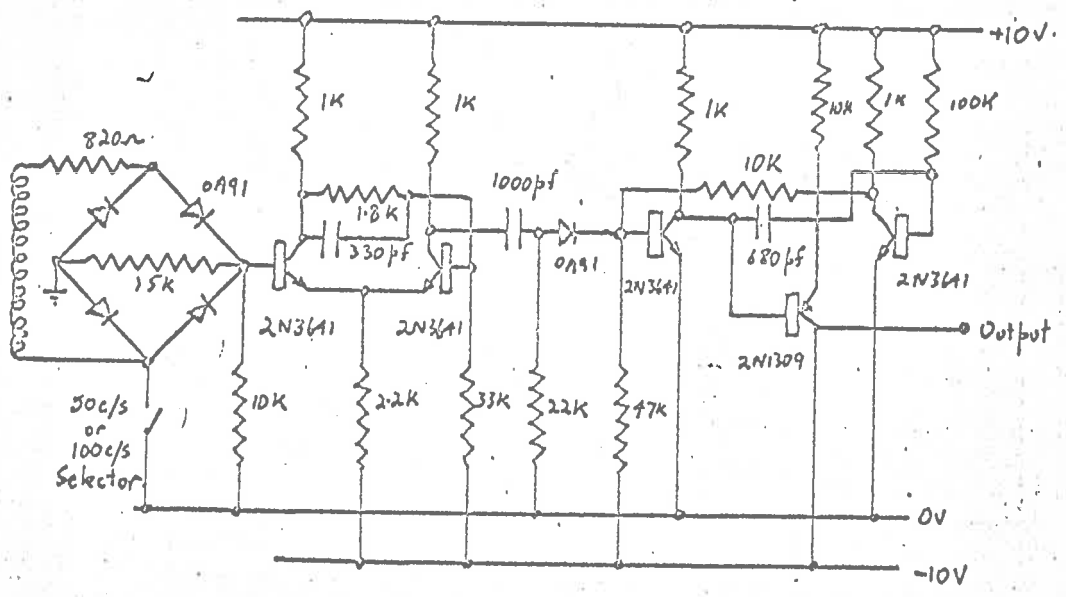

Fig. I(b) The input circuit for the clock including the Schmitt trigger and monostable circuits.

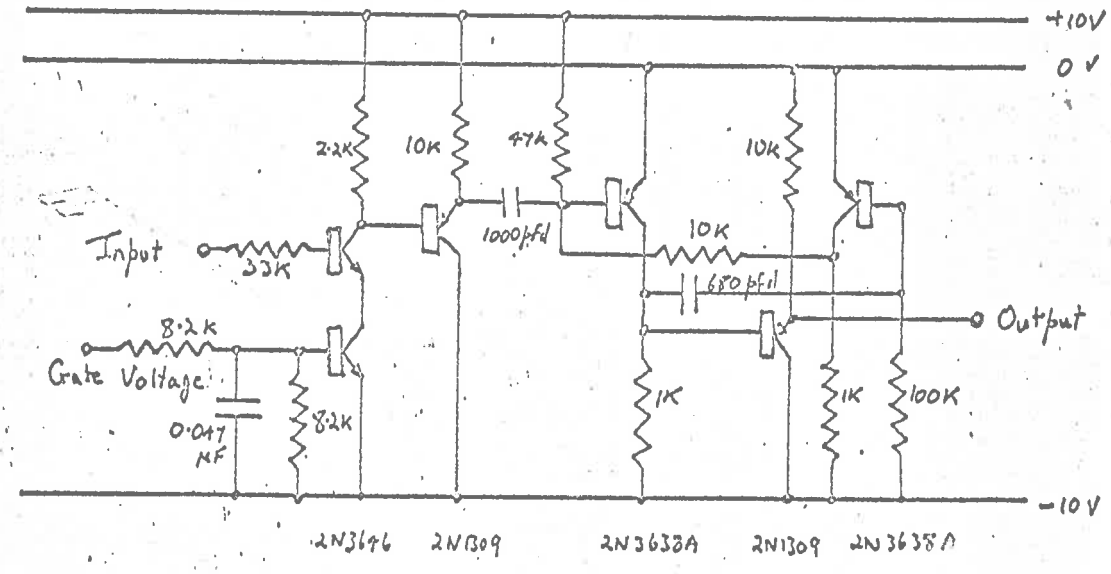

Fig. I(c) The series gate and output monostable circuit

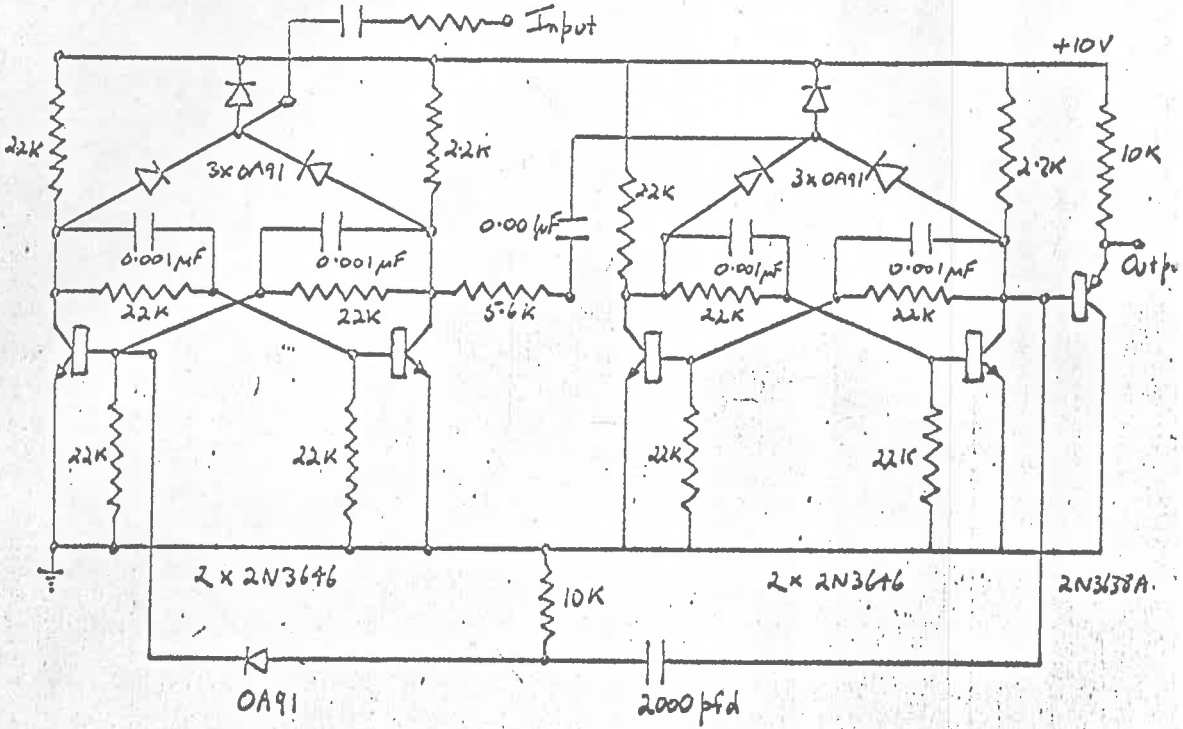

Fig. I(d) The circuit for the divide by 3 "binary"

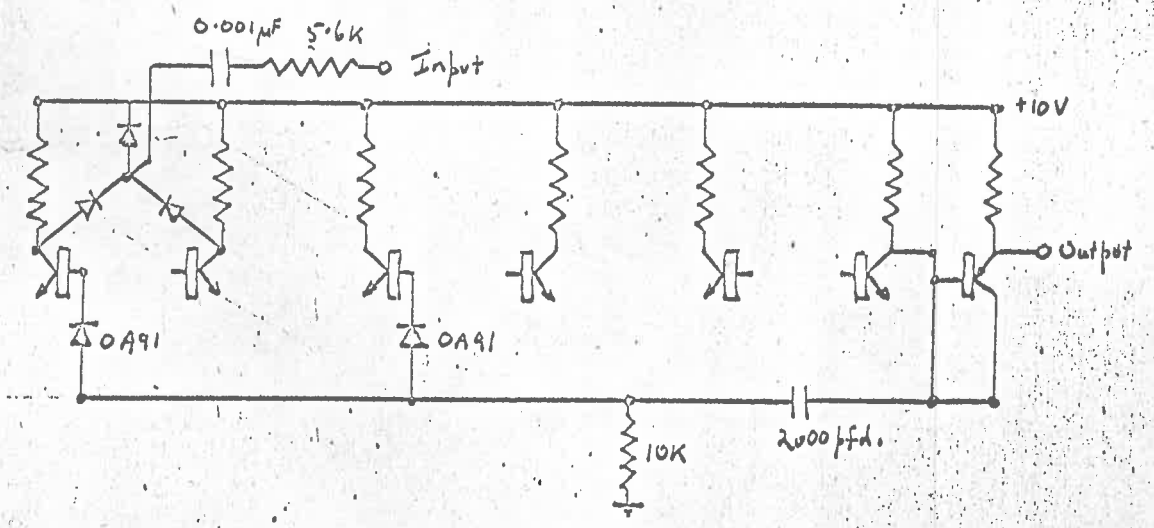

Fig. I(e) The divide by 5 configuration

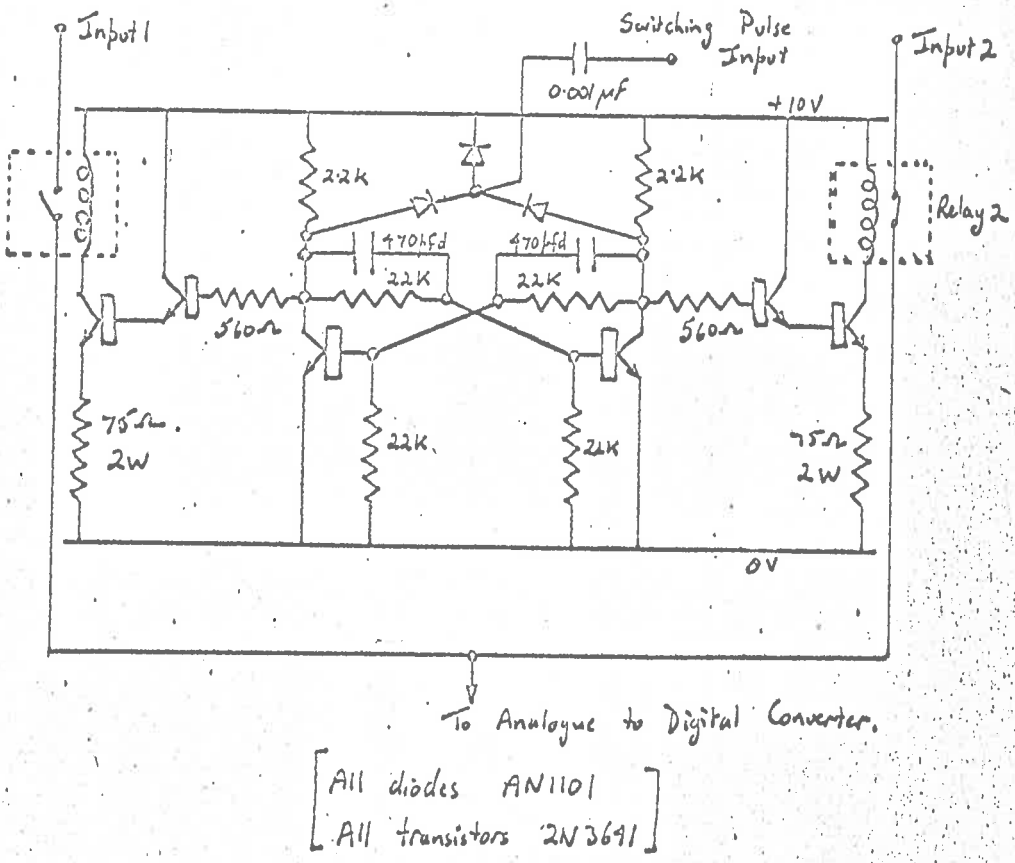

Fig. I(f) The switching circuits for the inputs to the analogue to digital converter

The start, stop and reset operations of the system are controlled by relays and an inhibit voltage is applied to the multichannel analyser when the system is in the stop mode. The reset control is used to clear all the binaries and to set the switch S in a predetermined position.

APPENDIX II

Circuits for Molecular Oxygen Data-Handling System

As was mentioned in chapter 5, the data-handling system used for the molecular oxygen experiment was a more recent version of the one developed for the molecular hydrogen experiment which is described in Appendix I. The logic of operation of the new system is identical to that described in Appendix I for the hydrogen system and the electronics was only re-designed to conserve space, to produce greater reliability and to allow easier maintenance. All these factors were achieved by the use of integrated circuits and printed circuit boards, and the ability to connect digital signals (e.g. counter outputs) to the multichannel analyser on command was also incorporated in the system. The only other major difference between the systems was the ability of the more recent version to handle four independent inputs.

A detailed circuit for the system is given in figure II. Fairchild industrial integrated circuits were used throughout the counting and g ating units.

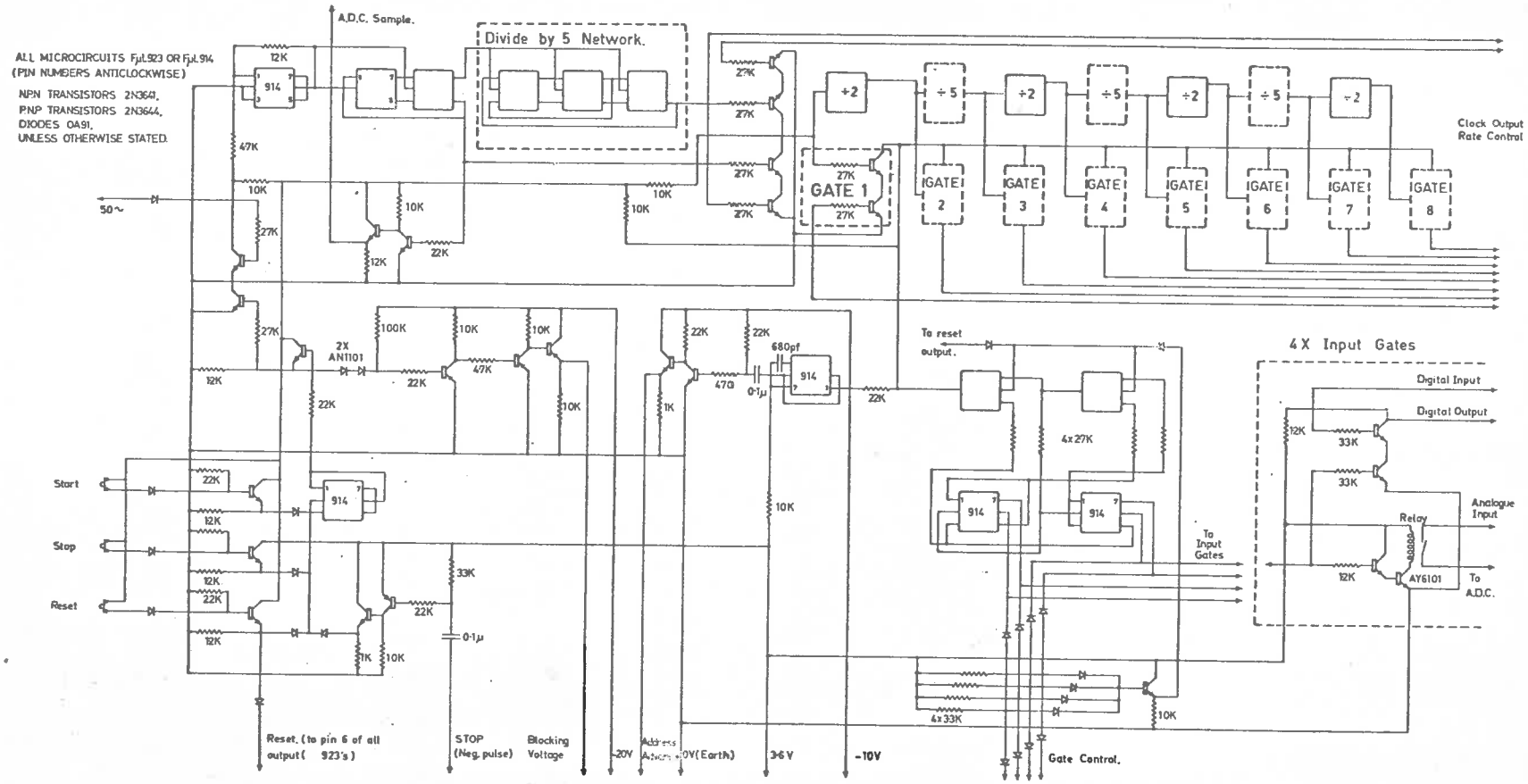

Fig. II Circuit for the modified data-handling system

APPENDIX III

Publications

The following papers have been written on the work described in this thesis.

1. "An Experimental Determination of the Oscillator Strengths for some Transitions in the Lyman Bands of Molecular Hydrogen".
   G.N. Haddad, K.H. Lokan, A.J.D. Farmer and J.H. Carver. J. Quant. Spect. Radiat. Transfer, 8, 1193 (1968).

2. Experimental Oscillator Strengths for the Schumann-Runge Band System in Oxygen".
   A.J.D. Farmer, W. Fabian, B.R. Lewis, K.H. Lokan and G.N. Haddad. J. Quant. Spect. Radiat. Transfer, 8, 1739 (1968).

3. "A Digital Data-Handling System for Recording Vacuum Ultraviolet Absorption Spectra".
   K.H. Lokan, G.N. Haddad, A.J.D. Farmer, W. Fabian, B.R. Lewis and D.G. McCoy. In preparation.

BIBLIOGRAPHY

Bates, D.R. (1949) Proc. Roy. Soc. (Lond) A196, 217.

Bethke, G.W. (1959) J. Chem. Phys. 31, 669.

Beutler, H. (1934) Z. Phys. Chem. 27, 287.

Beutler, H. (1935) Z. Phys. Chem. 29, 315.

Beutler, H. Deubner, A. and Junger, H.O. (1936) Z. Physik. 99, 181.

Blake, A.J., Carver, J.H. and Haddad, G.N. (1966) J.Q.S.R.T. 6, 451.

Born, M. and Oppenheimer, R. (1927) Ann. Physik. 84, 457.

Boyce, J.C. (1941) Rev. Mod. Phys. 13, 1.

Breene, R.G. (1957) Rev. Mod. Phys. 29, 94.

Brix, P. and Herzberg, G. (1954) J. Chem. Phys. 21, 2240.

Bunch, S.M., Cook, G.R., Ogawa, M. and Kuhler, A.W. (1958) J. Chem. Phys. 28, 740.

Carroll, P.K. (1959) Astrophys. J. 129, 794.

Cashion, J.K. (1966) J. Chem. Phys. 45, 1037.

Childs, D.R. (1964) J.Q.S.R.T. 4, 283.

Cook, G.R. and Metzger, P.H. (1964) J.O.S.A. 54, 968.

Coolidge, A.S., James, H.M. and Vernon, E.L. (1938) Phys. Rev. 54, 726.

Condon, E.U. (1928) Phys. Rev. 32, 858.

Condon, E.U. and Shortley, G.H. (1935) "The Theory of Atomic Spectra (C.U.P.)

Curry, J. and Herzberg, G. (1934) Ann. d. Phys. 19, 800.

Dennison, D.M. (1926) Phys. Rev. 28, 318.

Dieke, G.H. and Hopfield, J.J. (1927) Phys. Rev. 30, 400.

Ditchburn, R.W. and Heddle, D.W.O. (1953) Proc. Roy. Soc. (Lond) A220, 61.

Ditchburn, R.W. and Heddle, D.W.O. (1954) Proc. Roy. Soc. (Lond) A226, 509.

Dunham, J.L. (1932) Phys. Rev. 41, 721.

Franck, J. (1925) Trans. Farad, Soc. 21, 536.

Fraser, P.A. (1954) Can. J. Phys. 32, 515.

Fraser, P.A. and Jarmain, W.R. (1953) Proc. Phys. Soc. (lond) A66, 1145.

Fraunhoffer, J. (1817) Gilberts Ann. 56, 264.

Gilmore, F.R. (1965) J.Q.S.R.T. 5, 369.

Ginter, M.L. and Battino, R. (1965) J. Chem. Phys. 42, 3222.

Goldstein, R. and Mastrup, F.N. (1966) J.O.S.A. 56, 765.

Goody, R.M. (1964) "Atmospheric Radiation I: Theoretical Basis" (Oxford Monograph).

Haddad, G.N. (1967) "Thesis, University of Adelaide".

Helmann, H. and Laulicht, I. (1966). J. Chem. Phys. 44, 2398.

Heddle, D.W.O. (1960) J. Chem. Phys. 32, 1889.

Herzberg, G. (1950) "Molecular Spectra and Molecular Structure I: Spectra of Diatomic Molecules (D. vanNostrand).

Herzberg, G. and Howe, L.L. (1959) Can. J. Phys. 37, 636.

Herzberg, G. and Monfils, A. (1960) J. Molec. Spect. 5, 482.

Houser, J.E., Brooks, N.H. and Lawrence, G.M. (1968) J. Chem. Phys. 49, 5387.

Hopfield, J.J. (1930) Nature 125, 927.

Hori, T. (1927) Z. Physik. 44, 838.

Hulbert, H.M. and Hirschfelder, J.O. (1941) J. Chem. Phys. 9, 61.

Hylleraas, E.A. (1935) Z. Physik. 96, 643.

Hylleraas, E.A. (1936) Physik. Z. 36, 599.

Jain, D.C. (1964) J.C.S.R.T. 4, 427.

Jarmain, W.R. (1960) Can. J. Phys. 38, 217.

Jarmain, W.R. (1963a) Can. J. Phys. 41, 414.

Jarmain, W.R. (1963b) Can. J. Phys. 41, 1926.

Jarmain, W.R. and Fraser, P.A. (1953) Proc. Phys. Soc. (Lond) A66, 1153.

Klein, O. (1932) Z. Physik. 76, 226.

Knauss, H.P. and Ballard, S.S. (1935) Phys. Rev. 48, 796.

Kolos, W. and Wolniewicz, L. (1965) J. Chem. Phys. 43, 2429.

Kolos, W. and Wolniewicz, L. (1966) J. Chem. Phys. 45, 509.

Kolos, W. and Wolniewicz, L. (1968) J. Chem. Phys. 48, 3672.

Kronig, R de L. and Rabi, I.I. (1927) Phys. Rev. 29, 262.

Lee, P. and Weissler, G.L. (1952) Astrophys. J. 115, 570.

Leighton, R.B. (1959) "Principles of Modern Physics (McGraw-Hill).

Lyman, T. (1928) "The Spectroscopy of the Extreme Ultraviolet (Longmans Green and Co.)

Metsger, P.H. and Cook, G.R. (1964) J.C.S.R.T. 4, 107.

Nonfils, A. (1961a) Acad. Roy. Belg. Bull. Classe. Sci. 47, 585.

Nonfils, A. (1961b) Acad. Roy. Belg. Bull. Classe. Sci. 47, 816.

Nonfils, A. (1965) J. Molec. Spect. 15, 265.

Morse, P.M. (1929) Phys. Rev. 34, 57.

Namioka, T. (1964a) J. Chem. Phys. 40, 3154.

Namioka, T. (1964b) J. Chem. Phys. 41, 2141.

Namioka, T. (1965) J. Chem. Phys. 43, 1636.

Neblette, C.B. (1930) "Photography, its Principles and Practice (Van Nostrand, N.Y.)

Nicholls, R.W. (1956) Proc. Phys. Soc. (Lond) A69, 253.

Nicholls, R.W. (1960) Can. J. Phys. 38, 1705.

Nicholls, R.W. (1965a) J. Res. Nat. Bur. Stand. 69A, 369.

Nicholls, R.W. (1965b) Astrophys. J. 141, 819.

Nicholls, R.W. and Jarmain, W.R. (1956) Proc. Phys. Soc. (Lond) A69, 253.

Numerov, B. (1933) Publ. de l'Observ. Astrophysique Central de Russie 2, 188.

Ory, H.A. and Cittlemann, A.P. (1964) Astrophys. J. 139, 357.

Peek, J.M. and Lassettre, E.N. (1963) J. Chem. Phys. 38, 2392.

Pekeris, C.L. (1934) Phys. Rev. 45, 98.

Pell, J.D. and Karl, G. (1966) Can. J. Phys. 44, 1467.

Rees, A.L.G. (1947) Proc. Phys. Soc. (Lond) A59, 998.

Richards, W.G. and Barrow, R.F. (1964) Proc. Phys. Soc. (Lond) 83, 1045.

Rowland, H.A. (1882) Phil. Mag. (5) 13, 469.

Rydberg, R. (1931) Z. Physik. 73, 376.

Samson, J.A.R. (1967) "Techniques of Vacuum Ultraviolet Spectroscopy" (John Wiley and Sons Inc.)

Schumann, V. (1901) Ann. D. Phys. 4, 642.

Schumann, V. (1903) Smithsonian Contributions to Knowledge no. 1413.

Singh, N.L. and Jain, D.C. (1962) Can. J. Phys. 40, 520.

Spindler, R.J. (1965) J.Q.S.R.T. 5, 165.

Spindler, R.J. (1966) NASA rept. AVSSD-0287-66-RR.

Struve, O. and Elvey, C.T. (1934) Astrophys. J. 79, 409.

Stokes, G.G. (1880) Collected Papers 4, 267 (University Press, Cambridge).

Tanaka, Y. (1944) Sci. Rep. Inst. Phys. Chem. Res. (Tokyo) 42, 49.

Tilford, S.G., Vanderslice, J.T. and Wilkinson, P.G. (1965) Astrophys. J. 141, 1226.

Tousey, R. (1962) Appl. Opt. 1, 679.

Van der Held, E.F.M. (1931) Z. Physik. 70, 508.

Vanderslice, J.T., Mason, E.A., Maisch, W.G. and Lippincott, E.R. (1960) J. Chem. Phys. 32, 515.

Wacks, M.E. (1964) J. Chem. Phys. 41, 930.

Watanabe, K., Inn, F.C.Y. and Zelikoff, M. (1953) J. Chem. Phys. 21, 1026.

Watanabe, K. (1958) Adv. Geophys. 5, 157.

Werner, S. (1926) Proc. Roy. Soc. (Lond) A113, 107.

Wilkinson, P.G. and Mulliken, R.S. (1957) Astrophys. J. 125, 594.

Wilkinson, P.G. and Byram, E.T. (1965) Appl. Opt. 4, 581.

Wolniewicz, L. (1966) J. Chem. Phys. 45, 515.

Yamada, H. (1968) J.Q.S.R.T. 8, 1463.

Zare, R.N. (1965) J. Molec. Spect. 15, 117.

I hereby give my consent for this thesis to be available for loan or photo-copying.

A.J.D. Farmer.